

8-2016

Cardiovascular and hematopoietic responses to volatile benzene exposure.

Wesley Tyler Abplanalp
University of Louisville

Follow this and additional works at: <https://ir.library.louisville.edu/etd>

Part of the [Cellular and Molecular Physiology Commons](#)

Recommended Citation

Abplanalp, Wesley Tyler, "Cardiovascular and hematopoietic responses to volatile benzene exposure." (2016). *Electronic Theses and Dissertations*. Paper 2508.
<https://doi.org/10.18297/etd/2508>

This Doctoral Dissertation is brought to you for free and open access by ThinkIR: The University of Louisville's Institutional Repository. It has been accepted for inclusion in Electronic Theses and Dissertations by an authorized administrator of ThinkIR: The University of Louisville's Institutional Repository. This title appears here courtesy of the author, who has retained all other copyrights. For more information, please contact thinkir@louisville.edu.

CARDIOVASCULAR AND HEMATOPOIETIC RESPONSES TO VOLATILE
BENZENE EXPOSURE

By

Wesley Tyler Abplanalp

B.S., Indiana University, 2007

M.S., University of Louisville, 2015

A Dissertation

Submitted to the Faculty of the
University of Louisville School of Medicine
in Partial Fulfillment of the Requirements
for the Degree of

Doctor of Philosophy in Physiology and Biophysics

Department of Physiology
University of Louisville,
Louisville, Kentucky

August 2016

CARDIOVASCULAR AND HEMATOPOIETIC RESPONSES TO VOLATILE
BENZENE EXPOSURE

By

Wesley Tyler Abplanalp

B.S., Indiana University, 2007
M.S., University of Louisville, 2014

A Dissertation Approved on

August 2, 2016

By the following Dissertation Committee:

Aruni Bhatnagar, Ph.D.

Timothy O'Toole, Ph.D.

Dale Schuschke, Ph.D.

David Lominadze, Ph.D.

Stanley D'Souza, Ph.D.

ACKNOWLEDGEMENTS

The commencement and completion of my graduate of my graduate career could not have been achieved without support and patronage of many people. Closest to me, I would like to thank my wife Sarah. Her constant encouragement and understanding were of immense consolation. I would also like to thank my parents, Larry and Kaye, who encouraged me to pursue a life and career that encourages curiosity, exploration and challenge. I am unspeakably grateful to have them in my life. My sister, Katie, and brother, Kristafer, have always been sources of comfort, excitement, and creativity. Additionally, I would also like to thank my co-mentors, Drs. Bhatnagar and O'Toole. While their personalities may serve as a study in contrasts, their professional commitment to a rigorous scientific process is undeniably mirrored. I am unendingly grateful to them for extending this opportunity have a graduate career in their company. Especially, to Dr. O'Toole, who has taken so much time in his mentorship role. Also, I recognize my advisory committee members. Their involvement and feedback has been deeply valued. Lastly, I thank current and former members of the center who have been indispensable to this work. It's been a privilege to work with this wonderful and varied team.

ABSTRACT

CARDIOVASCULAR AND HEMATOPOIETIC RESPONSES TO VOLATILE
BENZENE EXPOSURE

Wesley T. Abplanalp

August 2, 2016

The rapid and recent increase in the global epidemic of diabetes and cardiovascular disease suggests a strong component of the environment is contributing. Benzene is a ubiquitous volatile pollutant generated by cigarette smoke, automobile exhaust, wildfires and industrial activities. Consequently, it is found in almost all urban and rural air samples. Benzene is known to cause hematotoxicity and its metabolism generates oxidative stress. Although, benzene has been studied for many years, few investigations have probed what influence benzene exposure may have on other physiological processes. Here we hypothesize that benzene metabolism by hepatic-CYP450 2E1 generates oxidative stress and inflammation, which then promote insulin resistance and endothelial dysfunction. To test this hypothesis, we measured hematological progenitor differentiation and circulating blood cell types as well as indices of oxidative stress, vascular damage, insulin resistance and stem cell function to assess relative sensitivity of hematological and vascular biomarkers. Our findings show that benzene-exposed mice exhibit oxidative stress, inflammation, vascular damage, insulin resistance, thrombosis with diminished vascular repair capacity

at levels similar to hematological changes typically found in acute studies assaying for the lowest observed adverse effect level. These data suggest that individuals exposed to this ubiquitous air pollutant are likely to experience inflammation and vascular complications.

TABLE OF CONTENTS

	PAGE
ACKNOWLEDGEMENTS	iii
ABSTRACT	iv
CHAPTER I	
<i>GENERAL INTRODUCTION</i>	
Air Pollution – Ancient and Recent	1
Benzene – Chemical Description	11
Benzene – Industrial and Commercial Uses	14
Benzene Absorption, Distribution, Metabolism and Excretion	17
Role of CYP2E1 in Benzene Metabolism and Toxicity	21
Hepatic Inflammation and Insulin Resistance	29
Insulin Signaling and Mechanisms for Insulin Resistance	32
Role of Hepatic Insulin Resistance on Glucose Production	36
Dyslipidemia as a Biomarker of Hepatic IR	37
Thrombosis and Hepatic IR	38
Hepatic IR and Inflammation	39
Goals of the Project	40

CHAPTER II

GENERAL CHARACTERISTICS OF BENZENE EXPOSURE

Introduction	42
Methods	44
Results	48
Discussion	77

CHAPTER III

BENZENE EXPOSURE AND INSULIN RESISTANCE

Introduction	85
Methods	86
Results	89
Discussion.....	150

CHAPTER IV

BENZENE EXPOSURE AND HEMATOPOIETIC AND ENDOTHELIAL PROGENITOR CELLS

Introduction	160
Methods	162
Results	166
Discussion.....	184

CHAPTER V

<i>CONCLUDING DISCUSSION.....</i>	190
-----------------------------------	-----

REFERENCES	196
CURRICULUM VITAE	212

LIST OF FIGURES

FIGURE	PAGE
1. Schematic of benzene metabolizing enzymes and metabolites	23
2. Benzene exposure system	50
3. Verification of benzene exposure and metabolism	52
4. Benzene and tissue injury	57
5. Benzene and plasma lipids	59
6. Benzene and platelet aggregates	62
7. PLAgg formation and TEMPOL intervention	69
8. Benzene exposure, circulating immune cells and HFD	73
9. Benzene exposure, monocyte subpopulations and HFD	75
10. Schematic of benzene-induced liver injury and insulin resistance	92
11. Benzene exposure and glycemc indices	94
12. Glycemc indices in animals 4wks-post exposure	96

13. Glucose tolerance tests and insulin tolerance tests	
after benzene exposure	98
14. Insulin-stimulated Akt phosphorylation in liver	100
15. Insulin-stimulated Akt phosphorylation in skeletal muscle	102
16. Phospho-Akt induction capacity	104
17. Schematic of benzene-induced liver injury and	
insulin resistance emphasizing ROS production	106
18. Benzene-induced markers of oxidative stress	108
19. Schematic of benzene-induced liver injury and	
insulin resistance highlighting inflammatory signaling	110
20. Nuclear Factor kappa-B (NF κ B) phosphorylation in liver	112
21. Nuclear Factor kappa-B (NF κ B) p65 phosphorylation in skeletal	
muscle	114
22. NF κ B-targeted cytokines	116
23. Benzene exposure and cytokine regulating proteins	119
24. IRS-2 pan-tyrosine phosphorylation in liver	120
25. Schematic of benzene-induced liver injury and insulin resistance	
with anti-oxidant intervention	126

26. TEMPOL intervention and glycemic indices	128
27. TEMPOL reverses glucose intolerance	130
28. Anti-oxidant intervention and Akt phosphorylation	132
29. Schematic of benzene-induced liver injury and downstream changes influenced by TEMPOL intervention	134
30. TEMPOL and oxidative stress	136
31. TEMPOL and inflammatory signaling	138
32. Anti-oxidant and SOCS proteins	140
33. Anti-oxidant and IRS-2 phosphorylation	142
34. HFD-fed mice, benzene exposure and FPG	144
35. Insulin-stimulated Akt phosphorylation and HFD	146
36. miRNAs, PTEN expression and benzene exposure	148
37. Benzene exposure and bone marrow-resident hematopoietic stem cell populations	169
38. Benzene exposure and HSC CFU outgrowth	171
39. Circulating and bone marrow-derived EPCs and benzene exposure	173
40. HFD, benzene exposure and bone marrow-resident hematopoietic stem cells	176

41. Benzene, HFD and HSC CFUs	178
42. Benzene, HFD and circulating and BM EPCs	180
43. EPC adhesion, proliferation and benzene exposure	182

LIST OF TABLES

TABLE	PAGE
1. Physical characteristics of benzene	12
2. Complete blood counts	54
3. Circulating microparticle levels	61
4. Complete blood count panels and TEMPOL	68
5. Complete blood count and 8wks of HFD.....	71
6. Complete blood count and 18wks of HFD	72
7. Characteristics of response to benzene exposure	193
8. Indices of oxidative stress, inflammation and IR	194
9. Hematopoietic and endothelial progenitor cells	195

CHAPTER I

GENERAL INTRODUCTION

Air Pollution – Ancient and Recent

Since the dawn of the Industrial Revolution Western civilization has gained tremendous economic prosperity. The Industrial Revolution allowed society to exponentially increase the production of goods, specialize in division of labor, enabled opportunities for greater geographic and social mobility, and it created technological innovation that provided relief from much of the physical toil of agrarian society. However, the opulence of this movement was shrouded in a fog of particulate haze. The energy driving much of this revolution was primarily coal-based, and unclean to burn and handle. Coal-burning furnaces emit many noxious chemicals such as benzene, arsenic, lead, cadmium, carbon monoxide, particulates, and sulfur and nitrogen dioxides (1). However, in modern times, airborne toxic events like the episodes in the Meuse Valley in 1930, in the town of Donora, Pennsylvania in 1948, and in London in 1952 led to undeniable evidence that industrial and residential air pollution was negatively impacting lives. Though carefully coordinated efforts to mitigate effects of air pollution did not begin until recently, the evidence for air pollution adversely affecting human health can be found in some of the oldest of human societies.

Archaeological evidence suggests that pollutants were widely experienced in groups that lived before current documentary records. For example, lung

tissue from mummified (intentional or not) human remains can be rehydrated by paleopathologists to ascertain pulmonary health at time of death. In Egypt, it has been seen that mummies demonstrate signs of pneumoconiosis (2), a lung disease typically associated with inhalation of dust, characterized by inflammation, coughing, and fibrosis. This would be expected in places with high concentrations of wind-blown sand (i.e. Egypt). Moreover, these paleopathological studies on pneumoconiosis have been performed on sixteenth century Peruvian miners and among East Anglian flint-knappers (3) finding similar results. Additional carbon deposits suggesting anthracosis are seen more broadly, as expected in persons frequently exposed to wood smoke over a lifetime. These studies suggest that indoor air pollution has been a hindrance to health since man first learned to use fire and would have been a problem whether people lived in urban or rural areas, and would have been exacerbated by poorly ventilated living conditions.

The problem of outdoor pollution grew more important with the development large cities and industrial activity, and it has been recognized as such almost since the dawn of its production. The *astynomoi* (city magistrates) of ancient Greece were charged with removing malodorous rubbish from town and controlling this kind of annoyance. More to the point, the Roman courts heard civil lawsuits over smoke pollution and made some efforts to house polluting industries outside of wealthy communities (4). Additionally, Roman senator Sextus Julius Frontinus (c. 40 – 103 Common Era [CE]) in *De Aqueductibus Urbis Romae* felt that it was of utmost importance to supply water

to Rome, which would alleviate broader sanitary concerns and purify the air. Even the Hippocratic Corpus contains a volume titled *Air, Water and Places* describing the importance of climate and the properties of air (including metalliferous content). Another medical giant, Galen, once wrote to his patient Marcus Aurelius that a great part of pestilence was the corruption of air. Additionally, the Arab world connected air pollution and health at an early date through miasmatic beliefs (5).

During these times in antiquity wood was a primary fuel (and a source of benzene exposure). It was not until the late 1200s CE that we have documentation that London moved to coal during a wood shortage. As quickly as coal entered society, people were equally swift to recognize the need to regulate its use. In the 1285 CE a petition was sent to a group of officials stating that since the switch from wood to sea-coal, the “air is infected and corrupted to the peril of those frequenting and dwelling those parts.” Continued enquiry by investigators like John Graunt (*Natural and Political Observations*), John Evelyn (*Fumifugium, or the Smoake of London Dissipated*), John Arbuthnot (*Concerning the Effects of Air on Human Bodies*) and John Hall (*Cautions Against the Immoderate Use of Snuff*) catalogued what demographic and environmental data was available in 16th, 17th and 18th centuries to infer the health effects of air pollution.

Two additions to society became notably impactful on personal exposure to air pollution. One such addition was the chimney which allowed for better ventilation of homes and use of bituminous coal, which would produce a noxious smelling and intense smoke (more so than so-called sea-coal). The other was

the steam engine. The steam engine could be recognized as a point source for soot release. Still, as areas rapidly scaled up their industry, the emissions became universally distributed and distressing (6). The grey colored rain would stain clothes hanging to dry (cream clothes were preferred over white) (7), black umbrellas were used to protect the worn clothes on the street, interiors of homes used dark wall coverings so as not to be noticeably stained by soot, and the sulfur dioxide weathered carved stone and corroded metal works (8). The trend in the 19th century was a new interest in the well-being of cities because of the mass migration of people into these centers providing employment opportunities. This attention brought awareness to the increased mortality in urban areas and brought about legislation to mitigate issues (9). However, while smoke abatement and air pollution mitigation acts were frequently brought forth, emphasis was placed on commercial growth and so industry maintained an advantage with legislators (10). Additionally, a lack of technologies to control air emissions kept industrialists and administrators from realizing a reduction in release (11). It is estimated that in places like London, pollutant concentrations would only have begun to decrease when railways systems were installed, allowing for a decrease in urban and industrial density, thus a diffusion of air pollution (12). The most reliable surrogate for a direct measurement of air pollution in this area was the presence of the iconic London fog.

Systematic developments in air pollution monitoring networks grew after a calling for more quantitative evidence to understand the relationship between “fogs” and increased mortality (13). These networks helped provide data for

epidemiological studies that demonstrated strong associations between pollution and negative health outcomes. However, causal mechanisms were, and are, poorly understood. Primary founts of information and action sprung from extreme cases, in which medical experts linked increases in mortality to these severe events. The most infamous of these occurred in the Meuse Valley, Belgium (1930), Donora, USA (1948), Pozo Rico, Mexico (1950) and London, England (1952). An estimated 4000 excess deaths occurred from the 1952 London fog incident that were associated with angina, suggesting a cardiovascular susceptibility. Moreover, an ordinance passed in Pittsburgh (1946) against air pollution may have been the first of its kind in the United States, though there was little scientific data to give the directive credence (14). Work since the 1950s has become very sophisticated requiring multidisciplinary teams involving aerosol engineers, physiologists and molecular biologists to understand how the mechanism by which pollutants effect human health.

Now in the 21st century, the emissions have become more varied in both composition and locality. While coal-derived emissions were initially limited to the Western civilization, they have lost their prevalence in the west and are more abundant elsewhere (e.g. China, India, Vietnam, etc.). In the United States, emissions are as much by petroleum combustion engines as coal combustion power plants as well as from other industrial emissions. Additionally, with the rampant spread of tobacco smoking in the 20th century, the world's smoking population has reached one billion users (15, 16). Tobacco smoke, auto exhaust, and industrial emissions (including coal, wood smoke, etc.) are the most

prevalent sources for human benzene exposure (17). The intensity of pollution will depend on the types of sources unique to an area (personal / commercial vehicles, industry), the density of those sources, and the emission rate of those sources, as well as by prevailing weather conditions and geography.

Accordingly, the very definition of “air pollution” is somewhat broad - “The presence in or introduction into the air of harmful or poisonous substances, especially as a result of human activity,” according to the Oxford English Dictionary. While this umbrella definition covers any noxious air pollutant constituents, as described (supra vide) the development and availability of technology to understand the composition of our own atmospheres has progressed at a surprisingly rapid rate allowing aerosol scientists and technologists to detect and quantify the concentration of thousands of chemicals in the air. The presence of large air monitoring networks and access to health outcomes allows epidemiologists to assess pollutant exposure levels of millions of individuals both at home and at work, and to assess the degree to which pollutant exposure is associated with different health outcomes. Before these networks became available there were no quantifiable toxicological approach to assess the dose-response of pollutants. For instance, during the tragic London fog incident of 1952, it is reported that 12,000 people died and 100,000 were laid ill by the pollution and stalled weather patterns around downtown London. Thousands of tons of black soot, particulates, sulfur dioxide were suspended in the air due to substantial coal combustion from factories along the river Thames. The PM₁₀ (particulate matter >10µm in diameter) concentrations were estimated

to be between 3,000 and 14,000 $\mu\text{g}/\text{m}^3$, but there was no accurate method in place for measuring this fraction at the time (18, 19). While the increased rate in mortality accompanying the fog was undeniable, no subtle changes in health status seemed verifiable. A similar 1948 incident in the small town (pop. 12,000) of Donora, Pennsylvania led to an estimated 20 casualties and 6,000 cases of respiratory and cardiovascular distress – half of the town. Incidents like this led to the passing of the Air Pollution Control Act of 1955 by the US congress, citing that air pollution is a national priority, but it left the interpretation and enforcement of this up to the states. This act did, however, pave the way for the Clean Air Act of 1963 which is considered to be the most influential and comprehensive air quality laws in the world (20). Given the minimal quantitative evidence available at the time, this was a notable endeavor. Not surprisingly therefore, the capacity to measure discreet constituents of air pollution and monitor their effect on human health has led to increased regulation. Six of the most monitored inhalable contaminants in the United States (by the Environmental Protection Agency [EPA]) are particulate matter, ozone, carbon monoxide, lead, sulfur dioxide, and nitrogen dioxide. While particularly problematic pollutants may vary from region to region, it has become evident that the sum of their actions is negative. The World Health Organization estimates that 1.5 billion people are exposed to hazardous elevated levels of pollution on a daily basis (21). Furthermore, seven million deaths are attributed to air pollution and each year with 200,000 of those deaths in the United States (22).

Many air pollutants are associated with negative effects on cardiovascular health. For instance, one of the EPA's closely monitored pollutants, fine particulate matter (PM_{2.5}), has an aerodynamic diameter small enough to be easily inhaled and can lodge deep in the lungs where it can stimulate an inflammatory response just prior to the left atrium and ventricle or translocate across the alveoli of the lungs into the circulation and interact directly with the endothelium. Rigorous epidemiological studies, along with laboratory research, have shown that increases in PM_{2.5} is associated with premature death in vulnerable populations (with cardiovascular disease [CVD] or lung disease), myocardial infarction, arrhythmia, aggravated asthma, decreased lung function and inflamed airways (23-25). Additionally, 80% of the total PM_{2.5} mortality is due to CVD (26). People with CVD, lung disease, or who are children or elderly are the most affected populations. Ultimately, research shows that for every 10µg/m³ of urban PM_{2.5} the mortality ratio rate (RR) is 1.13, demonstrating a strong correlation between pollution levels and mortality (27, 28).

Another closely monitored pollutant is ozone. Ozone appears in the stratosphere ("ozone layer") and in the troposphere (the lowest layer of the Earth's atmosphere). "Nose level" ozone, that of the troposphere, is what agencies monitor to assess health impacts. Troposphere ozone contributes to presence of angina, airway inflammation, reduced lung function, emphysema, and throat irritation (29-31). An evaluation between daily mortality counts and ambient ozone concentration in 95 large U.S. communities over the period of 1987-2000 found a 0.5% overall excess risk in non-accidental daily mortality for

each 20 ppb ozone increase in the 24-hour average ozone concentration the same day and a cumulative 1.04% excess risk for each 20 ppb increase in the 24-hour average concentration during the previous week (32). This finding was significant even after controlling for confounders like particulate matter or other pollutants.

Other closely monitored constituents like carbon monoxide (CO) reduce capacity for blood to deliver oxygen to tissues by competitively binding to hemoglobin over oxygen (O₂). This hypoxic state primarily affects the cardiovascular and nervous systems. Furthermore, CO is generated by the incomplete combustion of fossil fuels (making CO rather than CO₂) and is frequently emitted from automobile exhaust. Nitrogen dioxide (NO₂), another byproduct of fossil fuel combustion is a major cause of acid rain (along with sulfur dioxide) and greatly inflames bronchial airways, making populations with a pulmonary or cardio-pulmonary susceptibility at greater risk for complications (33). Understanding how these pollutants act alone, as well as in mixed model, real world scenarios will help to elucidate the true impact of these chemicals on population health.

Pollutants such as benzene, though ubiquitous in urban and rural environments (from the National Human Exposure Assessment Survey [NHEXAS]), are rarely monitored and thus it is difficult to ascertain the effect of these under-monitored chemicals on populations. While benzene for instance is known to be a carcinogen, it is unknown what, if any cardio-metabolic effects this pollutant might have. While a concomitant increase in the atmosphere is

corresponds to an increase in CVD, diabetes and obesity is difficult to conclude causation from these trends. However, molecular evidence supports a biological plausibility that benzene could cause low-grade inflammation and associated pathologies (i.e. CVD, diabetes). But because of limited monitoring resources, assessing the effect of under-monitored chemicals on health will most probably have to rely first on animal exposure studies to elucidate possible causality, before large scale human monitoring is implemented.

While the aforementioned pollutants are primarily generated by industrial and automotive activities, and accordingly monitored in public spaces, personal atmospheres may be further polluted through tobacco smoking activities. Environmental tobacco smoke (ETS) is an amalgam of pollutants known to have serious health consequences. Cigarette smoke contains roughly 4,000 different chemicals (34, 35). Solid particulates make up to 10% of tobacco smoke, while the rest is considered gases and aerosols. One of the major gases present is carbon monoxide, along with formaldehyde, acrolein, ammonia, nitrogen oxides, pyridine, hydrogen cyanide, vinyl chloride, N-nitrosodimethylamine, acrylonitrile and benzene. ETS comprises both the main and side streams of cigarette smoke. Frequency and volume of puffs, as well as the intensity of the “pull” on the cigarette contribute to the effect of the main stream cigarette smoke. The constituents of tobacco smoke will vary according to brand and country of origin. In 2009, the Family Smoking Prevention and Tobacco Control Act was signed into law giving the Food and Drug Administration (FDA) the authority to regulate the constituents of tobacco smoke found to be harmful. The FDA wishes to

collect more data on these harmful and potentially harmful constituents (HPHCs) of tobacco smoke in order to make safer cigarettes (36). One of these HPHCs is benzene, known to be a carcinogen and reproductive toxin, but suspected to be a cardiovascular toxicant as well. Thus, on account of the negative associations found with benzene and products containing benzene, there has been a desire to know more about industrially- and personally-generated benzene exposure.

Benzene

Chemical Description

Benzene is a clear, colorless aromatic hydrocarbon with an idiosyncratic sweet odor with olfaction detection at about 60ppm and olfaction recognition at approximately 100ppm (37). Gustation detection for benzene happens somewhere between and 4.5 ppm in solution for most people (37). Benzene contains 92.3% carbon and 7.7% hydrogen, with the molecular formula of C_6H_6 and molecular weight of 78.11 g/mol. The benzene molecule is the simplest of all aromatic hydrocarbons and can therefore be a source for the production of all other aromatic hydrocarbons. A further description of benzene's physical and chemical characteristics can be found in Table 1.

Benzene, the word, is derived from "gum benzoin" (a.k.a. benzoin resin) which is an aromatic resin. This resin has been used by European perfumers and pharmacists since the 16th century when it was made available from Asian trade routes. Benzoin resin was processed via sublimation to obtain benzoic acid and was known at the time as "flowers of benzoin" (38). Benzene

Table 1. Physical characteristics of benzene.

Characteristic	Information
Chemical	Benzene
Synonyms	Annulene, benzeen (Dutch), benzen (Polish), benzol, benzole; benzolo (Italian), coal naphtha, cyclohexatriene, fenzen (Czech), phene, phenyl hydride, pyrobenzol, pyrobenzole
Chemical formula	C ₆ H ₆
Molecular Weight	78.11
Color	Clear, colorless
Physical state	colorless to light yellow liquid
Melting point	5.5°C
Boiling point	80.1°C
Density at 15°C, g/cm³	0.8787
Odor	Aromatic
Odor Threshold	
Water	2.0 mg/L
Air	Detection: 61ppm Recognition: 97ppm
Conversion factors	1ppm = 3.26mg/m ³ at 20°C and 1atm pressure 1mg/m ³ = 0.31ppm

Physical characteristics of benzene related to molecular weight, melting point, and sensory detection levels.

was first isolated by the well-known English chemist Michael Faraday in 1825 from a substance known as “illuminating gas,” that was a mixture of hydrogen and hydrocarbon gases produced by destructive distillation of bituminous coal (or peat) commonly used at the time (39). Nine years later in 1834 the German chemist Eilhardt Mitscherlich developed another method for isolating benzene by heating benzoic acid with lime to produce benzene molecules. Yet another isolation technique using the more abundant coal tar was later developed by another German chemist A.W. von Hofmann in 1845 (40, 41). The structure of benzene was unknown at this point and would remain so until the mid-1860s when German chemists Joseph von Loschmidt and August Kekulé would independently propose the six carbon, cyclic arrangement with alternating single and double bonds. August Kekulé allegedly derived his inspiration for the benzene structure from the appearance of an ouroboros (i.e. a snake eating its own tail) in a dream that suggested the cyclic form of benzene (42). Of course the notion for this only gained credulity because of the rigorous experiments performed interrogating isomer derivatives of benzene. In 1929, the British X-ray crystallographer Kathleen Lonsdale confirmed that benzene had a single structure, composed of a resonance hybrid of August Kekulé’s cyclic, alternating double bond theory (43). Studies employing X-ray diffraction show benzene to be a planar structure with each carbon-carbon bond distance equal to 1.4 angstroms (Å).

Industrial and Commercial Uses

Benzene has many industrial and consumer uses. Industry employs benzene in adhesives and sealant chemicals, fuels and fuel additives, ion exchange agents, laboratory chemicals, plastics, processing aids and solvents (for cleaning or degreasing). Consumer products such as adhesives and sealants, automotive care products, cleaning and furniture care products, fuels, lubricants, greases, paints and coatings, plastic and rubber all typically involve benzene at some point in the production stage (17, 44).

Globally, approximately 30% of commercial benzene is produced by catalytic reforming. This process involves aromatic molecules being produced from dehydrogenation of cycloparaffins, hydroisomerization of alkyl cyclopentanes and the cyclization and subsequent dehydrogenation of paraffins (45).

Early uses of benzene were found in rubber solvents in mid to late 19th century Germany. Rubber solvents were a crucial part of making bicycle, wagon and automobile tires as well as canning seals. Benzene was such an effective solvent that it was used in most all rubber industry processes. Benzene continues to be used in manufacturing, notably in rubber, glue, and plastics industries. It is one of the top 20 chemicals produced by volume in the United States (46). Benzene is also found in crude oil petroleum and as such constitutes a sub-fraction of the raw products derived from deep drilling processes. Consequently, benzene is present in gasoline/petrol used for automotive engines. The absolute percent composition of benzene in end product

gasoline varies by country depending upon local law. In the United States, it is found at approximately 1% v/v in gasoline.

While benzene is an intentionally sourced and used chemical, it is often found in society as a combustion byproduct. Benzene is emitted from auto exhaust, coal and wood burning and from tobacco smoke. Tobacco smoke is the greatest source of benzene exposure for humans (47). This is driven by the relatively high concentration of benzene in cigarette smoke (35-70 ppm), though this varies by cigarette brand and smoking behavior (48). Tobacco smoke is such an abundant source of exposure to humans because of the overwhelming prevalence of tobacco smokers in the world. The World Health Organization (WHO) and the Journal of the American Medical Association (JAMA) have independently reported that there are approximately one billion smokers in the world, approximately 1 in 7 persons, globally (15, 16). Given that smokers expose individuals around them to benzene; it is not surprising that this is the primary source of benzene exposure in humans. However, tobacco smoke is not the primary source for anthropogenic benzene being released into the total environment though it does typically generate the most concentrated atmospheres of benzene in personal environments. Industrial emissions account for the greatest volumetric release of benzene at 3,500 tons per year in the US alone (49). Additionally, combustion engine exhaust contains volatile benzene and this is the second major source of exposure for humans. Benzene levels near roadways are elevated compared with up-wind measurements (50). Additionally, assessment of benzene within the cabin of automobiles during

driving has shown a 100% increase in ambient concentrations (51). These levels increase sharply in poorly ventilated areas. One study of a Los Angeles freeway tunnel measured ambient benzene at a level of >1000 ppm in the midst of rush hour traffic (52). Thus, urban benzene levels can vary greatly depending on ventilation, the concentration of benzene emitting sources and weather patterns that allow for or deprive areas of dispersing and diffusing movement of air. Benzene can also be found in the natural environment. Volcanic eruptions, forest fires and other sources of combusting carbon derived substances.

It is not uncommon in some industries to be exposed to high levels of benzene. The United States' Occupational Safety and Health Administration (OSHA) has established limits of acceptable occupational exposure loosely based upon health research findings. The exposure limits set by OSHA have a legal authority, meaning there's much greater incentive to follow OSHA guidelines (53). The National Institute for Occupational Safety and Health (NIOSH), a separate US government organization, also releases suggested thresholds for occupational exposure limits. However, NIOSH recommendations are not legally enforceable (54). NIOSH limits are often somewhat lower than OSHA's terms. For example, the 40h time weighted average (TWA) permissible exposure limit (PEL) is 1 ppm, whereas the NIOSH recommendations are 0.1 ppm for a 40h TWA PEL. The OSHA 15 min short term exposure limit (STEL) is 5 ppm whereas the NIOSH STEL is 1 ppm. One of the reasons for the conflicting limits between the two agencies stems from NIOSH's ability to update its recommendations based on current research findings without consideration of

costs to implement such changes in industrial practices. The OSHA guidelines are often said to target optimally reduced exposure levels while balancing practicality of implementation. Of note for contextual purposes, benzene concentration in main stream cigarette smoke is approximately 7 – 12 times the OSHA STEL. In 2009, FDA was granted authority to regulate the constituents of tobacco smoke and this will likely decrease the abundance of benzene in cigarettes. That said, no safe level of benzene exposure has been determined. The most frequently researched health outcome associated with benzene exposures is leukemia, and the rate of disease incidence appears to decrease in a linear fashion with ambient benzene reduction. Even at 0.3 ppb there is an excess lifetime cancer risk of 1 in 1,000,000 (55). However, this is a model-generated approximation and as benzene is rarely monitored even in metropolitan regions or in occupational environments where benzene exposure is likely, it is difficult to approximate the true impact of exposure on health.

Benzene Absorption, Distribution, Metabolism and Excretion

The toxicokinetics of benzene have been extensively studied. While inhalation exposure is the primary route of exposure, dermal and oral exposure can occur as well. However, inhalation exposure is most frequent. Absorbed benzene is rapidly distributed throughout the body and whatever is not quickly metabolized, accumulates in adipose tissues. The liver is the primary site of benzene metabolism into metabolites with various levels of reactivity. It is well known that benzene exposure is toxic and that this toxicity is dependent upon its

metabolism. However, no single metabolite has been found to be the major source of the characteristic hematopoietic and leukemic effects of benzene. At low exposure levels, benzene appears to metabolize quickly and is excreted via conjugated urinary metabolites. At high exposure levels, metabolic processes appear to be saturated and parent compounds may be excreted through exhalation. The hypothesis that benzene is rapidly absorbed is supported by results from a 23-person study who inhaled 47 – 110 ppm volatile benzene for 2 – 3h. These participants showed absorption was highest in the first 5 – 10 min of the experiment and then rapidly decreased. The first 5 min of exposure demonstrated 70 – 80% absorption, but this was decreased to 50% by 1h (56). This latter result was confirmed in a study of 6 volunteers exposed to 52 – 62 ppm benzene. Volunteers displayed 47% absorption after 4h of 52-62ppm exposure (57). Individuals exposed to a lower concentration (1.6 or 9.4 ppm) for 4h had 48% respiratory absorption at 9.4 ppm and those exposed at 1.6 ppm exhibited 52% respiratory absorption (58). Benzene exposure in cigarette smoke showed a similar 64% absorbance rate at concentrations of 32 – 69 ppm benzene (48).

Most data for benzene distribution in humans comes from case studies. These data suggest benzene is distributed throughout the body following blood absorption. Benzene deposits at a high rate in adipose tissue, which is in keeping with the lipophilic nature of the molecule, though it will be found elsewhere. Two studies have found benzene to be almost equally present in the blood and liver while brain contains nearly twice that of liver or blood (59, 60).

Benzene has been found to cross the placenta and is measurable in cord blood in concentrations equal to or greater than maternal blood (61). Benzene binds to plasma proteins and benzene metabolites can form covalent adducts with proteins from human blood and mice (62). However, adduct formation does not appear to prevent benzene distribution to other areas of the body. Furthermore, while benzene preferentially deposits in adipose, tissue concentrations will also depend on blood perfusion rate to the tissue (possibly explaining the high concentration in the brain).

Benzene achieves different equilibria in different tissue compartments. One experiment with rats exposed to 500 ppm benzene found that benzene stopped increasing in concentration in the bone marrow and blood 2 and 4h, respectively, after exposure indicating saturation. Supporting this, benzene metabolites phenol, catechol and hydroquinone (HQ) have been detected in the blood and bone marrow 6h after exposure, though metabolite concentrations were significantly higher in bone marrow (63). A study of dogs exposed to benzene at 800 ppm x 20d found 20 times more benzene in adipose, bone marrow and urine than blood (64).

Prior to metabolism, benzene is not toxic. However, most mammalian species express at least one isoform of the enzyme responsible for benzene metabolism. This enzyme is known as cytochrome P450 2E1 (CYP2E1). The majority of benzene metabolism occurs in the liver and centers on the formation of ring hydroxylated compounds. Early work attempting to delineate pathways of benzene metabolism showed hydroxylation of benzene to catechol, phenol,

hydroquinone and 1,2,4-benzenetriol (65-67). These hydroxylated metabolites are excreted as glucuronides and ethereal sulfates in the urine. However, the most commonly used, and debatably the most sensitive urinary metabolite currently used in assessing benzene exposure is *trans,trans*-muconic acid (*t,t*-MA). The production of *t,t*-MA involves a ring opening step to create *trans,trans*-muconaldehyde (68, 69). This was most convincingly established by Parke and Williams who exposed rabbits to [¹⁴C]benzene and were able to reliably detect and measure [¹⁴C]*t,t*-MA in the excreted urine (66).

The two pathways, ring hydroxylation and ring opening have been confirmed in other species (70-73). The hydroxylated compounds are broken down to sulfate conjugates and glucuronides and are often termed “detoxification products” because the conjugation leads to elimination and inhibits the generation of toxic intermediates (derived from hydroxylated benzene metabolites). A less abundant metabolite is S-phenylmercapturic acid (SPMA), which is a glutathione (GSH) conjugate. These metabolites act as a mechanism to detoxify the reactive benzene oxide, the first benzene metabolite to be formed. Additionally, *t,t*-muconaldehyde is converted to a less reactive metabolite (*t,t*-MA).

Available human data suggest that exhalation is the primary route of excretion for unmetabolized benzene (74). However, metabolized benzene in the form of phenol, SPMA, HQ and *t,t*-MA is excreted through the urine. Human studies showing respiratory excretion of unmetabolized benzene at 16-40% after 2-3h of 47-110 ppm benzene exposure also show that only 0.07-0.2% of unmetabolized benzene is excreted through the urine (56, 75). Thus, the

remainder is largely metabolized with a small portion of the benzene being deposited in lipid substances. Subsequently these excreted conjugate metabolites are used to monitor benzene exposure. Urinary phenol in workers exposed to 1-200 ppm benzene showed a 0.881 correlation coefficient with benzene exposure levels (76). Consequently, SPMA and *t,t*-MA are also frequently used markers of exposure with *t,t*-MA being demonstrated to be a reliable biomarker of low dose benzene exposure (77).

Role of CYP2E1 in Benzene Metabolism and Toxicity

As seen in Figure 1, the first step in benzene metabolism involves the CYP2E1 catalyzed oxidation of benzene to benzene oxide (78). Benzene oxide is in equilibrium with benzene oxepin (79). While several pathways are involved in benzene metabolism, CYP2E1 is the most frequently involved enzyme. The predominant pathway in benzene metabolism then involves non-enzymatic rearrangement to form phenol (80). Phenol is oxidized in the presence of CYP2E1 to catechol or HQ, and these metabolites are further oxidized by myeloperoxidase (MPO) to 1,2- and 1,4-benzoquinone (BQ) (81). This reaction is reversible, the metabolites 1,2- and 1,4-BQ are reduced to catechol and HQ, respectively, by NAD(P)H;quinone oxidoreductase (NQO1) (81). Additionally, catechol and HQ can be converted to 1,2,4-benzenetriol via CYP2E1 catalysis. Each of the phenol-derived metabolites can undergo glucuronic or sulfate conjugation (81, 82). Other pathways involved in benzene oxide metabolism involve reaction with glutathione (GSH) to form SPMA (70, 81), and the iron

catalyzed ring-opening conversion to *t,t*-MA, presumably by the *trans,trans*-muconaldehyde intermediate (81, 83).

In studies using products of CYP2E1 it has been found that significant oxidative stress and corresponding hepatotoxicity occurs. In fact, effects such as ethanol-induced liver injury seem to be largely driven by CYP2E1-derived oxidative stress. To understand the effects of this enzyme we should outline the background of the family of cytochrome P450 enzymes. The cytochrome P450 enzymes (or CYPs) are considered a super family of heme proteins acting as terminal oxidases in a mixed function oxidation system that metabolize many endogenous and exogenous substrates (e.g. steroids, fatty acids, xenobiotics, drugs, toxins) (84). CYPs are present in nearly all organisms and a nomenclature was developed for the P450 family based on the sequence identity of different enzymes (85, 86). CYPs are involved in mono-oxygenation, peroxidation, reduction, de-alkylation, dehalogenation, and epoxidation (87-89). Enzymes of the P450 family convert non-polar compounds into more polar metabolites that are easily excreted, conjugated with phase II enzymes into extractable metabolites.

Necessary for enzymatic function of CYPs is oxygen activation and this can result in production of ROS. Oxygenated P450 complex can form superoxide anion radicals (O_2^-), while decay of peroxy P450 -complex or dismutation of O_2^- may form hydrogen peroxide (H_2O_2) (90-92). The ROS are

Figure 1.

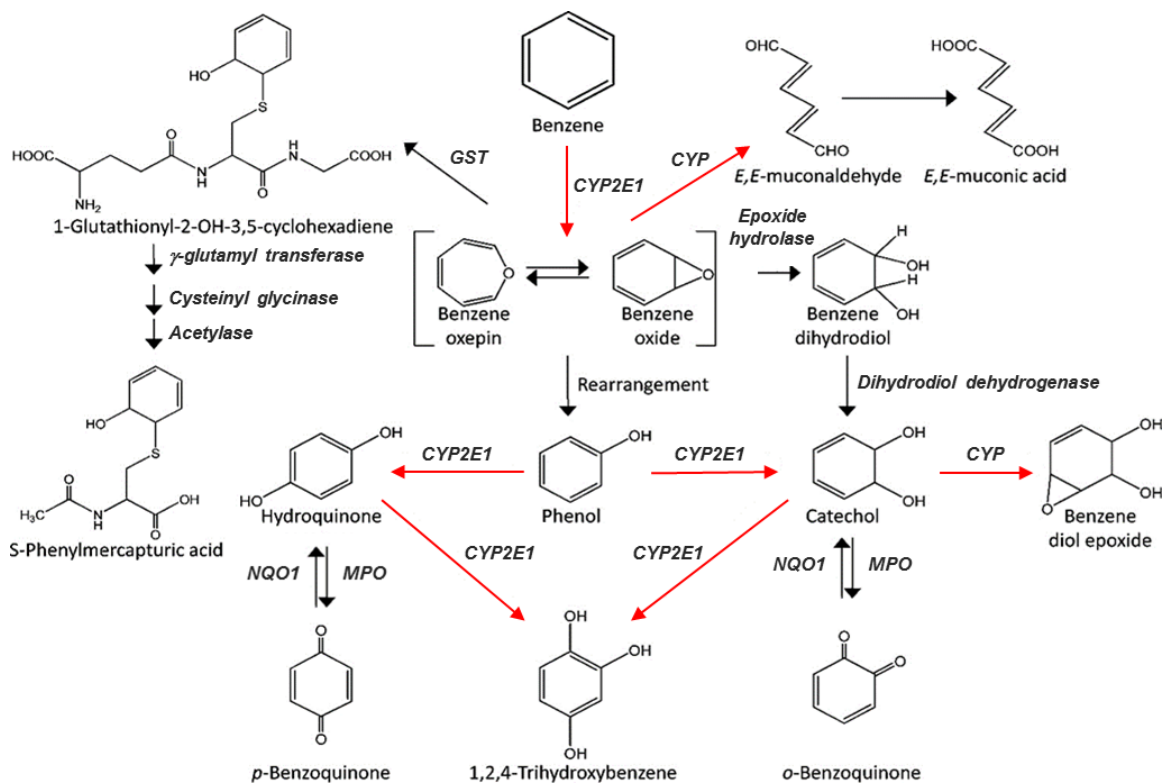


Figure 1. Schematic of benzene metabolizing enzymes and metabolites.

Benzene is first metabolized by *CYP2E1*, yielding benzene oxide which is in equilibrium with benzene oxepin. Either of these molecules may undergo spontaneous rearrangement to form phenol. Phenol is then further metabolized by *CYP2E1* to form hydroquinone or catechol. Hydroquinone and catechol can be further metabolized by *CYP2E1* to produce 1,2,4-Trihydroxybenzene. Hydroquinone can also be metabolized into *p*-benzoquinone by *MPO*, and *p*-benzoquinone can be cycled back to hydroquinone by *NQO1*. Catechol can also be metabolized by *MPO* to generate *o*-benzoquinone, and this can be cycled back to hydroquinone by *NQO1*. Catechol may also be metabolized to benzene diol epoxide. Additionally, the generation of *E,E*-muconaldehyde from benzene oxide may then be further metabolized into *E,E*-muconic acid, which is the most frequently measured benzene metabolite. Benzene oxepin is metabolized by *GST* to 1-Glutathionyl-2-OH-3,5-cyclohexadiene that is further metabolized to S-phenylmercapturic acid.

implicated in many major disorders such as ischemia-reperfusion injury, atherosclerosis, diabetes and inflammation (93-97). ROS generation from the CYP450 family of enzymes is well-documented (92, 98). ROS become toxic to cells because they react with most cellular macromolecules. This causes protein denaturation, DNA damage (e.g. breaks, adducts, etc.), DNA base removal or modifications that result in mutation, peroxidation of lipids (membrane damage and production of 4-hydroxynonenal [4-HNE] and malondialdehyde [MDA]) (99, 100). Many mechanisms (enzymatic and not) have evolved that confer protection of cells from ROS. Examples include catalase and GSH (peroxidase) that removes H_2O_2 ; superoxide dismutases removal of O_2^- ; GSTs removal of reactive intermediates and lipid aldehydes as well as thioredoxin, metallothioneins, heme-oxygenases and other enzymes (101, 102). Therefore, oxidative stress or ROS toxicity lies in the imbalance in rates of ROS production compared with ROS sequestration by anti-oxidant mechanisms along with rate of repair to cellular macromolecules. However, low levels of ROS can be crucial to homeostatic signaling transduction and cellular physiology (103).

CYP2E1 is a key player in hepatic injury after exposure to its substrates (e.g. benzene, EtOH, acetaminophen). *In vitro* studies with HepG2 cell lines demonstrated increased oxidative stress and mitochondrial damage by addition of polyunsaturated fatty acids (PUFAs), EtOH, iron or depletion of GSH (104). Additionally, oxidative stress induced by exposure to EtOH was reduced in CYP2E1KO mice (105). Molecular oxygen is an important substrate for CYP2E1, as relative to other CYP enzymes. CYP2E1 demonstrates high NADPH oxidase

activity and is loosely coupled with NADPH cytochrome P450 reductase (106, 107). CYP2E1 has been shown to be a highly efficient initiator of NADPH-dependent lipid peroxidation.

CYP2E1 can be induced by many factors, and many of the substrates of CYP2E1 can induce their own metabolism (108, 109). Metabolic conditions may also induce CYP2E1. In chronically obese, high-fat diet fed rats, CYP2E1 levels were found to be elevated (110). Also, CYP2E1 has been found to be elevated with long term fasting or starvation in rats (111, 112). Diabetes has been shown to increase CYP2E1 mRNA and protein levels several fold (113). Additionally, this may be influenced by insulin bioavailability as insulin has been shown to decrease CYP2E1 expression at post-transcriptional levels *in vitro* (rat hepatoma cell line) (114, 115). Correspondingly, hepatic CYP2E1 expression is increased in rats by streptozocin.

Data have been accumulated to support the involvement of CYP2E1 in the oxidation of benzene. Quite notably is the protection from any detected toxicity in CYP2E1^{-/-} (or CYP2E1KO) mice after exposure to 200ppm benzene 6h/d for 5d. The wild type animals in this study experienced severe cytotoxicity and genotoxicity. Pretreatment of mice with pan-CYP inhibitors decreased benzene metabolite formation and resulting genotoxicity (determined by alkaline comet assay) in benzene-exposed mice. Additionally, CYP2E1KO mice showed a greater than 90% reduction in formation of benzene metabolites like phenol, catechol and HQ after benzene exposure (116-118). Conversely, CYP2E1 inducers (3-methylcholanthrene and β -naphthoflavone) increase benzene

metabolism and benzene clastogenicity (chromosome breakage) (119). Furthermore, to validate toxicological murine studies involving CYP2E1, humanized CYP2E1 transgenic mice were compared with wild type mice. This study found substrate metabolism rate and capacity by human and murine isoforms of CYP2E1 to be similar *in vivo* (120). Occupationally, exposed workers with a phenotype associated with rapid CYP2E1 metabolism demonstrated increased susceptibility to benzene hematotoxicity when compared with slowly metabolizing isoforms (121). CYP2E1 is the primary catalyzing enzyme of benzene metabolism, though CYP2B1 and CYP2F2 may also play minor roles (<5% of benzene metabolism) (122-127). Additionally, ethanol (EtOH) and aniline are metabolized by CYP2E1 and are inducers of CYP2E1 expression. CYP2E1 is also associated with the generation of hydroxyl radicals, likely by excess cycling (126-129). The hydroxyl radical formation by CYP2E1 may also be involved in the benzene ring opening pathway, yielding *trans,trans*-muconaldehyde. Metabolites phenol, HQ, BQ and catechol can increase CYP2E1 expression in humans (130). Therefore, increased susceptibility to benzene exposure may occur if one is exposed to chemicals that induce CYP2E1 expression or activity. The induction of CYP2E1 by benzene (and its metabolites) with succeeding generation of oxygen and hydroxyl radicals is likely to be associated with known toxicities of benzene exposure (129, 131-139).

A growing body of evidence suggests that CYP2E1-mediated toxicity is largely driven by oxidative stress. For example, treating CYP2E1 expressing HepG2 cells with EtOH or arachidonic acid (CYP2E1 substrates) results in

increased oxidative stress as reflected by increased lipid peroxidation and increased dichlorofluorescein fluorescence. Low levels of arachidonic acid and other substrates acted as sensitizing factors. Moreover, treatment with antioxidants like vitamin E, trolox or ascorbic acid prevented toxicity in this cell line and similar results have been reported elsewhere (140-143). Additionally, CYP2E1-expressing cell lines generally show increased levels of antioxidant enzymes such as GSH, catalase, and heme-oxygenase. This may be an evolved, self-regulating mechanism to mitigate oxidative stress and is likely triggered by oxidant stimuli. Further regulation has been seen when this increasing expression of anti-oxidant enzymes is inhibited by treatment with exogenous anti-oxidants. Functionally this proved adaptive as these cells were less susceptible to oxidative stress mediated damage after exposure to H₂O₂, MDA or 4-HNE (144, 145).

A common model for CYP2E1-dependent oxidative stress and subsequent toxicity involves the following. Increasing CYP2E1 expression is induced by presence of substrates, likely via post-transcriptional mechanisms involving enzyme stabilization against degradation. CYP2E1, which is a loosely coupled enzyme, generates ROS (e.g. H₂O₂, O₂⁻, etc.) during the catalytic cycle. The presence of iron causes stronger oxidants to be formed (i.e. ferryl species, hydroxide species, and 1-hydroxyethyl radicals). Following this, hepatic cells induce expression of anti-oxidant enzymes as a response to perceived oxidative stress. However, these elements are overwhelmed in time and CYP2E1 generated oxidants begin to have their effect. Toxicity may be due to cell

membrane damage by lipid peroxidation and production of lipid aldehydes, damage to DNA or by protein oxidation and enzymatic inactivation. Mitochondria are also likely to be damaged by CYP2E1 oxidants, that is the decrease of the mitochondrial membrane potential ($\Delta\psi_m$) driven by increased mitochondrial membrane permeability stimulating pro-apoptotic pathways. Decreased ATP production could induce necrosis. Many CYP2E1 generated ROS can leave hepatocytes and influence nearby cells, stimulating collagen production and a fibrotic response (146, 147). Inevitable inflammation and cell damage occurring during this process exacerbates hepatocyte sensitivity as cells with increased CYP2E1 activity were sensitized to $TNF\alpha$ mediated cell death (148), suggesting a dangerous positive feedback loop.

Hepatic Inflammation and Insulin Resistance

Summary of Hepatic Insulin Resistance and Pathology

Chronic inflammation induces insulin resistance in the liver. Long term inflammation corresponds with and is driven by increased levels of cytokines (e.g. $MIP-1\alpha$, $IL-1\beta$, $IL-6$, $TNF-\alpha$) and/or adipokines (e.g. leptin and resistin). Cytokines inhibit insulin signaling in the liver by production and activation of suppressors of cytokines (SOCS) proteins, kinases (e.g. $IKK\beta$, PKC) and protein tyrosine phosphatases (e.g. PTEN). These factors inhibit insulin signaling at insulin receptor and insulin receptor substrate (IRS) locations. This impairment can decrease glucose production by insulin in liver cells and can trigger

hyperglycemia. Initial incidence of hepatic insulin resistance is concomitant with the increased production of hepatic VLDL that occurs through changes in apoB synthesis and degradation and *de novo* lipogenesis, or increased free fatty acid flux from adipose to liver. Insulin resistance often stimulates the production of C-reactive protein (CRP) and PAI-1, which are markers of inflammation. These abnormalities in liver insulin signaling tend to promote atherosclerosis. Elevated glucose levels promote endothelial dysfunction and changes in the extracellular matrix, increased cell proliferation and impairment of LDL receptor mediated uptake resulting in decreased clearance of LDL. A subset of the LDL fraction, small dense LDL (sdLDL) has a higher affinity to intimal proteoglycan driving increased infiltration of LDL particles into the arterial wall.

The liver plays a key role in metabolism throughout the body involving protein, carbohydrate and lipid utilization as well as xenobiotic break down and detoxification. The liver is integral to processes such as glycogenolysis, gluconeogenesis, glycogenesis, lipogenesis, cholesterol synthesis, coagulating factor production (e.g. fibrinogen), conversion of ammonia to urea, synthesis and excretion of bile, plasma protein production, and synthesis of inflammatory proteins (149). Several of these functions are rigidly controlled by hormones such as insulin, a circulating molecule with widespread effects on metabolism throughout the organism. This hormone facilitates glucose utilization (especially in skeletal muscle and adipose tissues) and inhibits hepatic glucose production by blocking glycogenolysis and gluconeogenesis. Insulin is central to additional cellular processes like protein production, synthesis and storage of lipids, cellular

growth, differentiation and proliferation (150). In an insulin resistant phenotype, standard levels of insulin are no longer able to affect a response in liver, muscle and adipose tissues. The location of the insulin resistance may produce changes in how the phenotype presents. Insulin resistance in liver tissue impairs glycogen synthesis, increases glucose production, lipogenesis and protein synthesis. Insulin resistance in skeletal muscle diminishes glucose uptake and insulin resistance in adipose tissue increases hydrolysis of triglycerides resulting in elevated plasma free fatty acid levels (151). Combined, this produces a phenotypical display of hyperglycemia, hyperinsulinemia, and hyperlipidemia – hallmarks of type 2 diabetes mellitus (T2D) and pre-diabetes.

The terms insulin resistance, metabolic syndrome and syndrome x are often used in a nearly interchangeable manner. However, while insulin resistance is often highly associated with dyslipidemia, obesity, hypertension, and increased urinary albumin, insulin resistance is defined in terms of glucose intolerance and insulin resistance. Metabolic syndrome is defined by presence of insulin resistance along with at least two of the other maladies listed (152-154). Inflammatory markers have been proposed as additional markers to identify this process. The prevalence of insulin resistance or metabolic syndrome varies widely by culture, geographic region and often by gender. Comparing disparate groups across the globe, one sees prevalence rates of insulin resistance as high as 53% in Polynesian men (living in New Zealand) but as low as 6% in Chinese women (living in China) (155, 156). Within a cultural or geographic group, prevalence rates of insulin resistance will vary by sex. The prevalence of insulin

resistance in women is lower than men for Hispanic and Caucasian populations (living in the USA) while insulin resistance is less prevalent in men than women in many regions of Africa and South Asia (157).

Insulin Signaling and Mechanisms for Insulin Resistance

Insulin is a crucial telecrine hormone that controls glucose metabolism throughout most of the body. Insulin facilitates glucose uptake by muscle and adipose tissue, while inhibiting glucose release by liver and is crucial to metabolic homeostasis. Insulin regulates protein synthesis by controlling amino acid uptake and decreasing protein degradation (proteolysis), thus having an anabolic effect. Insulin also controls lipid metabolism by increasing fatty acid synthesis, promoting esterification of free fatty acids and decreasing lipid breakdown (lipolysis). Insulin is also involved in cellular processes such as growth, proliferation, survival and differentiation (158).

The cellular effects of insulin are mediated by a surface membrane protein known as the insulin receptor. Insulin receptor is a heterotetramer expressed on most cells, including liver and skeletal muscle cells. When insulin binds to its receptor, a cascade of events is initiated involving receptor auto-phosphorylation of tyrosine residues, tyrosine phosphorylation of docking proteins such as IRS 1-6, src homology 2 (Shc), Casitas B-lineage lymphoma (Cbl) and GRB-associated binder-1 (Gab-1) that successively trigger downstream signaling molecules. Data from knockout animal models suggest that specific IRS molecules have unique roles in different tissues. In skeletal muscle, pancreatic β cells and

adipose tissue the molecule IRS-1 appears to be the primary mediator of insulin signaling (158, 159). However, IRS-2 is the main mediator for insulin signaling in liver metabolism and β cell proliferation (160) while IRS-3 likely is an important mediator in adipose tissue (161).

Insulin activates three pathways in cells. The pathway of greatest interest is the phosphatidylinositol-3-kinase (PI3K) pathway, which regulates insulin's metabolic effects (glucose, protein and lipid metabolism). Phosphorylated IRS proteins generate binding sites for PI3K that allows for activation of PI3K. PI3K in turn activates kinases such as 3-phosphoinositide-dependent kinase (PDK) (159). Protein kinase B (PKB), also known as Akt (akt8 virus oncogene cellular homolog) and some forms of protein kinase C (PKC) are substrates for PDK (162). Akt regulates the effects of insulin on such things as glucose transport, suppression of hepatic gluconeogenesis, protein synthesis and lipogenesis. A second pathway, the mitogen-activated protein kinase (MAPK) pathway controls the mitogenic growth and cellular differentiation. The third pathway is the Cbl associated/Cannabinoid receptor type 1/G-binding protein TC-10 (CAP/Cbl/Tc10) pathway. This signaling pathway regulates glucose transporter 4 (GLUT4), in muscle and adipose tissue.

Insulin resistance is characterized by the incidence of normal insulin concentrations being unable to sequester circulating glucose in an adequate fashion. That is the pancreatic β cells must secrete more insulin (hyperinsulinemia) to overwhelm the elevated circulating glucose levels (hyperglycemia). Eventually, it is believed, the pancreas cannot secrete sufficient

levels of insulin to maintain homeostatic glucose levels and this inability results in frank T2D.

While much is yet unknown concerning the molecular causation of insulin resistance, it is likely that signaling events downstream from the receptor are the primary causes for insulin resistance (163). Factors such as decreased insulin production and insulin receptor mutations may play a significant role in pathologies at a population level as well. Yet, a great deal of evidence from animal and human investigations supports the model that IR is primarily due to defects in signaling pathways in target tissues. In humans with T2D, decreased auto-activation of the insulin receptor has been observed in skeletal muscle (164). Additionally, down regulation of Akt or PI3K has been reported muscle of obese and lean subjects (165, 166). Thus, reduced levels and decreased phosphorylation of insulin signaling pathways have been described in the tissues of obese and T2D subjects.

There are several hypotheses for how particular mechanisms influence these signaling pathways (167). Down regulation or up regulation of specific components of insulin signaling like Akt, insulin receptor or IRS-2 can induce insulin resistance. However, differential expression of these signaling components will have different global effects depending on the affected tissue (149). A couple of interesting examples include how IRS-1 knockout (KO) mice were described to be insulin resistant, but not hyperglycemic (168) while IRS-2 KO mice were found to be hyperglycemic due to insulin resistance in the liver and β cell secretion failure (169). Other pathways may be influenced through

post-transcriptional modifications that alter the efficiency of the insulin signaling pathway. Kinases such as stress-activated protein kinase, PKC, and c-Jun N-terminal kinase (JNK) can phosphorylate IRS-1,2 at threonine and serine residues, thus inhibiting insulin signaling (170). SOCS proteins (notably SOCS-1,3) are inhibitory factors that influence signal transduction. These proteins block insulin signaling by competing with IRS-1,2 for association with insulin receptor and by increasing IRS-1,2 degradation (171). Insulin resistance could also occur by an increased activity of phosphatases that dephosphorylate transitional signaling molecules. Two major phosphatases involved in this activity are protein tyrosine phosphatase 1B (PTP1B) and phosphatase and tensin homologue (PTEN) (172, 173). It has been reported that PTP1B KO mice are resistant to weight gain and have greater insulin sensitivity when exposed to a HFD (174). Correspondingly, the liver and skeletal muscle tissues of obese, IR and T2D subjects tend to have higher levels of PTP1B than insulin sensitive, lean subjects (175). Liver overexpression of PTP1B in mice demonstrated hepatic and systemic insulin resistance (176). Molecules such as PTEN have been shown to inactivate PI3K via dephosphorylation and the inhibition of PTEN expression has been found to reverse hyperglycemia in diabetic mice (173). Other molecules such as SH2-containing inositol 5' phosphatase-2 (SHIP2) have an inhibitory effect on insulin signaling (177).

Role of Hepatic Insulin Resistance on Glucose Production

In subjects with T2D or IR the hallmark hyperglycemia is typically the result of two factors: peripheral tissue insulin resistance and uninhibited gluconeogenesis/glycogenolysis from hepatic cells resistant to insulin. Hepatocyte production of glucose is typical during the fasting state and inhibited during the fed state in insulin sensitive cells. The regulation of glucose production in the liver occurs by insulin-mediated inhibition of the gluconeogenic enzymes phosphoenolpyruvate carboxykinase (PEPCK) and the glucose-6 phosphatase (G6Pase). Of note, Akt appears to be necessary for the transcriptional inhibition on PEPCK and G6Pase (177). This action involves the phosphorylation of FoxO (a transcription factor), driving cytosolic translocation of FoxO proteins, transcriptional inactivation and thus the inhibition of PEPCK and G6Pase (178).

Impaired insulin signaling molecules in T2D and IR subjects is an expected observation and highly correlates with elevated fasting plasma glucose (FPG) levels. Hepatic insulin receptor knockout animals demonstrate serious glucose intolerance (179), yet deletion of the insulin receptor only in skeletal muscle and adipose yielded normoglycemic and normoinsulinemic levels (180, 181). This indicates that hepatic insulin resistance may play the major role in the development of glucose intolerance and hyperglycemia. Murine experiments utilizing a liver-specific IRS-2 KO model found significant insulin resistance and elevated FPG (160). Additionally, insulin resistant mice with the Foxo-1 gene knocked down had decreased G6Pase levels (182). Collectively, these results

suggest that resistance to insulin action in the liver leads to elevated FPG levels and disease progression towards T2D and CVD.

Dyslipidemia as a Biomarker of Hepatic IR

It was previously discussed that IR, metabolic syndrome and T2D are often associated with dyslipidemia. Data from non-diabetic insulin resistant subjects suggests that IR plays a crucial role in establishment of dyslipidemia (183). This lipid dysregulation is characterized by an increase in LDL and possible increase in triglycerides (TRG) and decrease in HDL (184) and this is thought to be associated with excessive hepatic generation of VLDL1 (185).

Insulin is implicated in this process because it regulates proteins involved in the metabolism of VLDL. Assembly of VLDL begins with lipidation of apolipoprotein B100 (apoB100) by microsomal triglyceride transfer protein (MTP) in the rough endoplasmic reticulum of the liver and this leads to generation of triglyceride-poor VLDL particles (VLDL2) (186) and additionally lipidated to form mature VLDL1 (187). VLDL is secreted from the liver and converted to IDL by lipoprotein lipase in the periphery. IDL is hydrolyzed by hepatic lipase to form cholesterol-rich LDL and is removed by LDL receptor-mediated uptake (185).

One manner in which insulin regulates this process is by inhibiting the rate of apoB synthesis and degradation in hepatocytes (188). Assembly and secretion of VLDL is inhibited by insulin via downregulation of MTP in the liver and enhanced post-translational degradation of apoB (189, 190). Conversely, it has been demonstrated in rat hepatocytes that inhibition of PI3K (part of the

insulin signaling pathway) increases apoB secretion (191-193). Correspondingly, T2D subjects have reduced PI3K activity and PI3K signaling, which leads to elevated VLDL levels (and hyperglycemia) (163). Another mechanism by which insulin may increase circulating lipid levels is by a transcription factor involved in *de novo* lipogenesis. Insulin promotes lipogenesis via increased transcription and activity of sterol response element-binding proteins (SREBP1-c). SREBP1-c controls the expression of several genes regulating the generation and absorption of cholesterol, phospholipids, triglycerides and free fatty acids (194).

Thrombosis and Hepatic IR

IR and T2D are highly associated with states of increased thrombogenic potential. There are many ways in which thrombosis may be dysregulated in IR including platelet hyperactivity, hypercoagulability, endothelial dysfunction and hypofibrinolysis which further contribute to IR's associated increased CVD risk. Nitric oxide (NO) inhibits platelet aggregation and NO bioavailability has been shown to decrease with inflammation and insulin resistance (195, 196). Inhalation of NO protects against human platelet aggregation and overexpression of NO in mice protects against high fat diet induced insulin resistance and weight gain (197, 198). Oxidative stress often drives decreased NO bioavailability and induces inflammation and logically is associated with states of IR and T2D. Additionally, increased PAI-1 has been found in states of IR associated with increased thrombogenicity (199). Human population studies have found that while elevated PAI-1 predicts myocardial infarction, this predictive ability is lost

after adjustment for IR, suggesting that IR may be a requirement for elevated PAI-1 in subjects susceptible to myocardial infarction (200-202). However, the primary source of PAI-1 and the mechanisms tied to inflammation and IR that might regulate PAI-1 are still poorly understood and debated.

Hepatic IR and Inflammation

There are many mechanisms by which inflammation may lead to IR. IRS-1,2, critical members of the insulin signaling pathway, are normally phosphorylated on tyrosine residues when active. Serine (or aberrant threonine) phosphorylation of IRS-1,2 can inhibit their downstream effects, as can the inhibition of their phosphorylation. Additional kinases such as inhibitor of NF- κ B (IKK), PKC and JNK can regulate IR generated by inflammatory factors (203). These kinases can regulate transcription factors such as nuclear factor kappa B (NF- κ B) and activator protein-1 (AP-1) and the transcription factors upregulate inflammatory gene expression (e.g. MIP-1 α , IL-1 β , IL-6, TNF- α). SOCS proteins recruited to negatively regulate cytokines can then also inhibit insulin signaling via competitive binding with IRS-1,2 to insulin receptor or enhanced degradation of IRS-1,2 (203). Additional evidence supports the ability of kinases and cytokines to alter insulin sensitivity. For instance, IKK- β (a regulator of cytokine producing NF- κ B) can block insulin signaling via inhibitory serine residue phosphorylation on IRS-1 or activating NF- κ B (triggering aforementioned cytokine generated IR). This cytokine regulating kinase has been shown to be important in altering systemic insulin sensitivity of mice in global and liver-specific

KO mice (204, 205) supporting the notion that cytokine-induced inflammation plays a key role in systemic IR, but also that liver inflammation is sufficient to generate systemic IR.

Additional studies have demonstrated a link between macrophage-generated cytokines and IR (206-208). Though cytokines may derive from many cell types, it is speculated that macrophages are the major systemic source of cytokines. Also, as hepatic tissue is responsible for filtration and metabolism of toxic products, it is reasonable to speculate that the liver will encounter relatively high levels of pro-inflammatory stimuli. Furthermore, the liver comprises 80-90% of the body's macrophages (208). Thus, the liver may play an especially critical role in macrophage-mediated inflammation and IR.

Goals of the project

The overarching hypothesis of this project is that exposure to benzene, generates, inflammation, insulin resistance, and vascular dysfunction. It is proposed that the oxidative stress caused by benzene metabolism generates inflammatory responses hepatically and systemically that could lead to insulin resistance. Given the high prevalence of benzene in the atmosphere and the high probability of exposure could make benzene a relevant player in the global epidemic of T2D. Moreover, oxidative injury caused by benzene exposure may lead to vascular damage peripherally and impair bone marrow-resident endothelial progenitor cells required for the repair of vascular injury. A reduction in repair capacity and increased injury by benzene exposure could contribute to

cardiovascular disease. Studies of smoking populations (high benzene exposure) show both increased incidence of diabetes and cardiovascular disease. Thus, understanding the context of how these diseases progress, especially in reference to hematotoxicity, will give critical insight not only into whether hematological or vascular biomarkers are more sensitive to benzene, but also whether benzene exposure has the capacity to induce cardiometabolic injury. Hence, the aim of this project was to examine the systemic effects of (Chapter II), to elucidate whether benzene exposure affects insulin sensitivity and to understand the mechanism underlying benzene toxicity (Chapter III), and lastly to assess the effects of benzene exposure on the abundance and function of medullary hematopoietic and endothelial stem cells (Chapter IV).

CHAPTER II

GENERAL CHARACTERISTICS OF BENZENE EXPOSURE

Introduction

Benzene is a ubiquitous environmental pollutant. In the United States, it is one of the top 20 chemicals produced by industrial sources, which yearly release over 6.7 million pounds of benzene in the air (17, 49). Humans are primarily exposed to benzene found in mainstream or secondhand cigarette smoke. Mainstream cigarette smoke contains 35-70 ppm benzene, and even higher concentrations of benzene are generated from other tobacco products such as water pipes, cigars and pipe tobacco (48, 209, 210). Thus, benzene concentrations are found at high levels from indoor and outdoor sources (211).

Although the effects of benzene on hematopoiesis and leukemia have been extensively studied, other sensitive biomarkers of benzene toxicity have gone largely unreported (212, 213). Moreover, the hallmark hematological changes (e.g. decreased lymphocytes, erythrocytes, hematocrit, T- and B-cells) are somewhat variable and dependent upon route of administration (e.g. inhalation vs. dermal absorption), dose and duration of exposure (214-216). The highest allowable dose of benzene exposure in a work environment (known as the STEL, PEL) is largely determined by the no observed adverse effect level (NOAEL) reported by the Agency for Toxic Substances and Disease Registry

(53). Importantly, limits of exposure concentration vary based on the duration of the exposure. These limits are defined as acute (1-14d), intermediate (>14-364d) and chronic (365d or greater) exposures (17). Benzene was recognized as a hematotoxic agent in the late 19th century after concentrated, acute exposures and has been studied more carefully in low dose, chronic exposures in the context of hematopoiesis and circulating bone marrow-derived cells (217, 218). As more is understood about benzene metabolism, oxidative stress, and associated complications, it is useful to approach these relevant exposure studies with a fresh perspective (219, 220). Our exposure model included acute (2wks) and intermediate (6wks) exposure durations. These sub-chronic exposures have benzene concentrations (50 ppm) very similar to that of what is found in main-stream cigarette smoke. Additionally, 50 ppm benzene is well within the range found in poorly ventilated, highly trafficked automotive areas, as well as that found in industrial activities involving benzene (e.g. plastics, petroleum, shoe industries). These acute and intermediate exposures are at relatively low concentrations compared with reported LOAELs (17).

To investigate what general physiological changes occur after 50ppm volatile benzene x 6h/day x 2wks or 6wks, we measured body mass, organ weights, complete blood counts and cellular biological outcomes such as platelet-leukocyte aggregates, immune differential panels, circulating microparticles. While aspects of reporting immune cell changes following benzene exposure have been published, these data are typically undocumented while traditional blood count (WBC, NE, MO, etc.) tests are more frequently reported. However,

because immune cells are derived from the bone marrow and are crucial to the survival of any organism because of their protective capacity, the response of these cells to environmental exposure tells us much about the ability to fight disease, autoimmune dysregulation and inflammation-driven disease processes. Additionally, changes in the markers of platelet function and vascular stasis are virtually undocumented in benzene-exposed organisms.

Here we report on novel biomarkers for benzene exposure as well as traditional measurements to allow for greater physiological context, and a better understanding of systemic toxicity due to benzene exposure.

Methods

Volatile Benzene Exposures

All procedures were approved by the University of Louisville Institutional Animal Care and Use Committee. C57BL/6J (wild-type; WT) mice were purchased from The Jackson Laboratory (Bar Harbor, ME). At 10 and 20wks of age, male mice were placed on either a normal chow diet or a 60% high fat diet (HFD; Research Diets Inc., #D12492) for the duration of the exposure. For the HFD intervention, animals were placed on this diet for 4 or 14wks prior to start of inhalation exposure and were maintained on this diet until necropsy. Water and diet were provided *ad libitum*. Anti-oxidant, 4-Hydroxy TEMPO (Sigma) was administered at 1mM in drinking water *ad libitum*, changed daily. Benzene atmospheres were generated from liquid benzene (Sigma-Aldrich) housed in a Kin-Tek Laboratories (La Marque, TX) permeation tube. A carrier gas (N₂) was

delivered to the permeation tube at 100mL/min and diluted with 3L/min HEPA and charcoal filtered room air where upon the atmospheres were delivered to a custom vapor system (Teague Enterprises, Inc., Woodland, CA, USA). Throughout the exposures, benzene concentration was continuously monitored by an in-line photo ionization detector (ppb RAE, Rae Industries, Sunnyvale, CA, USA) upstream of the cage insert vapor delivery unit (Teague Enterprises, Inc.) mounted on a standard polycarbonate rat cage (41 cm x 34 cm x 21 cm). Filtered air or benzene was distributed through a fine mesh screen at 3L/min with a cyclone-type top that distributes air within 10% of the mean concentration at six locations in the cage (Figure 2). Mice were exposed to 50ppm benzene (Figure 3A) for 6 h/day for 2wks or 6wks. Exposure assessment in individual animals was verified by GC/MS measurement of urinary *t,t*-MA (Figure 3B).

Complete Blood Counts and Plasma Biochemistry

After exposures, animals were euthanized by intraperitoneal injection of 100uL of pentobarbital solution (40mM in PBS). Peripheral blood was collected by cardiac puncture in 0.2M EDTA coated syringes. Peripheral blood was then transferred to Eppendorf tubes containing 20µL 0.2M EDTA and gently mixed. From this aliquot, 25µL of blood was used per animal for complete blood count analysis (CBC; Hemavet 950FS, Coulter Counter, Oxford, CT). Plasma HDL and LDL cholesterol, triglycerides, total protein, albumin (Cholesterol CII Enzymatic Kit; L-Type TG-H Kit; Bradford reagent, bromocresol green, Wako, Richmond, VA, USA), ALT, AST (Infinity, ThermoElectron, Louisville, CO, USA), levels were

measured using commercially available assay reagents as indicated. Assays were performed using calibrated standards in 96-well plates.

Metabolite Analysis by GC/MS

Samples applied for GC/MS analysis were re-dried under vacuum desiccation for a minimum of 24h prior to being derivatized under dried nitrogen using bistrimethyl-silyl-trifluoroacetamide. The GC column was 5% phenyl and the temperature ramp was from 40° to 300° C in a 16 min period. Samples were analyzed on a Thermo-Finnigan Trace DSQ fast-scanning single-quadrupole mass spectrometer using electron impact ionization. The instrument was tuned and calibrated for mass resolution and mass accuracy on a daily basis. The information output from the raw data files was automatically extracted as discussed below.

Platelet-Leukocyte Aggregates, Immune Differential Panels, Microparticle Detection and Flow Cytometry

To measure the platelet-leukocyte aggregates (PLAgg), whole blood (100 μ L per assay) was diluted with 400 μ L of 1 X Tyrodes solution (Sigma). Cells were fixed with 50 μ L 16% paraformaldehyde (PFA) for 10-30min. The sample was then lysed with 2 mL of Milli Q water and centrifuged at 400 x g for 5 min at room temperature (RT). Samples were then decanted and 5 μ L FcBlock (Miltenyi Biotec) was added to each tube for 10 min incubation at 4°C. The staining cocktail (CD41 FITC, CD45 APC, and CD11b eFluor605NC [eBiosciences]) was

then added to the appropriate samples and incubated for 30 min at 4°C, after which samples were washed with Tyrodes solution, and centrifuged at 400 x g for 5 min at RT. Unstained samples were used as a negative control. Samples were again decanted, vortexed and resuspended in 250µL Tyrodes. Samples were then acquired on an LSRII flow cytometer on low speed for 10,000 WBC by scatter. Enumeration of PLAggs was achieved by gating for CD45⁺ cells, along with a CD41⁺ marker and further refinement of the population occurred using CD11b⁺ cells from the parent population.

For the immune differential, 100µL whole blood was aliquoted into a 5mL falcon tube and 1mL of 1x BD PharmLyse (BD BioSciences) was added to each sample and incubated for 10min at RT. Samples were then centrifuged at 500 x g for 5 min at RT and decanted. The samples were then washed twice with 1mL 1% BSA/PBS buffer and centrifuged at 500 x g for 5 min at RT. Samples were again decanted, vortexed and 5µL of 50µg/mL Fc block was added to each tube for 10 min at 4°C. Then appropriate antibodies were added (NK1.1 FITC, Ly6C PE, CD8a PerCP-e710, CD62L PE-Cy7, CD19 APC, Gr-1 Alexa 700, CD3e APC-e780, CD11b e605 NC, CD4 e605 NC [eBiosciences]) and incubated for 30 min at 4°C. Unstained samples were used as a negative control. Samples were then washed with 1mL 1% BSA/PBS buffer and centrifuged at 500 x g for 5 min at RT, decanted, and vortexed. The addition of 250µL 1% BSA/PBS buffer was added to each sample and data was acquired on high speed for 90 s on an LSRII flow cytometer.

Microparticles of platelet and endothelial origin, were measured using a standard protocol (221). Briefly, 100 μ L of plasma was centrifuged for 2 min at 11,000 x g at 4°C in a fixed-angle rotor centrifuge. Supernatant was transferred to a new 1.5 mL Eppendorf tube and centrifuged for 45 min at 17,000 x g at 4°C. The supernatant was then aspirated and resuspended in PBS/ 2.5mM Ca²⁺. An aliquot of the microparticle suspension was added to separate Falcon FACS tubes with appropriate antibodies (Annexin V-Pacific Blue [Life Technologies], Flk-1-APC [eBiosciences], CD41a-FITC [eBiosciences], CD62E-PE [BD Pharmingen], CD143 [R&D Systems]) and incubated for 30 min while unstained samples were used as a negative control. The anti-mouse CD143 antibody was labeled with a Zenon Alexa Fluor 488 Goat Labeling Kit (Life Technologies). After staining, 10 μ m counting beads (Spherotech) were added to the sample at 50 beads/ μ L of sample. Size beads (1 μ m, 2 μ m, Life Technologies) were used to identify populations less than 1 μ m in diameter. The samples were then run on an LSRII and 20,000 events were collected.

Results

Exposure to volatile benzene alters CBCs in mice. C57BL/6, male mice exposed to 50ppm volatile benzene for 6h/d x 14d showed little difference in complete blood cell counts, with no cytopenias (Table 2) or change in body weight. In contrast, benzene-exposed animals demonstrated a trending increase in most cell types but only had a significant increase in neutrophils (0.365 \pm 0.117 k/ μ L HFA, 0.486 \pm 0.215 k/ μ L benzene), red blood cells (8.27 \pm 0.63 M/ μ L HFA,

9.53±2.18 M/ μ L benzene), percent eosinophils, percent basophils and red cell distribution width (RDW) (n=38/group). Mice exposed to 50ppm benzene for 6h/d x 6wks demonstrated significant cytopenias compared with their HFA-exposed counterparts. Benzene-exposed animals demonstrated a significant decrease in many cell types, most of myeloid origin (see Table 2, n=20/group). These data suggest that the trademark myeloid-associated cytopenias associated with benzene exposure do not present in the peripheral blood until 6wks of benzene exposure.

Liver assessment and plasma biochemistry is disrupted in benzene-exposed mice. While no difference was seen in body weight or in the change in body weight during an exposure, the liver:body weight ratio was increased after 2wks of benzene exposure (Figure 4F). This change was not observed in the 6wk exposure cohort when compared with HFA controls.

Mice exposed to benzene for 2wks demonstrated significantly elevated plasma alanine aminotransferase (ALT) levels compared with HFA-exposed controls (35.6±3.2 IU/L HFA, 47.1±8.6 IU/L Benzene, n=20/group). However, this was not observed after 6wks of exposure (Figure 4A). Furthermore, aspartate aminotransferase (AST) levels were increased in benzene-exposed animals compared with HFA-exposed controls (62.5±11.4 IU/L HFA, 88.3±23.9 IU/L Benzene, n=10/group). Similar to ALT, there was no corresponding increase in AST after 6wks of benzene exposure compared with HFA-exposed controls (n=10/group) (Figure 4B) indicating that there may be a compensatory

Figure 2.

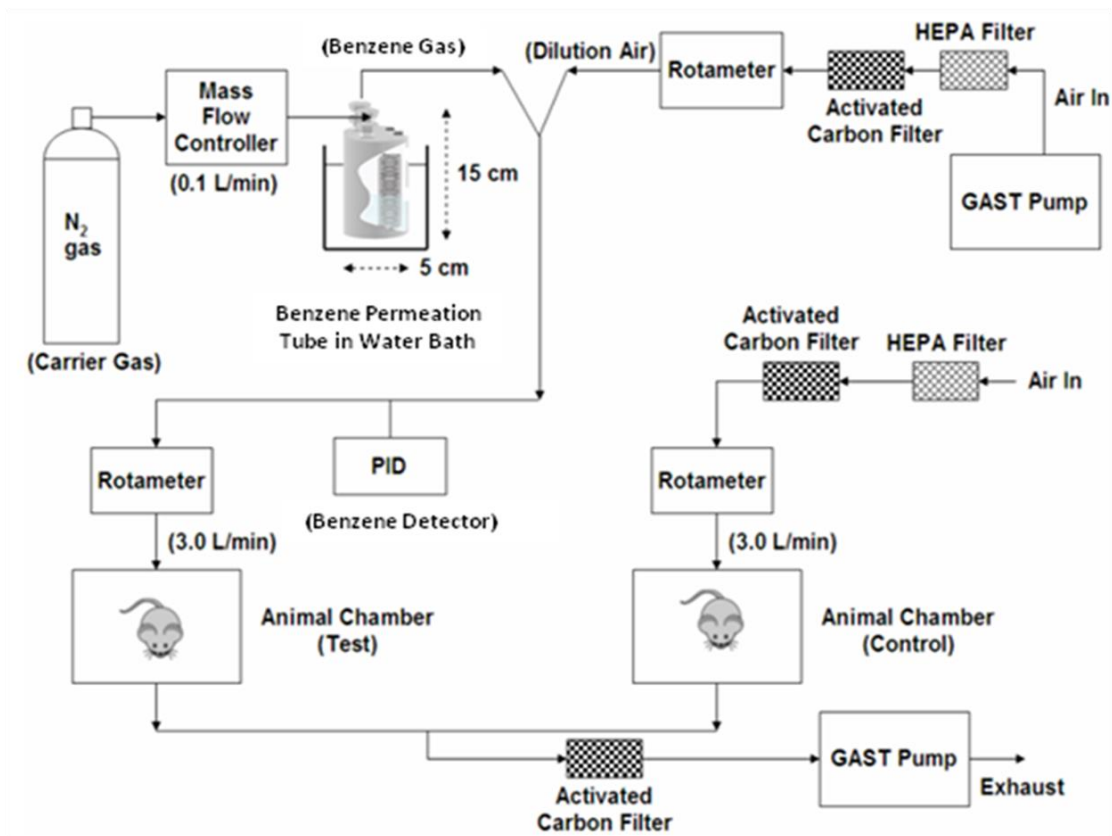
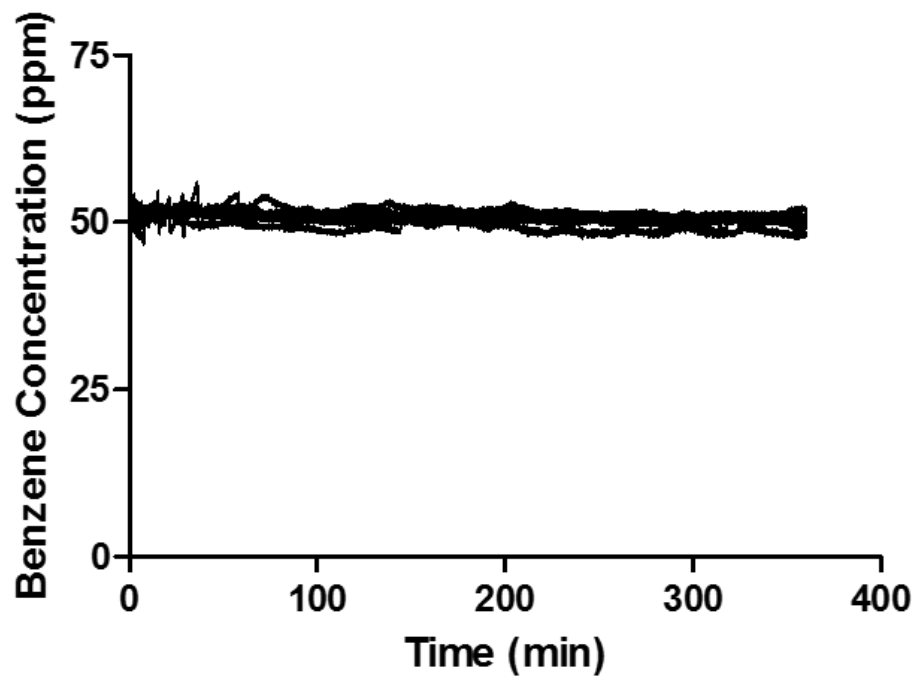


Figure 2. Benzene exposure system. Schematic showing the benzene exposure apparatus used in these studies. Benzene was delivered using a N₂ carrier gas to move concentrated benzene to a line where it was diluted with HEPA-filtered air. The benzene concentration (measured in ppm) was monitored by a ppbRAE unit before the gas mixture arrived at the animal chamber. A rotameter placed before the ppb RAE unit allowed personnel to dilute the concentrated flow of benzene to a controlled concentration. Additionally, the mass flow controller utilized between the carrier gas supply and the benzene permeation tube enabled a constant flow rate of flow through the permeation tube while a water bath containing the benzene permeation tube maintained constant temperature to allow for controlled benzene vaporization and transport by the carrier gas. Mice exposed to HEPA-filtered air have carbon and HEPA-filter upstream of the animal chamber and air is pumped through the system by a GAST pump. Benzene and HFA are exhausted through carbon and HEPA filters before leaving the system in a fume hood validated by the University of Louisville's Department of Environmental Health Services to manage the flow of this apparatus.

Figure 3.

A.



B.

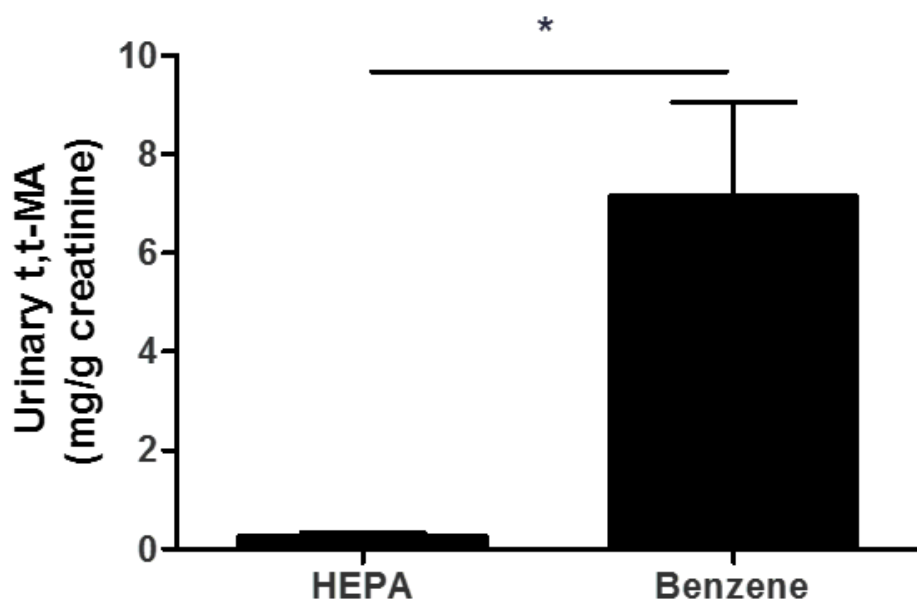


Figure 3. Verification of benzene exposure and metabolism. (A) Exposure chamber concentrations of benzene were determined by ppbRAE monitor logging. Illustrated are minute by minute benzene concentrations over one 14d representative exposure. (B) Urine collected from mice exposed to 50 ppm benzene or HFA for 14d was analyzed for the benzene-specific metabolite, *t,t*-MA. n=5 mice/treatment; *p<0.05.

Table 2. Complete blood counts.

Parameters - Mean (SD)	HEPA 2wks	Benzene 2wks	p-value	HEPA 6wks	Benzene 6wks	p-value
Leukocytes						
WBC (k/mL)	1.607 (0.376)	1.631 (0.340)	0.800	2.200 (0.782)	1.380 (0.099)	0.014 *
NE (k/ μ L)	0.365 (0.117)	0.486 (0.215)	0.018 *	0.379 (0.140)	0.199 (0.099)	0.006 *
LY (k/ μ L)	1.199 (0.322)	1.218 (0.278)	0.833	1.742 (0.641)	1.009 (0.246)	0.009 *
MO (k/ μ L)	0.084 (0.062)	0.118 (0.078)	0.092	0.073 (0.040)	0.041 (0.015)	0.037 *
EO (k/ μ L)	0.015 (0.016)	0.013 (0.018)	0.659	0.002 (0.004)	0.004 (0.008)	0.569
BA (k/ μ L)	0.002 (0.004)	0.002 (0.004)	0.491	0.003 (0.005)	0.002 (0.004)	0.628
NE (%)	18.72 (6.07)	19.88 (8.57)	0.500	17.57 (3.3)	14.59 (6.80)	0.234
LY (%)	74.67 (8.95)	74.19 (9.59)	0.822	79.16 (3.77)	81.49 (7.25)	0.382
MO (%)	4.44 (2.65)	4.73 (2.60)	0.644	2.92 (1.05)	3.39 (0.83)	0.282
EO (%)	0.075 (0.051)	0.250 (0.257)	0.001 *	0.106 (0.115)	0.041 (0.592)	0.215
BA (%)	0.039 (0.061)	0.006 (0.017)	0.012 *	0.146 (0.170)	0.000 (0)	0.024 *
Erythrocytes						
RBC (M/ μ L)	8.27 (0.63)	9.53 (2.18)	0.002 *	8.52 (0.60)	7.10 (2.40)	0.098
HGB (g/dL)	12.8 (2.3)	13.8 (3.3)	0.174	11.6 (0.8)	9.7 (3.6)	0.126
HCT (%)	44.7 (6.8)	47.1 (9.2)	0.216	38.0 (2.5)	32.8 (11.7)	0.202
MCV (fL)	49.5 (4.6)	50.0 (4.4)	0.614	44.6 (0.8)	45.8 (2.1)	0.112
MCH (pg)	14.2 (1.2)	14.4 (0.9)	0.369	13.6 (0.5)	13.4 (0.7)	0.613
MCHC (g/dL)	28.8 (1.8)	29.0 (1.8)	0.537	30.5 (1.4)	29.4 (1.9)	0.146
Thrombocytes						
RDW (%)	17.2 (1.1)	17.8 (1.2)	0.039 *	17.2 (0.5)	16.7 (0.8)	0.135
PLT (k/ μ L)	782 (148)	751 (179)	0.487	768 (71)	601 (195)	0.028 *
MPV (fL)	4.5 (0.4)	4.5 (0.5)	0.682	4.4 (0.1)	4.5 (0.1)	0.513

Mice were exposed to HFA or benzene for 2wks (second and third columns) or 6wks (fifth and sixth columns) and complete blood counts were measured. n=20-26 mice/treatment; *p<0.05.

mechanism providing protection for hepatic and systemic tissue. Additionally, no significant difference was seen in the ALT:AST ratio between 2wk benzene-exposed and HFA-exposed control animals (Figure 4C), suggesting there is not an overt sign of liver (ALT) versus peripheral systemic injury (AST). Plasma albumin levels decreased after 2wks of benzene exposure compared with HFA-exposed controls (Figure 4D). Alternately, a small $11\% \pm 0.11$ increase plasma albumin was seen in benzene-exposed animals after 6wks of benzene exposure. Corresponding to the decrease in albumin after 2wks of benzene exposure is a resultant increase in non-albumin protein levels. No change in NAP was demonstrated between HFA-exposed and benzene-exposed animals after 6wks of exposure (Figure 4E). The transient decrease in albumin may be related to either damage in the vasculature or an increase in the transport of benzene and other metabolites. The small increase in albumin after 6wks of benzene exposure may be associated with an increase in insulin resistance, which has been previously documented.

Despite changes in ALT and AST levels after 2wks of benzene exposure, no significant difference was found between various endothelial-derived microparticle (EMP) or platelet-derived microparticle (PMP) levels (Table 3). However, after 6wks of benzene exposure, a significant increase in all EMP populations (but not PMP) was found, with an average 1.5-fold increase over HFA-exposed animals.

Mild, but significant increases in HDL levels were seen in benzene-exposed animals after 2 and 6wks of exposure relative to HFA-exposed controls

(Figure 5A). Additionally, a substantial increase in LDL levels were found after 6wks of benzene exposure (25.6±3.3 mg/dL HFA, 34.2±4.1 mg/dL benzene, n=20/group), but not after 2wks of exposure (Figure 5B). Also, the ratio of LDL:HDL was significantly increased after 6wks of benzene exposure compared with HFA controls. Furthermore, benzene-exposed animals demonstrated an increase in total cholesterol compared with HFA-exposed controls at 6wks (107±5 mg/dL HFA, 120±7 mg/dL Benzene, n=20/group; *p<0.05) but not at 2wks (Figure 5D). Alternately, there was no significant increase in triglyceride (TRG) levels after 2 or 6wks of exposure.

Platelet-leukocyte aggregate formation is enhanced with benzene exposure. A consistent finding after 2 and 6wks of benzene exposure was the elevation of numbers of platelet-leukocyte aggregates (PLAggs) which showed 1.5-fold increase after 2wks of benzene exposure and 1.6-fold increase after 6wks of exposure (Figure 6). The relative increase in aggregation does not change with exposure duration (2 or 6wks) in our experiments (n=20/treatment; *p<0.05).

Circulating immune cell relative abundance is diminished in mice with benzene exposure. Natural Killer (NK) cells, B cells, CD4⁺ T cells, CD8⁺ T cells, granulocytes, monocytes and monocyte subpopulations were measured by flow cytometry. While NK cells, B cells and monocytes demonstrated a trending decrease with benzene exposure, these changes did not achieve statistical significance in 12-14wk old mice. Additionally, no monocyte subpopulations

Figure 4.

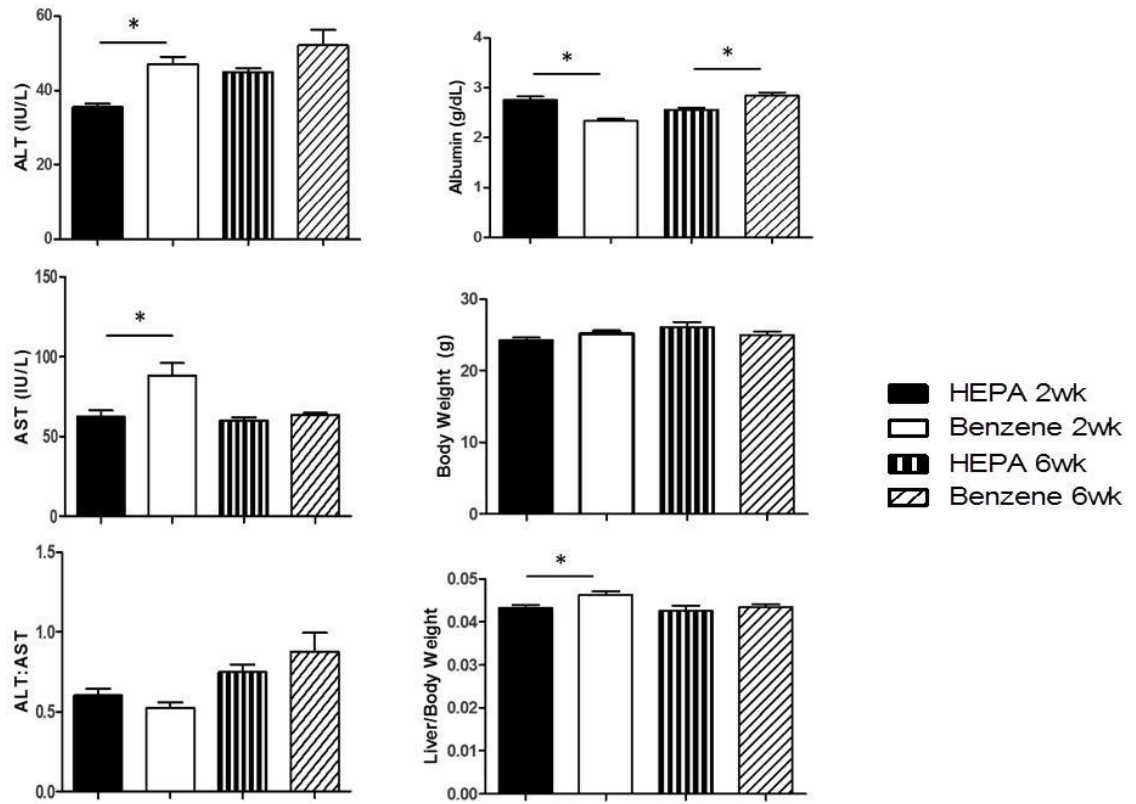


Figure 4. Benzene and tissue injury. Mice were exposed to HFA or 50ppm benzene for 2wks or 6wks as indicated in 4 separate exposures and blood collected at termination of exposure. Indices of liver injury, ALT (A), and systemic injury, AST (B), were measured in collected plasmas. In addition ALT:AST (C) and liver:body weight ratios (E) were determined. Albumin (D) was also measured in these plasma samples. n=15-20 mice/treatment; *p<0.05.

Figure 5.

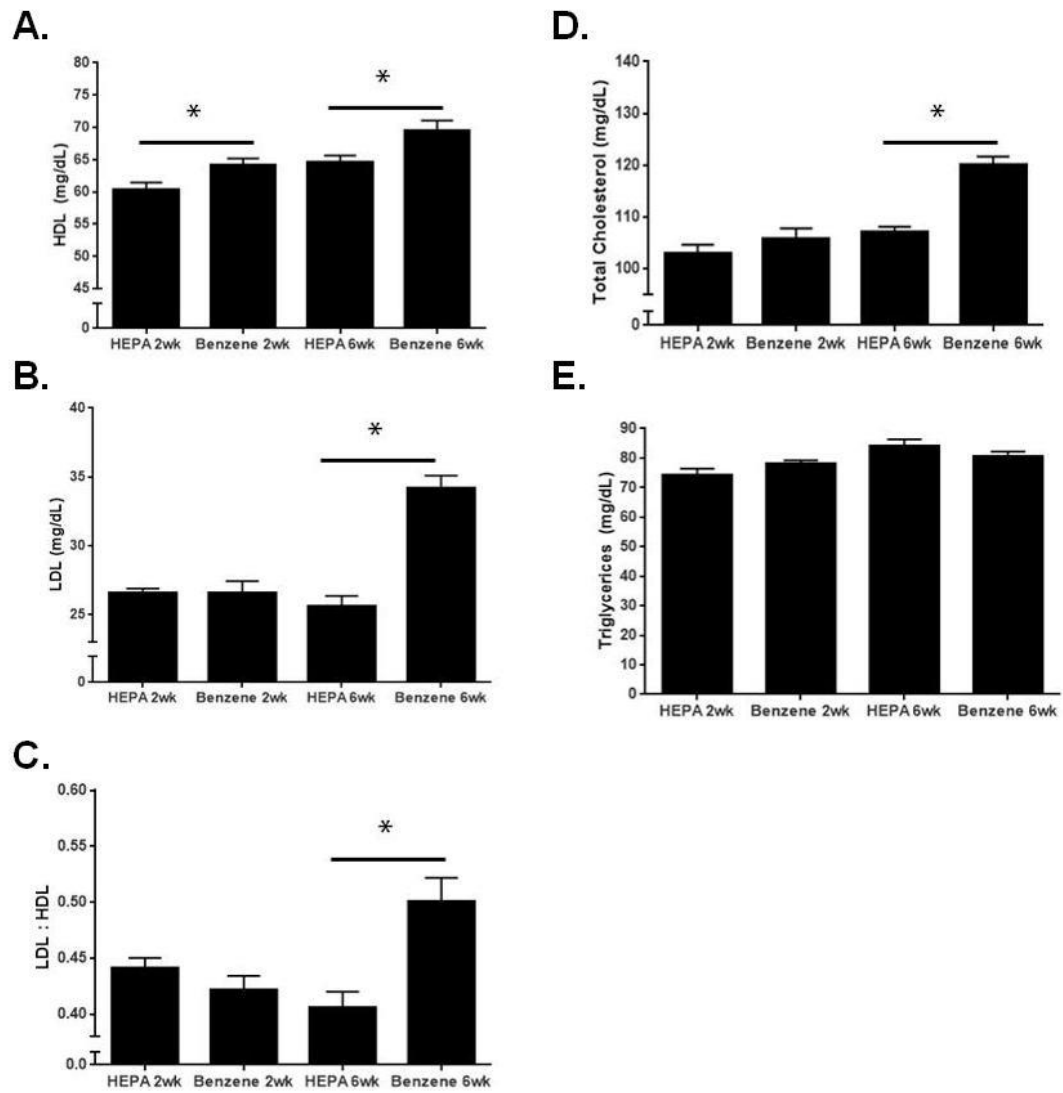


Figure 5. Benzene and plasma lipids. Mice were exposed to HFA or 50ppm benzene for 2wks or 6wks as indicated in 4 separate exposures and blood collected at termination of exposure. Plasma levels of HDL (A), LDL (B), total cholesterol (D) and triglycerides (E) were measured as outlined in Methods. We also calculated an LDL:HDL ratio (C). n=14-20 mice/treatment; *p<0.05.

Table 3. Circulating microparticle levels.

Microparticle Population	Microparticle Phenotype	Air	Benzene	p-value
		2wk Mean (StDev)	2wk Mean (StDev)	
Microparticle (non-specific)	<1um/AV+	1.6116 (1.4125)	1.1879 (1.0565)	0.2599
Platelet-derived Microparticle	<1um/AV+/CD41+	1.7062 (1.6673)	1.3278 (1.3652)	0.5495
Activated Endothelial-derived Microparticle	<1um/AV+/CD62E+	0.8346 (0.6287)	0.5758 (0.3904)	0.2571
Activated Lung Endothelial-derived Microparticle	<1um/AV+/CD62E+/CD143+	0.6060 (0.4486)	0.3561 (0.2280)	0.1180
Lung-derived Microparticle	<1um/AV+/CD143+	1.0921 (0.9360)	0.7393 (0.6328)	0.3083
Endothelial-derived Microparticle	<1um/AV+/Flk+	0.9193 (0.7359)	0.5519 (0.3875)	0.1601
Lung Endothelial-derived Microparticle	<1um/AV+/Flk+/CD143+	0.9032 (0.7254)	0.5318 (0.3693)	0.1484

Microparticle Population	Microparticle Population	Air	Benzene	p-value
		6wk Mean (StDev)	6wk Mean (StDev)	
Microparticle (non-specific)	<1um/AV+	0.3771 (0.2037)	2.0693 (1.8137)	<0.0001 *
Platelet-derived Microparticle	<1um/AV+/CD41+	0.2793 (0.1769)	0.2487 (0.1042)	0.5632
Activated Endothelial-derived Microparticle	<1um/AV+/CD62E+	2.2299 (1.1452)	3.4797 (0.4293)	0.0003 *
Activated Lung Endothelial-derived Microparticle	<1um/AV+/CD62E+/CD143+	1.1499 (0.5525)	1.9073 (0.4550)	0.0001 *
Lung-derived Microparticle	<1um/AV+/CD143+	1.1586 (0.5531)	1.8651 (0.4378)	0.0001 *
Endothelial-derived Microparticle	<1um/AV+/Flk+	0.7206 (0.3566)	1.1771 (0.3128)	0.0001 *
Lung Endothelial-derived Microparticle	<1um/AV+/Flk+/CD143+	0.8673 (0.4903)	1.3308 (0.2619)	0.0015 *

Mice were exposed to HFA or 50ppm benzene for 2wks or 6wks as indicated in 4 separate exposures and blood collected at termination of exposure. Listed are the levels of 7 types of circulating microparticles. n=20 mice/treatment; *p<0.05.

Figure 6.

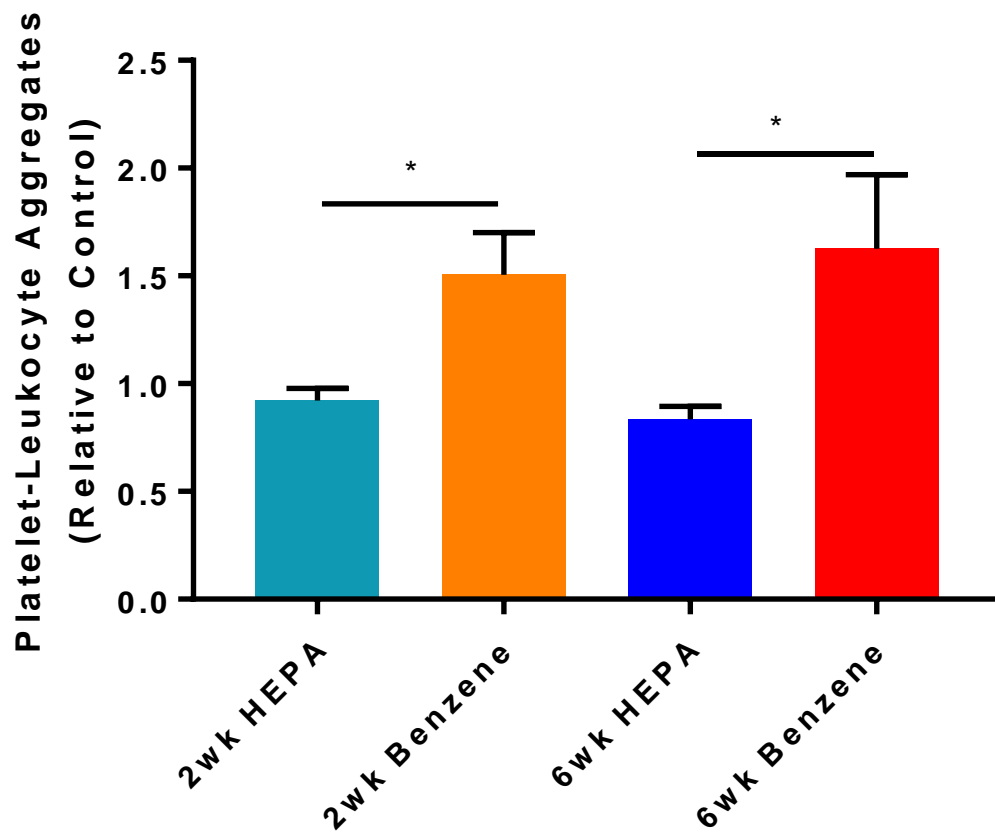


Figure 6. Benzene and platelet aggregates. Mice were exposed to HFA or 50ppm benzene for 2 or 6wks in 4 separate exposures and the relative abundance of PLAgg in whole blood was determined by flow cytometry. Indicated is the relative abundance of PLAgg normalized to HFA-exposed mice. n=16-20 mice/treatment; *p<0.05.

were significantly altered after benzene exposure though all trended towards a decrease (Figure 8).

Circulating microparticle levels increase after 6wks of benzene exposure.

Circulating microparticles were measured by flow cytometry methods investigating seven microparticle populations defined as: (1) microparticles (not specific to cell type of origin), (2) platelet-derived microparticles (PMP), (3) activated endothelial-derived microparticles, (4) lung, activated endothelial-derived microparticles, (5) lung-derived microparticles, (6) endothelial-derived microparticles (EMP), (7) lung, endothelial-derived microparticles. These microparticle populations were measured in animals on normal chow diet only after 2 and 6wks of benzene or HFA exposure.

Mice exposed to benzene for 2wks, compared with filtered air controls demonstrated no significant changes in any of the seven microparticle populations. However, mice exposed to benzene for 6wks demonstrated increases 6 of the 7 microparticle subpopulations (PMP remained unchanged). Total (non-specific) circulating microparticle levels, as well as activated endothelial-derived microparticles, lung, activated endothelial-derived microparticles, lung-derived microparticles, endothelial-derived microparticles, lung, endothelial-derived microparticles were increased from 1.5-fold (lung endothelial microparticles, $p=0.0015$) up to 1.7-fold (lung activated endothelial microparticles, $p=0.0001$) for specific microparticle subpopulations (Table 3).

Mice with benzene exposure plus anti-oxidant intervention have altered CBCs. To test the role of oxidative stress in the development of benzene related pathologies, we used an anti-oxidant intervention utilizing 4-Hydroxy TEMPO (TEMPOL) at 1 mM in drinking water (*ad libitum*). There were no cytopenias detected in mice receiving this TEMPOL intervention after 2wks of benzene exposure relative to HFA-exposed, TEMPOL administered controls. Minor differences between groups were seen in basophil count, basophil percent, percent hematocrit, mean corpuscular volume, and mean corpuscular hemoglobin concentration (see Table 4, n=20/group). However, significant differences were detected between the benzene-exposed animals with no intervention and the benzene-exposed animals with intervention. Benzene-exposed, TEMPOL treated animals demonstrated a decrease in neutrophil count, monocyte count, eosinophil count, percent monocytes, erythrocytes, hemoglobin, percent hematocrit, mean corpuscular volume and mean corpuscular hemoglobin (Table 4).

When assaying for PLAGgs it was noted that with the oxidative stress generated by CYP2E1 activity during benzene metabolism, an anticipated decrease in bioavailable NO is expected. One of the physiological roles of NO is to inhibit platelet aggregation. In our anti-oxidant (TEMPOL) intervention cohort we assayed for PLAGgs and found a trending decrease ($p=0.09$) in aggregation compared with benzene-exposed animals receiving no intervention (Figure 7).

Mice exposed to benzene and high fat diet rapidly develop cytopenias.

While mice 12-14wks of age fed a normal chow showed modest changes in circulating cell types (i.e. erythrocyte counts) after benzene exposure, mice on a 6wks HFD demonstrated cytopenias in WBC, neutrophils and lymphocytes after 2wks of benzene exposure. Mice on a HFD for 18wks did not demonstrate a more magnified cytopenia after 2wks of benzene exposure compared with NC benzene-exposed animals. However, the age matched 24wk old mice exposed to benzene but on a normal chow diet did demonstrate cytopenias (in WBC, neutrophils, lymphocytes and monocytes) after just 2wks of benzene exposure. Complete description of blood counts comparing benzene-exposed animals may be found in Tables 5 and 6.

Natural Killer (NK) cells, B cells, CD4⁺ T cells, CD8⁺ T cells, granulocytes, monocytes and monocyte subpopulations were also measured in mice administered a HFD in addition to benzene exposure. HFD increased sensitivity of the animals to benzene exposure. All cell types experienced a significant change with at least one of the exposure cohorts, with NK cells and granulocytes demonstrating the least change of all populations measured (Figure 8).

NK cells demonstrated a significant 74% ($p=0.0001$) decrease only in animals exposed to benzene that were on HFD for 18wks, while other benzene-exposed groups showed a trending decrease in these cells ($n=5$ /group). Granulocytes generally showed a trending decrease after benzene exposure compared with controls, though the changes did not reach significance. Changes in B cells followed the same downward trend after benzene exposure

as seen earlier. A significant decrease between 18wk HFD fed, benzene-exposed mice and HFD fed, HFA-exposed control was found as well as was their normal chow controls, age matched controls. An additional age-dependent 62% decrease ($p=0.03$, $n=5/\text{group}$) between benzene-exposed 12-14wk old animals and 24wk old animals was found (Figure 8).

Several changes were seen in the CD4⁺ T cell population following benzene exposure. Animals on an 18wk HFD and exposed to benzene experienced a 62% decrease ($p<0.0001$) in CD4⁺ T cells relative to the HFA exposed, 18wk HFD fed mice. Mice exposed to 8wk HFD and benzene demonstrated a significant decrease in CD4⁺ T cells compared with NC benzene-exposed controls. Additionally, an age dependent decrease was seen in CD4⁺ T cells after 2wks of benzene exposure for animals on a normal chow diet. CD8⁺ T cells were decreased in almost all benzene exposure cohorts (Figure 8).

Monocytes showed the same cytopenia trend as other cell types following benzene exposure. This diminution reached significance between 18wk HFD fed and benzene-exposed animals compared with HFD fed and HFA-exposed mice, as well as with their age-matched normal chow controls (Figure 9). A significant decrease was also seen between 8wk HFD fed and benzene animals and age matched benzene normal chow animals (61% decrease, $p=0.007$).

Table 4. Complete blood count panels and TEMPOL.

Parameters - Mean (SD)	HEPA Water	Benzene Water	p-value	HEPA TEMPOL	Benzene TEMPOL	p-value	p-value
Leukocytes							
WBC (k/ μ L)	1.607 (0.376)	1.631 (0.340)	0.8004	1.725 (0.531)	1.461 (0.414)	0.1084	0.1477
NE (k/ μ L)	0.365 (0.117)	0.486 (0.215)	0.0178 *	0.397 (0.172)	0.339 (0.105)	0.2327	0.0041 ‡
LY (k/ μ L)	1.199 (0.322)	1.218 (0.278)	0.8328	1.226 (0.416)	1.036 (0.297)	0.1418	0.0571
MO (k/ μ L)	0.084 (0.062)	0.118 (0.078)	0.0916	0.031 (0.012)	0.029 (0.015)	0.5806	<0.0001 ‡
EO (k/ μ L)	0.015 (0.016)	0.013 (0.018)	0.6592	0.003 (0.005)	0.002 (0.004)	0.6397	0.0068 ‡
BA (k/ μ L)	0.002 (0.004)	0.002 (0.004)	0.4914	0.000 (0)	0.002 (0.004)	0.0421 †	0.6948
NE (%)	18.72 (6.07)	19.88 (6.57)	0.5000	22.08 (5.39)	23.00 (6.31)	0.6419	0.1220
LY (%)	74.67 (8.95)	74.19 (9.59)	0.8225	75.24 (5.45)	73.93 (6.34)	0.5092	0.9026
MO (%)	4.44 (2.65)	4.73 (2.60)	0.6440	2.19 (1.04)	2.62 (1.33)	0.2793	0.0002 ‡
EO (%)	0.075 (0.051)	0.250 (0.257)	0.0008 *	0.0979 (0.117)	0.21 (0.25)	0.1015	0.5903
BA (%)	0.039 (0.061)	0.006 (0.017)	0.0121 *	0.000 (0)	0.123 (0.148)	0.0026 †	0.0039 ‡
Erythrocytes							
RBC (M/ μ L)	8.27 (0.63)	9.53 (2.18)	0.0016 *	8.33 (0.38)	8.13 (0.36)	0.1369	0.0004 ‡
HGB (g/dL)	12.8 (2.3)	13.8 (3.3)	0.1741	10.9 (0.7)	10.9 (0.5)	0.9230	<0.0001 ‡
HCT (%)	44.7 (6.8)	47.1 (9.2)	0.2159	39.1 (1.6)	37.3 (2.4)	0.0139 †	<0.0001 ‡
MCV (fL)	49.5 (4.6)	50.0 (4.4)	0.6144	47.0 (1.0)	45.1 (3.0)	0.0168 †	<0.0001 ‡
MCH (pg)	14.2 (1.2)	14.4 (0.9)	0.3686	13.1 (0.5)	13.3 (0.7)	0.3539	<0.0001 ‡
MCHC (g/dL)	28.8 (1.8)	29.0 (1.8)	0.5366	28.2 (0.7)	29.5 (1.2)	0.0006 †	0.2516
Thrombocytes							
RDW (%)	17.2 (1.1)	17.8 (1.2)	0.0385 *	16.6 (0.7)	16.8 (0.5)	0.2217	<0.0001 ‡
PLT (k/ μ L)	782 (148)	751 (179)	0.4871	699 (55)	677 (68)	0.2760	0.0550
MPV (fL)	4.5 (0.4)	4.5 (0.5)	0.6823	4.3 (0.2)	4.29 (0.2)	0.8913	0.1228

* = p-value < 0.05 between HEPA Water and Benzene Water

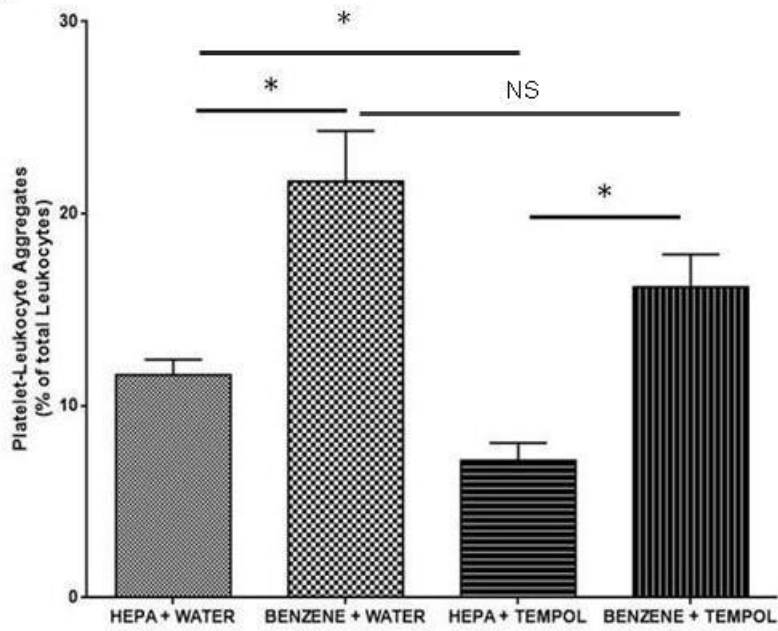
† = p-value < 0.05 between HEPA TEMPOL and Benzene TEMPOL

‡ = p-value < 0.05 between Benzene Water and Benzene TEMPOL

Mice were exposed to HFA or benzene for 2wks consuming normal drinking water (second and third columns) or water supplemented with 1mM TEMPOL (fifth and sixth columns) and complete blood counts were measured. n=18-26 mice/treatment; *p<0.05.

Figure 7.

A.



B.

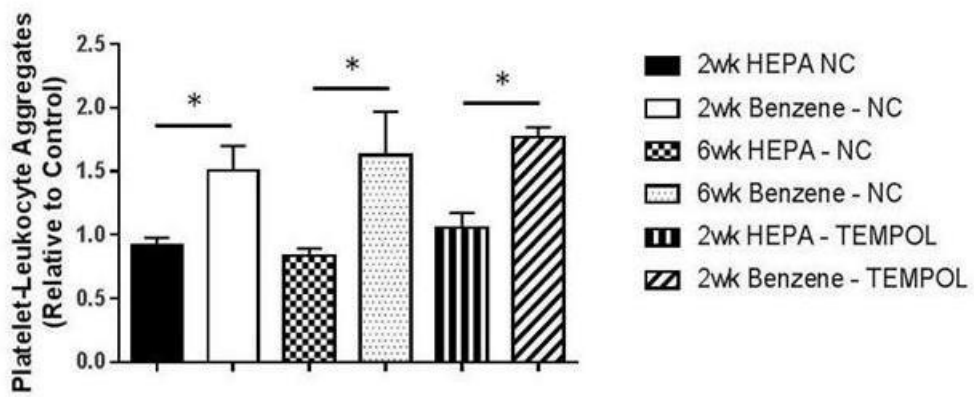


Figure 7. PLAGg formation and TEMPOL intervention. Mice were exposed to HFA or benzene for 2wks consuming normal drinking water or water supplemented with 1mM TEMPOL in 4 separate exposures and the abundance of PLAGg in whole blood was determined by flow cytometry (A). We also calculated the abundance relative to each treatment's control from 2wk (normal drinking water and TEMPOL-water) and 6wk HFA and benzene-exposed animals (B). n=15-20 total mice/treatment; *p<0.05.

Table 5. Complete blood count panel and 8wks of HFD.

Parameters - Mean (SD)	HEPA 14 weeks NC	Benzene 14 weeks NC	p-value	HEPA 14 weeks HFD - 8 weeks	Benzene 14 weeks HFD - 8 weeks	p-value	p-value
Leukocytes							
WBC (k/ μ L)	3.675 (0.251)	2.940 (0.024)	0.1188	3.432 (0.740)	2.000 (0.582)	0.0133 †	0.0971
NE (k/ μ L)	0.545 (0.150)	0.442 (0.095)	0.2877	0.742 (0.120)	0.460 (0.231)	0.0515	0.8778
LY (k/ μ L)	2.957 (0.258)	2.442 (0.303)	0.2349	2.610 (0.647)	1.570 (0.305)	0.0193 †	0.0731
MO (k/ μ L)	0.165 (0.076)	0.056 (0.022)	0.0598	0.078 (0.026)	0.050 (0.023)	0.1112	0.6870
EO (k/ μ L)	0.003 (0.005)	0.000 (0.000)	0.3910	0.000 (0.000)	0.000 (0.000)	-	-
BA (k/ μ L)	0.000 (0.000)	0.000 (0.000)	-	0.000 (0.000)	0.000 (0.000)	-	-
NE (%)	14.87 (3.96)	15.87 (4.65)	0.7367	22.00 (3.60)	21.43 (5.70)	0.8547	0.1312
LY (%)	80.44 (3.10)	82.20 (4.53)	0.5122	75.72 (3.90)	76.03 (5.67)	0.9210	0.0957
MO (%)	4.56 (2.07)	1.88 (0.50)	0.0788	2.21 (0.52)	2.51 (0.96)	0.5608	0.2446
EO (%)	0.133 (0.035)	0.036 (0.034)	0.0050 *	0.038 (0.026)	0.032 (0.044)	0.8022	0.8766
BA (%)	0.010 (0.020)	0.008 (0.018)	0.8809	0.030 (0.042)	0.000 (0.000)	0.1890	0.3739
Erythrocytes							
RBC (M/ μ L)	9.20 (0.60)	9.23 (0.96)	0.9495	9.38 (1.35)	8.23 (0.76)	0.1436	0.1067
HGB (g/dL)	11.3 (1.3)	11.8 (1.3)	0.5096	13.9 (1.9)	12.5 (1.1)	0.1728	0.4342
HCT (%)	42.8 (3.5)	43.2 (4.4)	0.8886	41.3 (5.7)	36.4 (3.9)	0.1594	0.0348 ‡
MCV (fL)	46.5 (1.0)	46.7 (0.2)	0.6665	44.0 (0.4)	44.2 (1.0)	0.6943	0.0046 ‡
MCH (pg)	12.2 (0.7)	12.8 (0.1)	0.1939	14.9 (0.3)	15.1 (0.3)	0.2138	<0.0001 ‡
MCHC (g/dL)	26.3 (0.9)	27.4 (0.2)	0.0920	33.8 (0.6)	34.3 (0.9)	0.3649	<0.0001 ‡
Thrombocytes							
RDW (%)	17.4 (0.3)	17.3 (0.5)	0.8897	18.3 (1.1)	17.9 (0.9)	0.5375	0.2481
PLT (k/ μ L)	657 (95)	664 (95)	0.9129	729 (79)	861 (23)	0.0178 †	0.0084 ‡
MPV (fL)	4.25 (0.06)	4.22 (0.08)	0.5460	4.60 (0.07)	4.60 (0.16)	1.0000	0.0031 ‡

*= p-value < 0.05 between HFA NC and Benzene NC

†= p-value < 0.05 between HFA+HFD and Benzene+HFD

‡= p-value < 0.05 between Benzene NC and Benzene+HFD

Mice were exposed to HFA or benzene for 2wks consuming normal chow diet (second and third columns) or HFD for 8wks (fifth and sixth columns) and complete blood counts were measured. n=10-26 mice/treatment; *p<0.05.

Table 6. Complete blood count panel and 18wks of HFD.

Parameters - Mean (SD)	HEPA	Benzene	p-value	HEPA	Benzene	p-value	p-value
Age	24 weeks	24 weeks		24 weeks	24 weeks		
Diet	NC	NC		HFD - 18 weeks	HFD - 18 weeks		
Leukocytes							
WBC (k/ μ L)	3.736 (0.760)	1.776 (0.247)	0.0030 *	3.708 (1.714)	1.544 (0.325)	0.0464 †	0.2424
NE (k/ μ L)	0.756 (0.215)	0.384 (0.147)	0.0150 *	0.892 (0.684)	0.462 (0.114)	0.2342	0.3765
LY (k/ μ L)	2.872 (0.696)	1.350 (0.153)	0.0070 *	2.718 (1.412)	1.024 (0.217)	0.0542	0.0278 ‡
MO (k/ μ L)	0.104 (0.0.0)	0.036 (0.015)	0.0039 *	0.092 (0.107)	0.054 (0.021)	0.4767	0.1593
EO (k/ μ L)	0.000 (0.00)	0.004 (0.005)	0.1778	0.006 (0.013)	0.004 (0.005)	0.7694	1.0000
BA (k/ μ L)	0.000 (0.00)	0.002 (0.004)	0.3739	0.002 (0.004)	0.002 (0.004)	1.0000	1.0000
NE (%)	20.42 (5.22)	21.16 (5.42)	0.8306	23.69 (10.48)	29.98 (3.35)	0.2598	0.0186
LY (%)	76.72 (5.86)	76.40 (5.96)	0.9330	73.94 (12.46)	66.40 (3.23)	0.2523	0.0158
MO (%)	2.83 (0.80)	2.21 (0.98)	0.3015	2.22 (1.89)	3.36 (0.72)	0.2608	0.0682
EO (%)	0.026 (0.040)	0.170 (0.233)	0.2411	0.118 (0.231)	0.190 (0.207)	0.6182	0.8895
BA (%)	0.000 (0.000)	0.066 (0.148)	0.3739	0.028 (0.063)	0.084 (0.147)	0.4668	0.8517
Erythrocytes							
RBC (M/ μ L)	8.62 (1.07)	8.28 (1.00)	0.6133	10.69 (0.90)	10.18 (0.76)	0.3671	0.0105 ‡
HGB (g/dL)	12.3 (1.4)	12.1 (1.4)	0.8616	15.1 (0.6)	15.0 (1.0)	0.7639	0.0068 ‡
HCT (%)	38.6 (4.4)	35.6 (4.3)	0.4831	47.4 (2.5)	44.9 (3.3)	0.2163	0.0095 ‡
MCV (fL)	44.8 (1.3)	44.2 (0.3)	0.3586	44.4 (1.9)	44.1 (0.5)	0.7301	0.8290
MCH (pg)	14.2 (0.2)	14.6 (0.2)	0.0205 *	14.2 (0.7)	14.7 (0.4)	0.2079	0.7924
MCHC (g/dL)	26.0 (12.6)	33.1 (0.4)	0.2752	31.9 (0.8)	33.3 (0.8)	0.0280 †	0.6184
Thrombocytes							
RDW(%)	18.3 (1.4)	17.5 (0.4)	0.2646	19.7 (1.8)	18.7 (0.5)	0.2884	0.0045 ‡
PLT (k/ μ L)	844 (157)	831 (84)	0.8795	663 (116)	565 (90)	0.1730	0.0013 ‡
MPV (fL)	4.66 (0.11)	4.48 (0.15)	0.0659	5.0 (0.4)	4.75 (0.4)	0.2517	0.2196

*= p-value < 0.05 between HFA NC and Benzene NC

†= p-value < 0.05 between HFA+HFD and Benzene+HFD

‡= p-value < 0.05 between Benzene NC and Benzene+HFD

Mice were exposed to HFA or benzene for 2wks consuming normal chow diet (second and third columns) or HFD for 18wks (fifth and sixth columns) and complete blood counts were measured. n=16-26 mice/treatment; *p<0.05.

Figure 8.

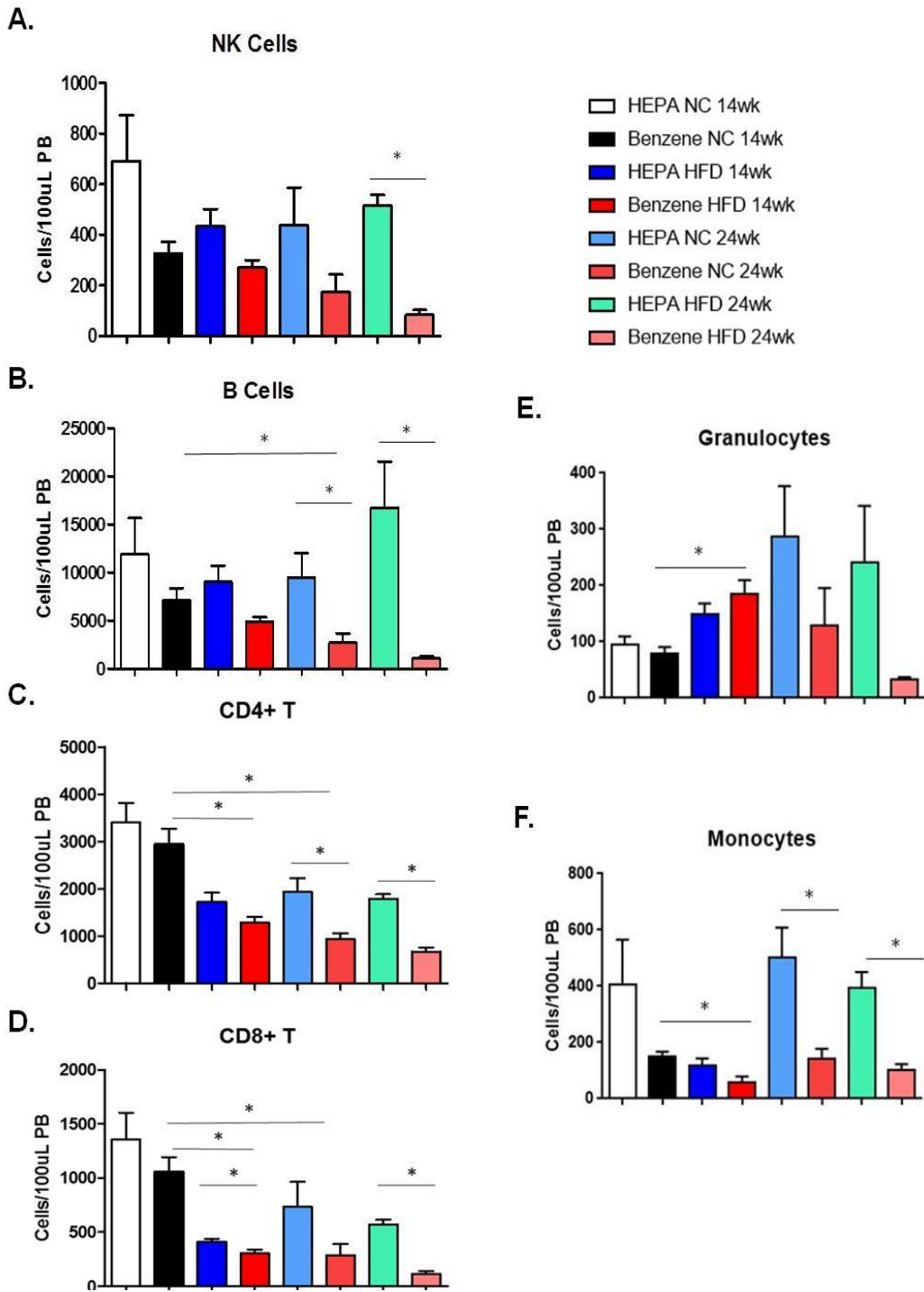


Figure 8. Benzene exposure, circulating immune cells and HFD. Mice were exposed to HFA or benzene for 2wks consuming normal chow diet, HFD for 8wks or HFD for 18wks and immune cell panels were measured by flow cytometry. Illustrated are levels of NK cells (A) B cells (B), CD4⁺ T cells (C), CD8⁺ T cells (D), granulocytes (E) and monocytes (F). n=5 mice/treatment;*p<0.05.

Figure 9.

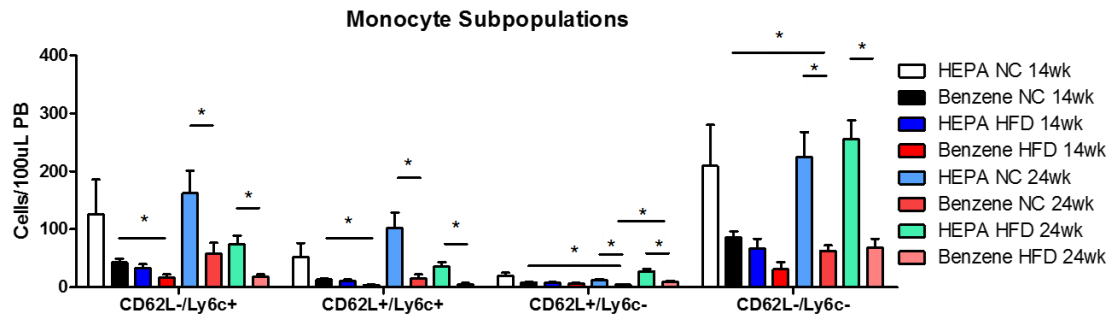


Figure 9. Benzene exposure, monocyte subpopulations and HFD. Mice were exposed to HFA or benzene for 2wks consuming normal chow diet, HFD for 8wks or HFD for 18wks and monocyte subpopulations were measured by flow cytometry. Illustrated are levels of CD62L⁻/Ly6c⁺, CD62L⁺/Ly6c⁺, CD62L⁺/Ly6c⁻, CD62L⁻/Ly6c⁻ cells. n=5 mice/treatment; *p<0.05.

Monocyte subpopulations were divided into four groups, each of which has a dynamic response to benzene exposure. The four populations are defined as CD62L⁻/Ly6c⁺, CD62L⁺/Ly6c⁺, CD62L⁺/Ly6c⁻ and CD62L⁻/Ly6c⁻. The monocyte subpopulation CD62L⁻/Ly6c⁺ showed trending decreases for all benzene exposure groups that yielded significant diminutions when comparing 18wk HFD fed and benzene-exposed mice compared with HFD fed and HFA-exposed controls. This trend was true for the 24-week old normal chow benzene-exposed animals compared with HFA-exposed controls (Figure 9). Decreases were also seen when comparing NC benzene-exposed animals to 8wk HFD and benzene-exposed animals. The CD62L⁺/Ly6c⁺ subpopulation showed significant changes in the same cohorts and in the same downward trend in cell abundance. Lastly, the CD62L⁻/Ly6c⁻ population demonstrated significant decreases in both 24wk old populations (HFD and NC) when comparing benzene-exposed animals with diet-matched HFA-exposed controls.

Discussion

The major findings of this study are that benzene exposure increases LDL, platelet-leukocyte aggregate formation and that high fat feeding coupled with benzene exposure induces hematotoxicity more rapidly than benzene exposure by itself. Additionally, these changes happen before hematological disruption seen in CBCs in animals on normal chow diet exposed to benzene. Meta-analyses by groups like the ATSDR allow for comparison of many endpoints at different exposure levels, but results are inconsistent between species, among

species of varying genotypes and occasionally among species of the same genotype (17). Thus having multiple toxicological endpoints measured at separate times will allow for relative toxicity assessment. This study also examines how lifestyle factors (i.e. HFD) may alter susceptibility to benzene exposure.

Our 2wk benzene exposure (NC diet) CBC data aligns well with what has been reported in the literature (215, 222), showing a small increase in erythrocytes and trending decreases in B and T cells. Likewise, the near pancytopenias seen after 6wks of 50 ppm benzene exposure (NC diet) demonstrates a stepwise progression towards hallmark hematotoxicity. Interestingly, TEMPOL intervention in benzene-exposed animals blocked the trending increases in circulating cells seen in benzene-exposed animals on normal drinking water. This change was seen in nearly all measured cell types. This suggests that oxidative stress plays a role in the early development of hematotoxicity. This notion is confirmed in other studies. Almost all studies studying chronic (i.e. >1 year) exposure to benzene in humans with genetic polymorphisms in GSTT1, GSTM1 or NQO1 that decrease function and in CYP2E1 or MPO that enhance function suggest that increased susceptibility to hematotoxicity is driven by decreased mitigation of oxidative stress (218, 223, 224). Quite surprisingly, one of these studies determined that GSTT1 null genotypes conferred greater susceptibility to leukopenias in workers chronically exposed to benzene than did polymorphisms in MPO or NQO1, which are enzymes directly involved in hydroquinone-benzoquinone cycling (223).

Importantly, we studied whether a HFD might influence susceptibility to benzene exposure. Given the global epidemic of diet-induced obesity it is imperative to recognize any increased risk posed by this ubiquitous pollutant. Obesity has been shown to increase the benzene metabolizing enzyme's (CYP2E1) expression and activity (225). Studies have also shown that CYP2E1 substrate exposure (i.e. ethanol) enhances sensitivity to benzene toxicity by increasing expression and activity of CYP2E1. Yet it is unknown whether diet, obesity or diabetes influences susceptibility to benzene toxicity. Thus we hypothesized that vulnerability to benzene exposure might be increased in mice fed a high fat diet. Mice on a HFD for 8wks or 18wks that were exposed to benzene demonstrated the same drastic and acute cytopenias. This may be due to enhanced oxidative stress and disruption of the vascular compartment often seen with high fat feeding, along with a disturbance in production of hematopoiesis. In obese states, adipocytes expand within the bone marrow niche which may then disrupt critical structural and chemical components to homeostatic hematopoiesis. Intercellular signaling chemicals (chemokines and cytokines) may inhibit cell cycle of renewing HSCs or egress of maturing cells from the bone marrow. This is the first and clearest indication in this study that suggests that lifestyle factors may increase susceptibility to benzene exposure. Data presented in chapter IV hint that increased adhesion to the bone marrow stroma may be an additional factor that potentiates toxicity by inhibiting cell egress from the medullary cavity. Indeed, one study assessing genetic polymorphisms in benzene-exposed workers with reduced WBCs found the gene

VCAM1 to play a critical role in increasing benzene susceptibility, theoretically likely by inhibiting mature cell mobilization (226).

Monocyte subpopulations were measured in an attempt to assess monocyte phenotype and possible functional changes that might suggest changes in other disease susceptibility. These subpopulations were determined by whether these cells were positively or negatively staining for markers for Ly6c and CD62L. Ly6c⁻ monocytes have been shown to secrete anti-inflammatory factors and promote tissue repair (227), whereas Ly6c⁺ monocytes are involved in phagocytosis and pro-inflammatory processes and are thought to be of relative equal abundance in mice with Ly6c⁻ monocytes, depending on the mouse strain (227). CD62L (L-selectin) is a crucial homing receptor which is required to initiate monocyte rolling and adhesion and is involved in inflammatory processes (228). However, all monocyte subpopulations show a strong decrease in abundance and may infer decreased overall monocyte activity in the organism.

We measured early endpoints affected by benzene exposure such as ALT, AST, albumin, NAP, liver:body weight and PLAGgs. Other investigations have documented that benzene exposure increases liver weights in rats, although additional hepatic markers were not measured to confirm findings (216). Here we demonstrate that liver:body weight ratios are increased after 2wks of exposure with corresponding increases in ALT and AST. ALT is used as a marker of hepatic injury, and increases in plasma levels of ALT reflect liver inflammation. AST is found in many organs such as striated muscle, liver, kidney, brain, and erythrocytes. Elevation of this enzyme is often associated with

skeletal muscle or cardiac damage (e.g., it is increased after myocardial infarction) (229). This transient increase is also associated with a decrease in plasma albumin protein and a corresponding increase in NAP. These results taken together suggest that exposure to benzene induces both hepatic and systemic inflammation and injury. However, albumin is primarily a carrier protein and it transports many metabolites, hormones, amino acids and products of toxic degradation (230). Therefore, depletion in albumin may also suggest that albumin is being depleted as a result of increased conjugated metabolite transport. Mice exposed to benzene for 6wks demonstrate a return to near normal levels of albumin, which may be due to increased hepatic production in response to increased demand via conjugated metabolite transport. Interestingly, though, long term insulin resistance is associated with elevated albumin levels in human subjects and thus the increase in albumin in benzene-exposed mice is likely a composite of increased hepatic production and a byproduct of insulin resistance (231).

Notably, circulating endothelial-derived microparticles (of any subpopulation) were not elevated after 2wks of benzene exposure. While these circulating microparticles are often used as a sensitive biomarker for endothelial dysfunction, the variability within our measurements due to flow cytometry limits of detection does not lend it to be a sensitive biomarker for subtle changes and may not be helpful as a determinant of vascular health in this specific instance (232, 233). However, there simply may be no change in circulating microparticles at this time.

A novel finding of this study is that PLAGg formation increases with benzene exposure. Generation of these aggregates, which is often an indicator of endothelial dysfunction, showed consistent, reproducible results and were consistently elevated after benzene exposure. There are many reasons why increased aggregation may take place. The PLAGg may arise due to increased oxidative stress and decreased nitric oxide bioavailability (234). Furthermore, PLAGg formation is strongly associated with inflammation (235, 236). We therefore utilized the TEMPOL intervention to assess what role oxidative stress may play in driving PLAGg formation following benzene exposure. While a trending decrease in PLAGg formation in TEMPOL administered, benzene-exposed animals was observed relative to benzene-exposed animals, the relative increase of PLAGg formation compared with the TEMPOL administered HFA-exposed animals was not diminished. This suggests that either ROS do not play a role in PLAGg formation following benzene exposure or that the dose of TEMPOL administered was not sufficiently high to return the PLAGg levels to baseline.

Another interesting finding from this study was the development of hypercholesterolemia in mice after benzene exposure. While HDL and LDL were both increased in mice with benzene exposure, LDL disproportionately increased over HDL. Total cholesterol was increased as well. The increase in LDL may be a sign of hepatocyte injury and insulin resistance. Other studies (that follow our findings in chapter III) have shown early development of hepatic insulin resistance and a strong link between hepatic insulin resistance and enhanced

LDL secretion. Treatment of hepatocytes with PI3-K inhibitors has demonstrated that the insulin signaling pathway is important for insulin-stimulated reduction in apoB secretion (191-193). Thus, many IR and T2D subjects with diminished PI3-K signaling show excessive release of LDL (163, 193, 237). Alternately, insulin stimulation can decrease expression of microsomal triglyceride transferase protein (MTP) through the MAPK pathway and increased MTP expression has been shown to increase LDL production (193, 237). Lastly, increased free fatty acid flux to these insulin resistant tissues can provide increased triglyceride uptake and therefore substrate for LDL production. These trends in LDL levels are in keeping with the increased HOMA-IR scores of benzene-exposed animals. Given the likelihood of hepatotoxicity after benzene exposure, this constellation of biological indicators would be likely to appear together as seen in this study.

Conclusions

Taken together, these results demonstrate that PLAGg formation, plasma enzyme detection are elevated in mice after 2wks of benzene exposure while CBCs remained unchanged at this time. Anti-oxidant intervention with TEMPOL appeared to protect from disrupted blood count disturbances and marginally decreased PLAGg formation, suggesting that oxidative stress plays a significant role in these processes. Additionally, PLAGg formation has not been associated with benzene exposure until this study. Interestingly, susceptibility to benzene exposure appears to increase with age in these animals (comparing 14 and 24 wk old mice), independent of diet as evidenced by cytopenias detected in CBC

and immune panels. Additionally, mice receiving 8wks HFD feeding and 2wks of 50ppm benzene exposure showed cytopenias similar to NC fed animals exposed to benzene for 6wks suggesting that 14wk old mice relative to 24wk old mice fed a HFD increases toxicity of benzene exposure.

CHAPTER III

BENZENE EXPOSURE AND INSULIN RESISTANCE

Introduction

Benzene is a ubiquitous volatile pollutant and is generated by petroleum, plastics, glue and shoe industries, automobile exhaust, wildfires and cigarette smoking. Benzene concentrations in glue, rubber and shoe factories can frequently be found to be >100 ppm and poorly ventilated, heavily trafficked tunnels have been measured to have >1000 ppm benzene. Consequently, benzene can be found in virtually all air samples (urban and rural) as was reported by the National Human Exposure Assessment Survey. Here we hypothesize that benzene metabolism by hepatic-CYP450 2E1 generates reactive oxygen species (ROS) which may cause inflammation, insulin resistance (IR) (Figure 10).

In our experiments, we exposed C57Bl/6 mice to 50 ppm benzene for 6h/d x 14d or 6wks. This concentration of benzene is similar to that found in main stream cigarette smoke, which is the primary source of global human benzene exposure. To test the role of ROS in these processes we utilized an anti-oxidant (4-hydroxy TEMPO, or TEMPOL) intervention to see if benzene induced metabolic changes could be mitigated. Additionally, we examined the effects of insulin resistance (IR) induced by a HFD, to assess whether greater CYP2E1

ROS generation exaggerates the effects of benzene. These interventions attempt to understand how oxidative stress is involved in the physiological response to benzene but also to understand how lifestyle choices may confer greater susceptibility to benzene toxicity. Given the pervasive nature of volatile benzene and its association with inflammation, we hypothesized that benzene exposure may contribute to the rapidly emerging global epidemic of human obesity, diabetes and cardiovascular disease.

Methods

Volatile Benzene Exposures

All procedures were approved by the University of Louisville Institutional Animal Care and Use Committee. Benzene exposures were performed as described in Chapter II. Briefly, mice were maintained on NC or HFD with normal drinking water or TEMPOL intervention and subsequently exposed to HFA or volatile benzene for 14d or 6wks. Necropsy was performed immediately after the final exposure.

***In Vivo* Assessment of Glucose Handling**

Fasting plasma glucose levels were recorded following a 6h fast with a standard glucose meter (Accu-check, Aviva) and glucose test strips (Accu-check, Aviva Plus). Fasting plasma insulin levels were measured by an ultrasensitive insulin ELISA assay (Mercodia) from supernatant of peripheral blood spun at 400 x g for 20min. As described before (238), glucose tolerance tests were performed

following a 6h fast by injection (i.p.) of D-glucose (1 mg/g) in sterile saline. Insulin tolerance tests were performed on nonfasted animals by i.p. injection of 1.0 U/kg Humulin R (Eli Lilly, Indianapolis, IN). Tissue specific insulin-stimulated phosphorylation of Akt analysis was conducted by injecting saline or insulin 15min prior to tissue extraction with immediate freezing in liquid nitrogen. Protein and RNA extracts from frozen samples were later obtained for Western blot analysis.

Western blotting and qPCR

Tissue homogenates were prepared from frozen tissue using a pulverizer or Dounce homogenizer and used for Western blot protein expression analysis. For quantitative RT-PCR, RNA extracted from tissues with a Qiagen miRNA isolation kit was used to assess NF κ B target expression of cytokines MIP-1 α , IL-1 β , IL-6, TNF- α , and adiponectin. Primers for mRNA targets were obtained from Integrated DNA Technologies and qPCR was performed using Universal SYBR Green PCR Master Mix (Stratagene). Analysis of miRNAs utilized the same Qiagen isolation kit and TaqMan primers, and master mixes (Applied Biosystems) was then used to generate cDNA and perform qPCR. Western blotting conditions were performed under standard conditions. Briefly, SDS-PAGE was performed for 1.25h at 125V, membrane transfers were conducted for 16-18h at 200mAmps, with blocking at room temperature for one hour with 5% non-fat milk solution followed by 2h incubation at room temperature with primary antibody. The blot was then washed three times with TBST, and the appropriate secondary

antibody was added to the blot with 5% non-fat milk and incubated at room temperature for one hour. The blots were developed using ECL developing solution (Thermo Fisher) and the image obtained on a Typhoon 7000 FLA (GE Healthcare) imaging system. Quantification of bands on the western blot was performed using ImageJ software (NIH.gov). Antibodies used for western blotting analysis were Akt, phospho-Akt (Ser473), NF κ B p65, phospho-NF κ B p65 (Ser536), phospho-pan-Tyrosine and PTEN (Cell Signaling), SOCS1 and SOCS3 (AnaSpec), IRS-2 (Abnova). Secondary antibodies were anti-mouse IgG and anti-rabbit IgG, HRP-linked antibodies (Cell Signaling).

Oxidative Stress Measurements

Glutathione (GSH) measurements were obtained using frozen liver and skeletal muscle specimens and analyzed using a kit BIOXYTECH GSH -412TM Colorimetric Determination Glutathione Kit (Oxis Research). Standard protocol given by the manufacturer was followed. Samples in a 96 well plate were read on a BioTek plate reader to obtain quantification capacity. To measure intracellular GSH, monochlorobimane dissolved in 100% ethanol to a stock concentration of 40 mM and stored at -20 °C was thawed and added to the leukocyte suspension from peripheral blood draw to a final concentration of 40 μ M and the cells were maintained at room temperature in the dark for 20min prior to analysis of the cells on the LSRII flow cytometer. To measure lipid peroxidation product malondialdehyde (MDA), we again utilized frozen liver and skeletal muscle tissues and employed the commercially available Lipid

Peroxidation (MDA) Assay Kit (Sigma). As before, we followed the standard protocol provided by the manufacturer and read the samples in a 96 well plate on a BioTek plate reader to obtain quantification by fluorescence optical density measurements (excitation 532nm, emission 553nm).

Results

Effect of benzene exposure on glucose and insulin levels. As seen in Figure 11, mice exposed to volatile benzene for 2wks showed an increase in FPG at day 14 of the exposure ($p=0.0004$). This significant increase in FPG was lost in animals exposed to benzene for 6wks, though an upward trend in glucose levels still remained ($p=0.097$). Additionally, FPI levels were elevated in mice after 2 ($p=0.034$) and 6wks ($p=0.0008$) of benzene exposure. HOMA-IR was significantly increased in benzene-exposed animals at 2 and 6wks (72% and 80%, respectively). Giving greater clarity to the phenotype, HOMA- β also exhibited significantly increased values after 2 and 6wks of benzene exposure (65% and 72%, respectively). Mice exposed to benzene or filtered air for 2wks and allowed to remain unexposed for 4wks (Figure 12) demonstrated significantly elevated FPG compared with HEPA controls. Correspondingly, FPI and HOMA-IR also trended towards an increase in animals exposed to benzene, but likely did not achieve significance because of the low number of animals available for insulin testing ($p=0.10$, $n=3$). HOMA- β did not show a significant change or strong trend with benzene exposure.

Glucose tolerance tests on benzene-exposed animals demonstrate a modest, but significant increase in area under the curve (AUC) after 2wks of benzene exposure relative to HFA-exposed animals (Figure 13). Interestingly, insulin tolerance tests demonstrated a remarkable decrease in insulin sensitivity as seen in the insulin tolerance test (ITT) AUC indicating that animals are requiring more insulin to sequester less glucose than controls. This is in keeping with a pre-diabetes phenotype.

Insulin signaling in the liver and skeletal muscle after benzene exposure.

Animals exposed to benzene for either 2 or 6wks of exposure demonstrated a significant decrease in insulin-stimulated phosphorylation of Akt in the liver (Figure 14). While 2wk HFA-exposed mice demonstrated a 2.8-fold ($p < 0.0001$, $n = 10$) induction of Akt phosphorylation upon insulin stimulation, benzene-exposed animals demonstrated no induction capacity of Akt phosphorylation. Additionally, 6wk benzene-exposed animals also exhibited an ablation in hepatic insulin signaling. Additionally, while skeletal muscle also exhibited a decrease in insulin-stimulated phosphorylation of Akt after benzene exposure, the magnitude of decrease was less than that seen in liver (Figure 15). The induction of phosphorylation of Akt in skeletal muscle of HFA-exposed mice was 2.5-fold ($p < 0.05$, $n = 10$) while benzene-exposed mice demonstrated an insignificant 1.6-fold increase in Akt phosphorylation (Figure 16), suggesting that benzene exposure decreases insulin-induced Akt phosphorylation.

Evidence of oxidative stress in the liver and skeletal muscle after benzene exposure. Indicators of oxidative stress were measured in the liver, plasma and

skeletal muscle by measuring GSH, monochlorobimane (MCB) and malondialdehyde (MDA) (Figure 18). Hepatic GSH levels were decreased from 12.2 ± 0.7 μ moles/g tissue in HFA-exposed mice to 9.0 ± 1.3 μ moles/g tissue in 2wk exposed benzene animals ($p < 0.0001$, $n = 9-10$). A 44% reduction ($p < 0.0001$, $n = 9$) of GSH was seen in livers of animals exposed to benzene for 6wks. Additionally, 6wk exposed animals exhibited an 18% reduction ($p = 0.028$) in hepatic GSH compared with animals exposed to benzene for 2wks. Skeletal muscle of 2wk exposed benzene mice also demonstrated a reduction in GSH (Figure 18). MCB, a GSH dye, was measured in stained circulating leukocytes of 2wk HEPA or benzene-exposed mice. HFA-exposed mice exhibited higher levels of MCB mean fluorescence intensity relative to benzene-exposed animals when measured by flow cytometry. Additionally, MDA, a lipid peroxidation product, was found to be of higher abundance in 2wk exposed benzene animals than HEPA exposed mice.

Evidence of inflammation-associated insulin resistance following benzene exposure. To understand whether ROS generation might be driving inflammation-driven IR, markers of inflammation such as NF κ B, cytokines, and suppressors of cytokines (SOCS) were assayed. Phosphorylation of NF κ B subunit p65 relative to total NF κ B (Figure 20) was found to be elevated in livers of mice exposed to benzene for 2wks and 6wks. Congruently, levels of NF κ B subunit p65 phosphorylation relative to total NF κ B p65 (Figure 21) exhibited an increase in skeletal muscle of mice exposed to benzene for 2wks and 6wks.

Figure 10.

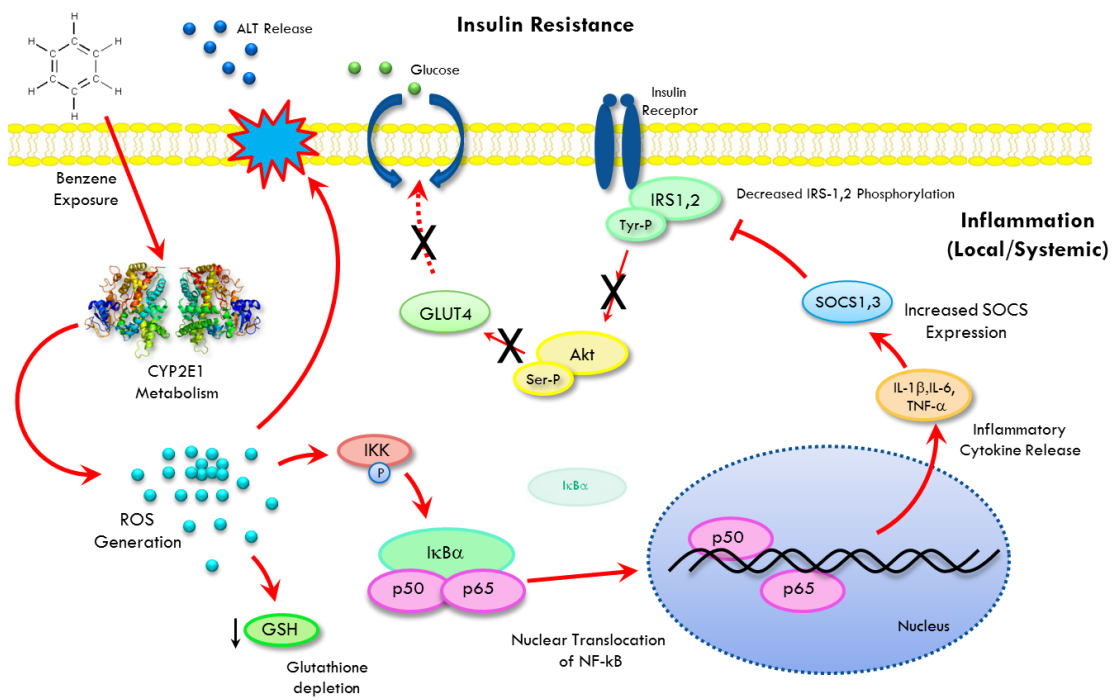


Figure 10. Schematic of benzene-induced liver injury and subsequent insulin resistance. In this proposed model for benzene-induced pathology, benzene metabolism by CYP2E1 generates oxidative stress, induces inflammatory signaling pathways, upregulates cytokines, and upregulates SOCS proteins thereby inhibiting insulin signaling pathways.

Figure 11.

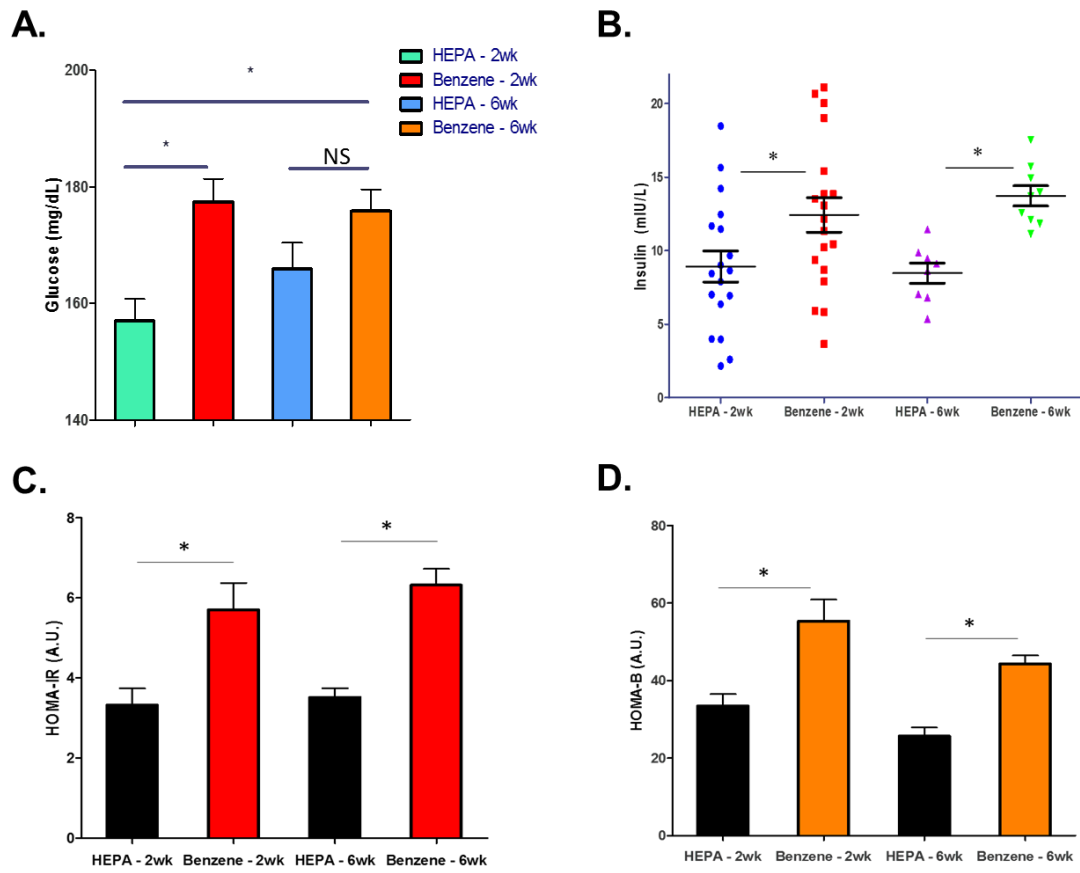


Figure 11. Benzene exposure and glycemic indices. Mice were exposed to HFA or 50ppm benzene for 2 or 6wks in 6 separate exposures, FPG and FPI were measured, and composite HOMA-IR and HOMA- β scores calculated. Indicated are absolute FPG (A), FPI (B), HOMA-IR (C) and HOMA- β (D). FPG: n=20-36 mice/treatment; FPI, HOMA-IR, HOMA- β : n=8-18 mice/treatment; *p<0.05.

Figure 12.

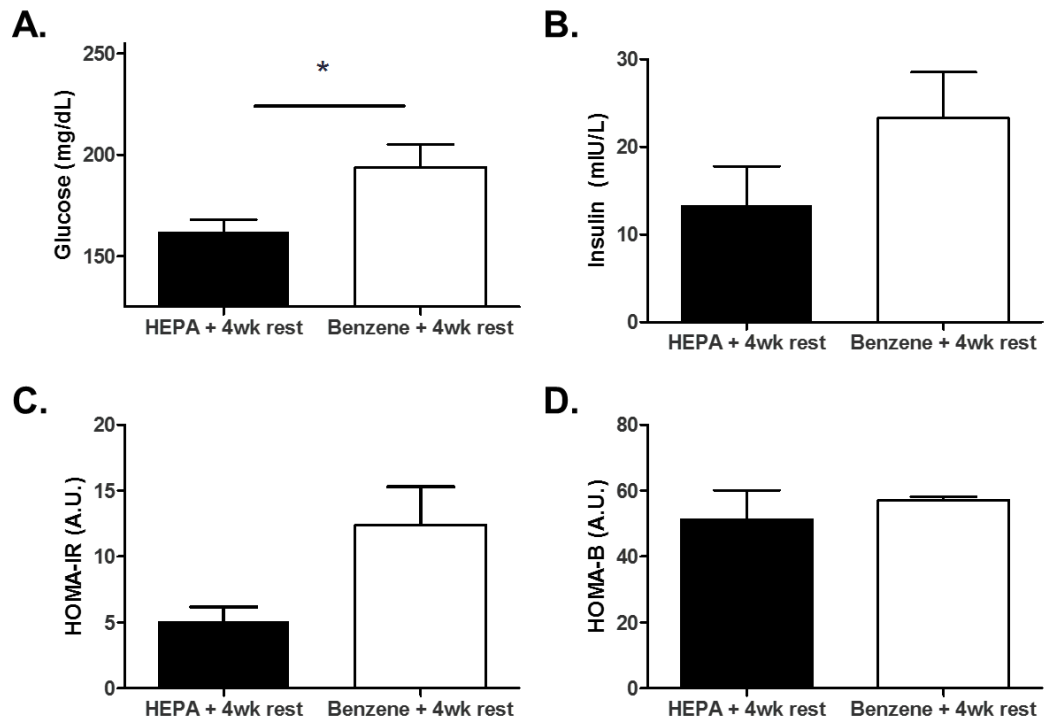


Figure 12. FPG, FPI, HOMA-IR and HOMA- β in animals 4wks-post exposure.

Glycemic indices were measured in animals exposed to benzene or HFA for 2wks and then left unexposed for 4wks. FPG (A), FPI (B), HOMA-IR (C) and HOMA- β were assayed after a 6h fast. FPG: n=7 mice/treatment; FPI, HOMA-IR, HOMA- β : n=3 mice/treatment; *p<0.05.

Figure 13.

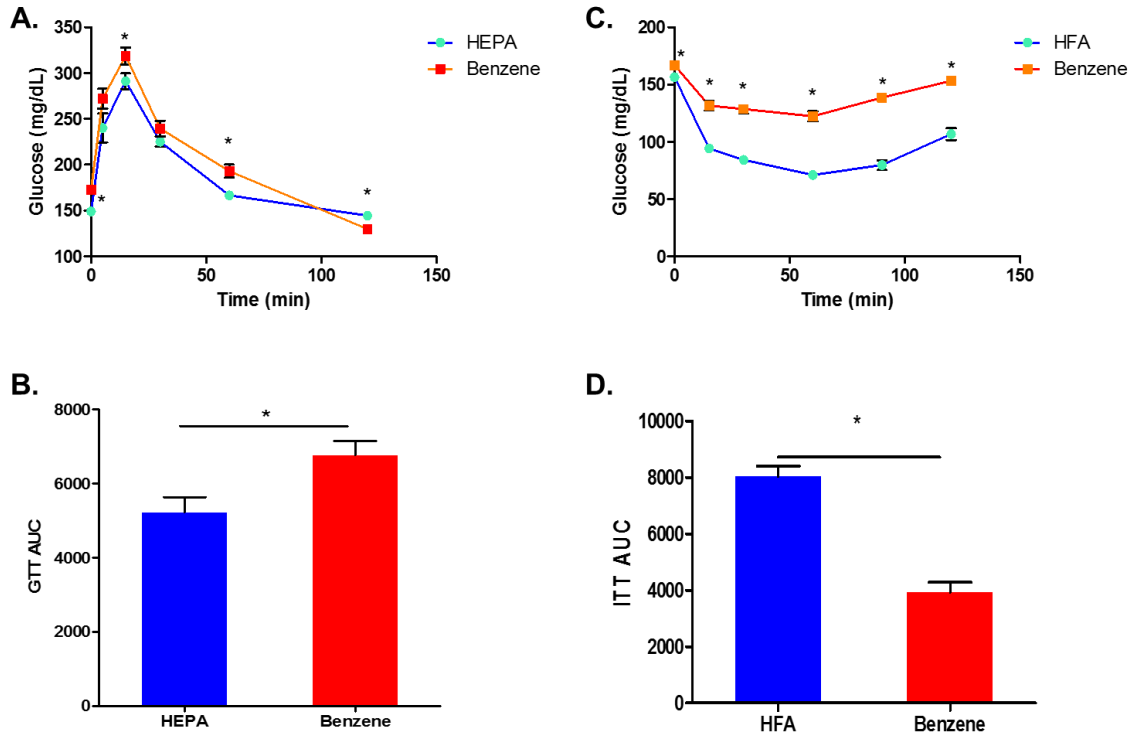


Figure 13. Glucose tolerance tests and insulin tolerance tests after benzene exposure. Mice were exposed to HFA or 50ppm benzene for 2wks and GTTs and ITTs were performed as described. Indicated are absolute glucose levels after glucose bolus for GTT (A), AUC score calculated for GTT (B), absolute glucose levels after insulin bolus for ITT (C) and AUC score calculated for ITT (D). n=10 mice/treatment; *p<0.05.

Figure 14.

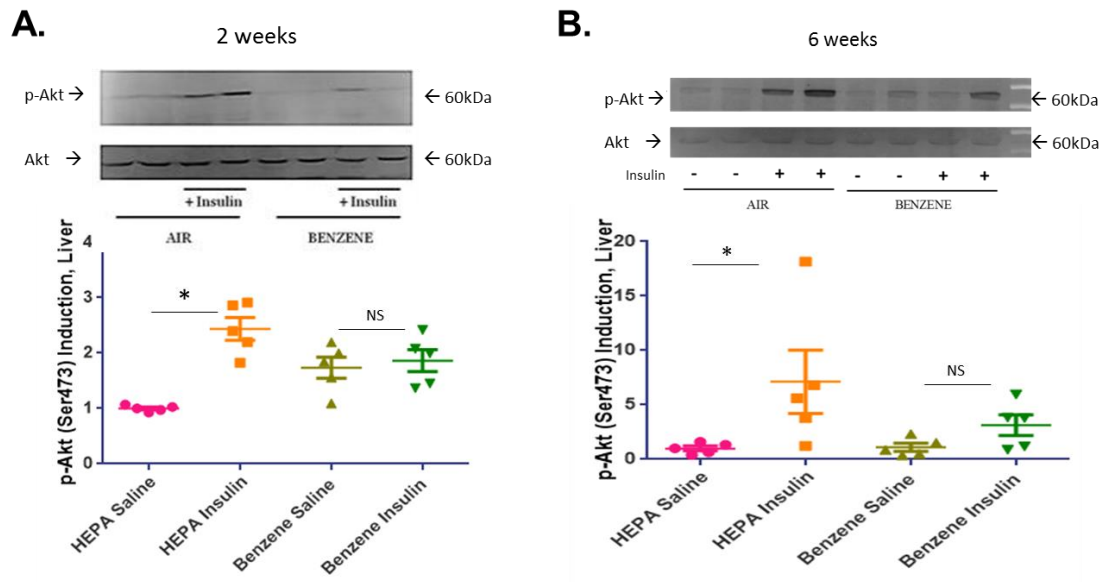
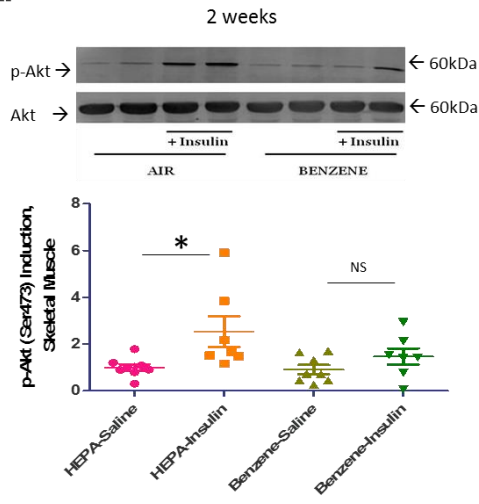


Figure 14. Insulin-stimulated Akt phosphorylation in liver. Mice were exposed to HFA or 50ppm benzene for 2wks (A) or 6wks (B) and then injected with saline or insulin 15min before euthanasia. Levels of insulin-stimulated phospho-Akt were then measured in homogenates of collected livers. Illustrated are representative blots of phospho-Akt and pan-Akt (upper panels). Also illustrated are grouped data from 2 individual experiments and 5 animals. *p<0.05.

Figure 15.

A.



B.

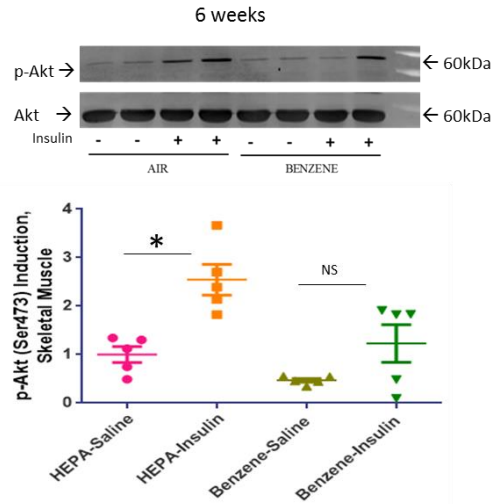


Figure 15. Insulin-stimulated Akt phosphorylation in skeletal muscle. Mice were exposed to HFA or 50ppm benzene for 2wks (A) or 6wks (B) and then injected with saline or insulin 15min before euthanasia. Levels of insulin-stimulated phospho-Akt were then measured in homogenates of collected skeletal muscle. Illustrated are representative blots of phospho-Akt and pan-Akt (upper panels). Also illustrated are grouped data from 2 individual experiments and 5 animals. * $p < 0.05$.

Figure 16.

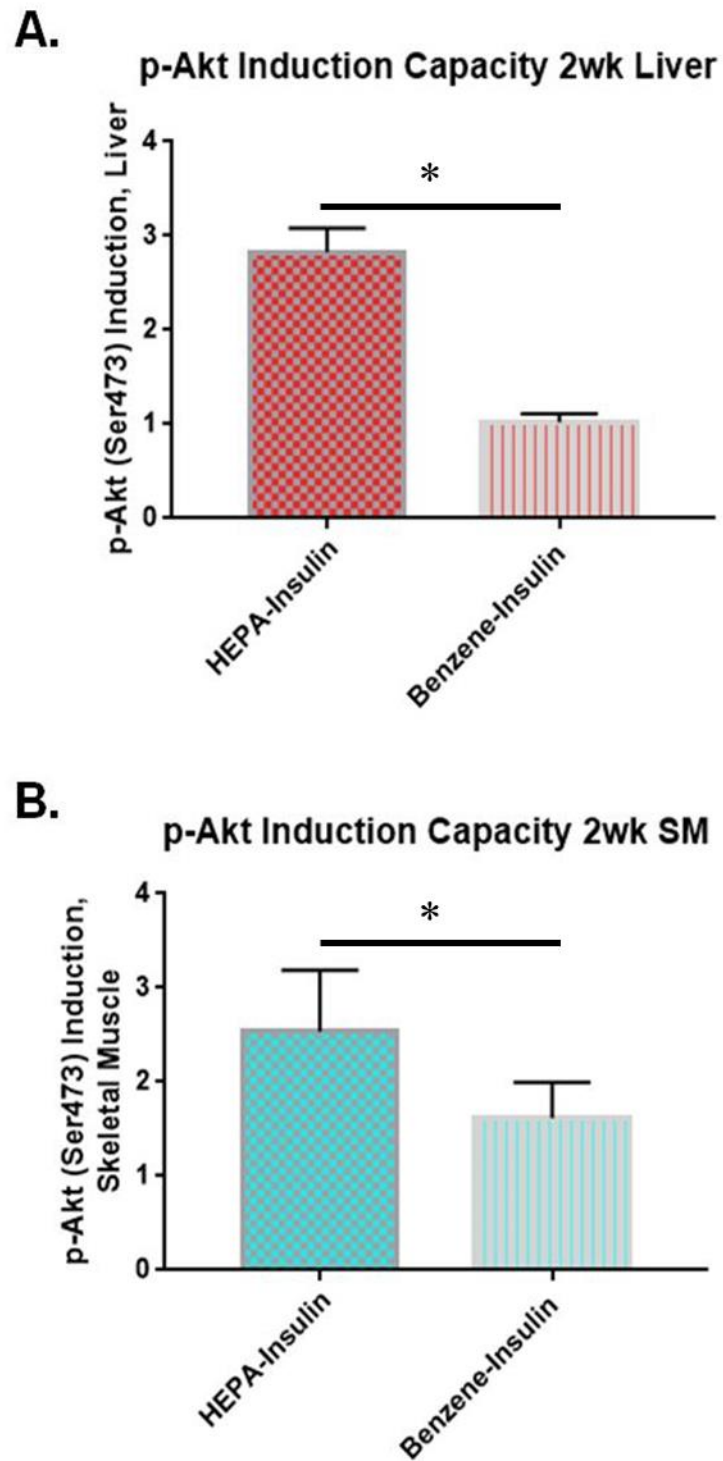


Figure 16. Phospho-Akt induction capacity. The capacity of tissue homogenates to induce Akt phosphorylation after insulin stimulation was measured by comparing each sample to its HFA control as illustrated for liver (A) and skeletal muscle (B) above. n=5 mice/treatment; *p<0.05.

Figure 17.

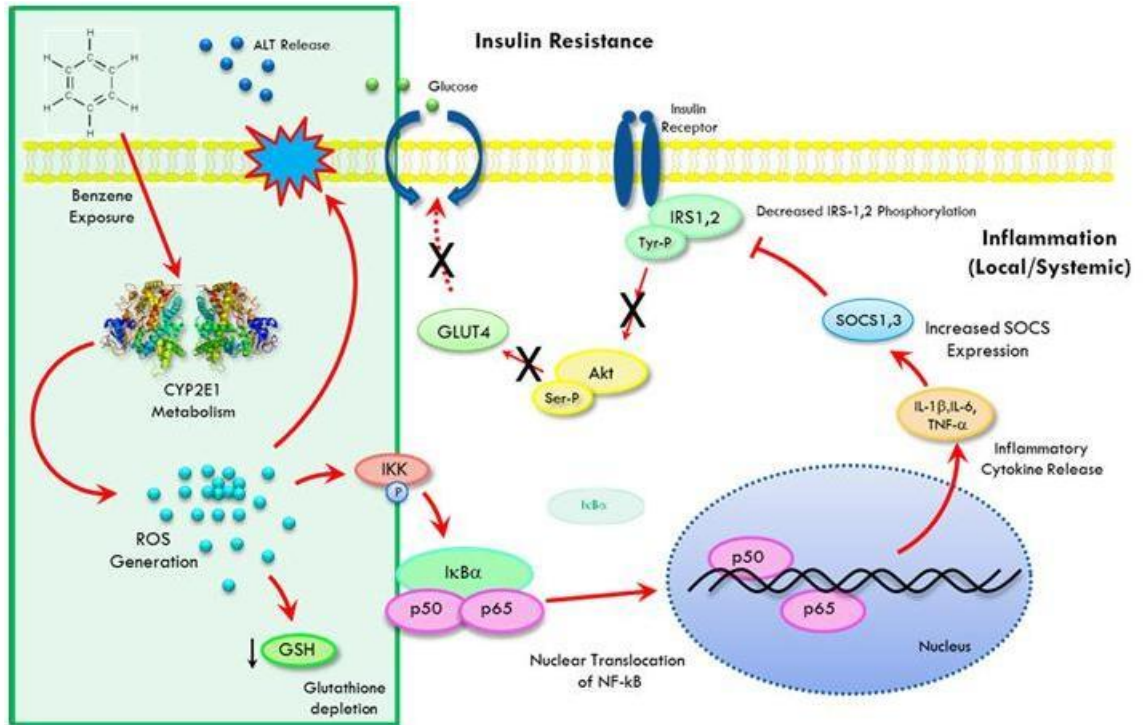
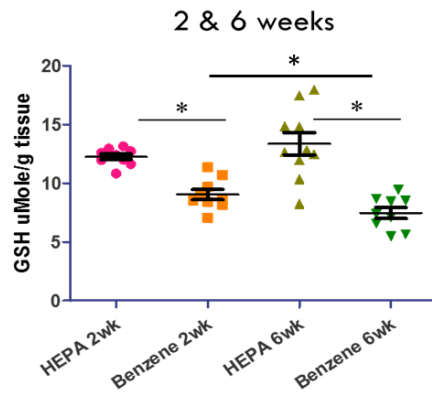


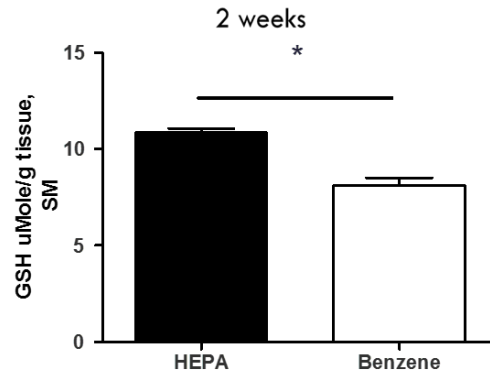
Figure 17. Schematic of benzene-induced liver injury and subsequent insulin resistance emphasizing ROS production. In this proposed model for benzene-induced pathology, benzene metabolism by CYP2E1 generates oxidative stress, induces inflammatory signaling pathways, upregulates cytokines, and upregulates SOCS proteins thereby inhibiting insulin signaling pathways. Here we highlight the ROS production of the schematic.

Figure 18.

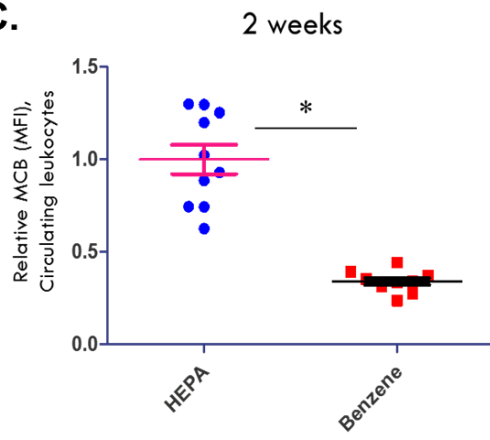
A.



B.



C.



D.

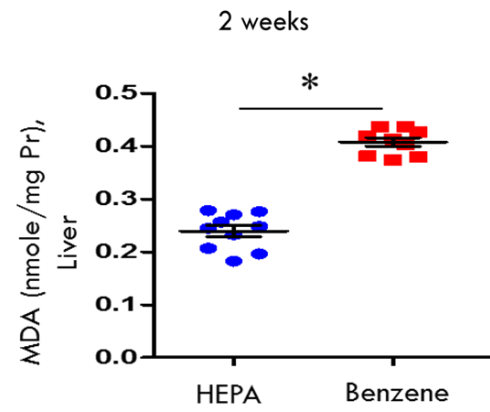


Figure 18. Benzene-induced markers of oxidative stress. Mice were exposed to HFA or 50ppm benzene for 2 or 6wks and euthanized. MCB levels were measured in circulating lymphocytes by flow cytometry and normalized to levels in filtered air-exposed animals (C). In addition, levels of GSH was measured in homogenates of liver (A) and skeletal muscle (B). MDA was measured in homogenates of liver (D). n=8-10 mice/treatment; *p<0.05.

Figure 19.

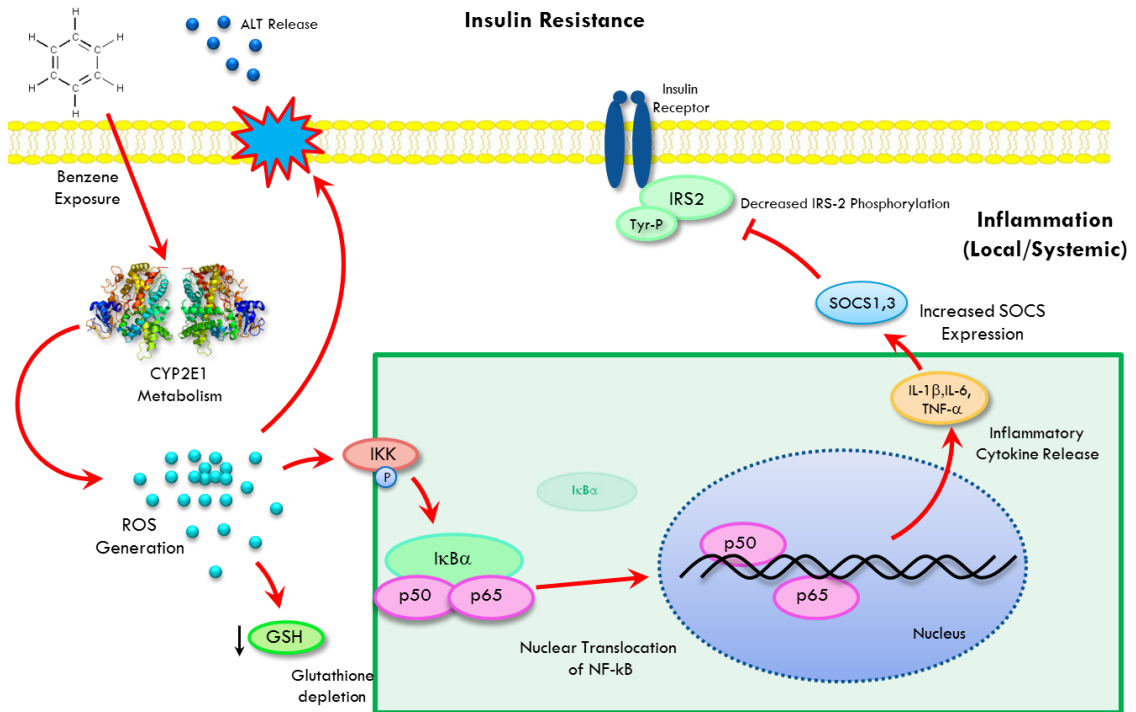


Figure 19. Schematic of benzene-induced liver injury and subsequent insulin resistance highlighting inflammatory signaling. Benzene metabolism by CYP2E1 generates oxidative stress, induces inflammatory signaling pathways, upregulates cytokines, upregulating SOCS proteins thereby inhibiting insulin signaling pathways. Here we highlight the inflammatory signaling pathways.

Figure 20.

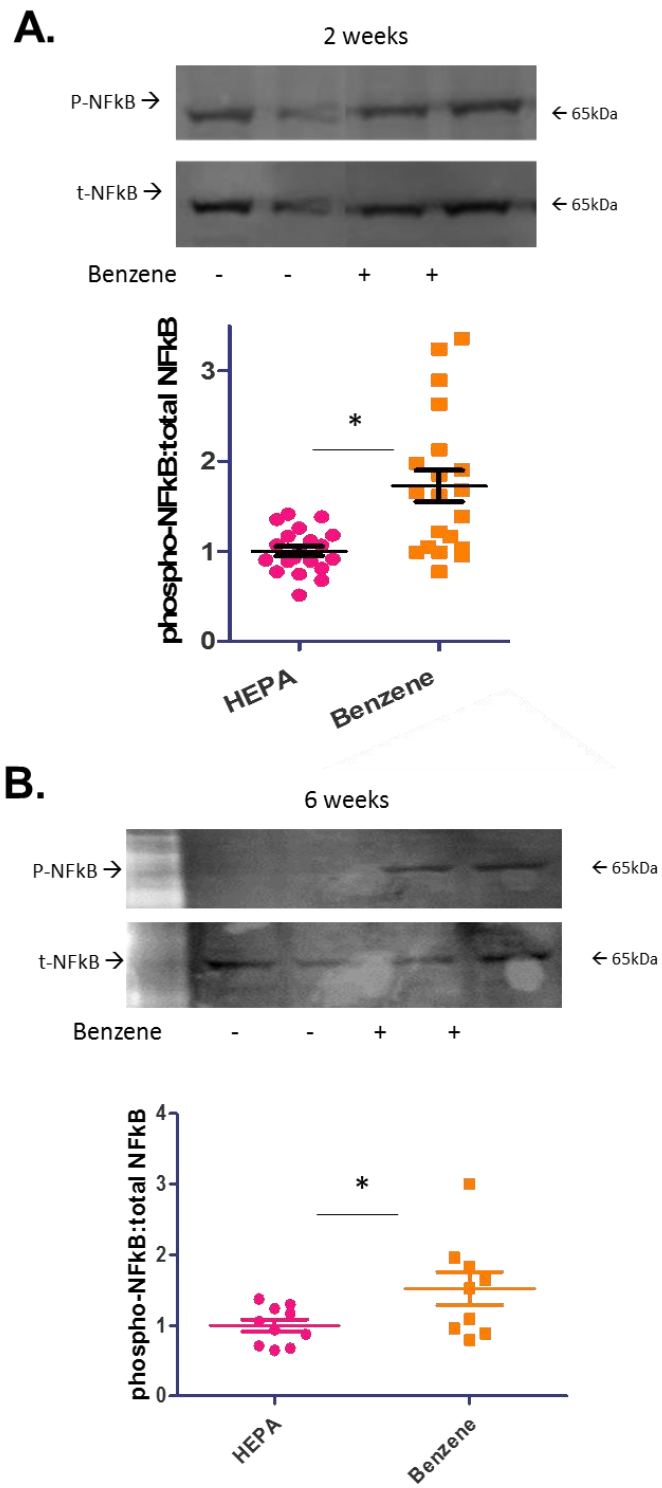


Figure 20. Nuclear factor kappa-B (NF κ B) phosphorylation in liver. Mice were exposed to HFA or 50ppm benzene for 2wks (A) or 6wks (B) and then euthanized. Levels of NF κ B p65 phosphorylation and total NF κ B p65 in liver homogenates were determined by Western blotting. Illustrated are representative blots (upper panels) and normalized data (lower panels). 2wk: n=20 mice/treatment; 6wk: n=8-10 mice/treatment; *p<0.05.

Figure 21.

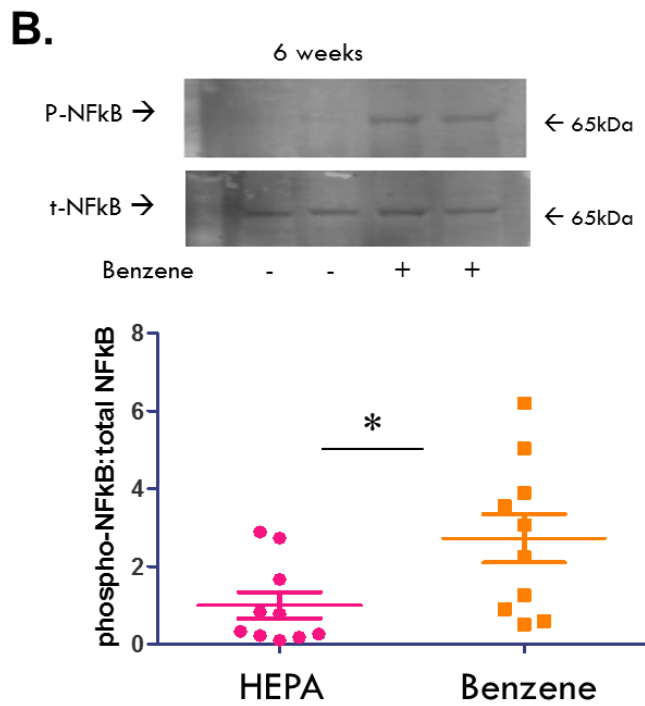
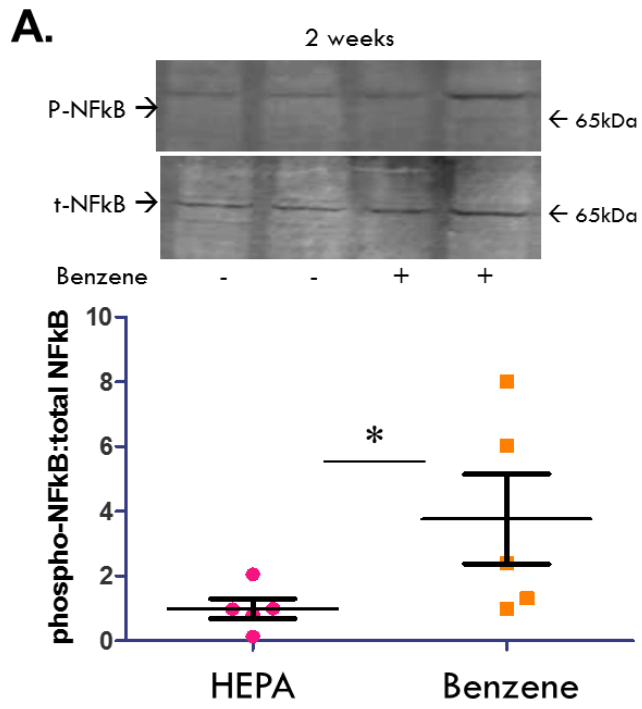


Figure 21. Nuclear factor kappa-B (NF κ B) p65 phosphorylation in skeletal muscle. Mice were exposed to HFA or 50ppm benzene for 2wks (A) or 6wks (B) and then euthanized. Levels of NF κ B p65 phosphorylation and total NF κ B p65 in skeletal muscle homogenates were determined by Western blotting. Illustrated are representative blots (upper panels) and normalized data (lower panels). 2wk: n=5 mice/treatment; 6wk: n=10 mice/treatment; *p<0.05.

Figure 22.

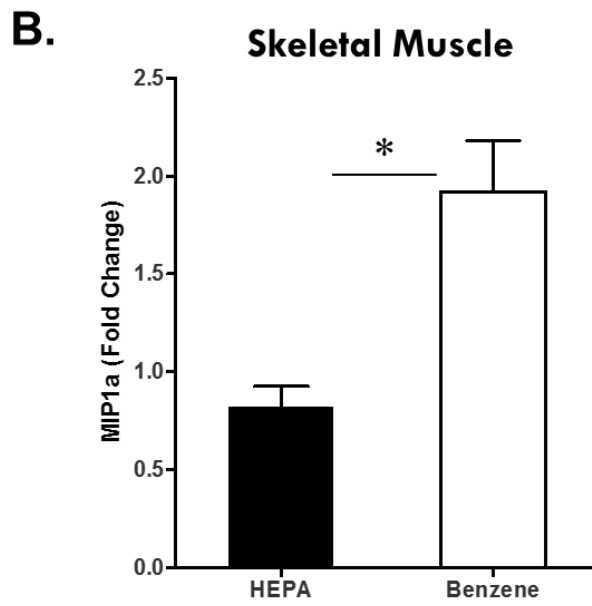
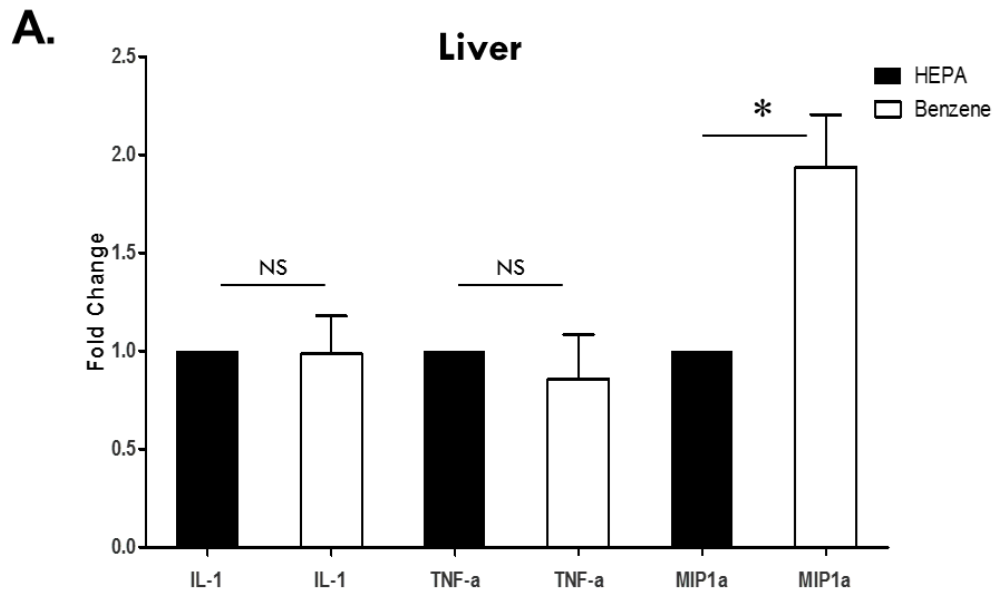


Figure 22. NF κ B-targeted cytokines. Mice were exposed to HFA or 50ppm benzene for 2wks and then euthanized. Quantitative PCR of selected cytokine transcripts was then performed on RNA preparations of liver (A) and skeletal muscle (B). Illustrated are the fold changes using GAPDH as housekeeping control gene. n=8-10 mice/treatment; *p<0.05.

Figure 23.

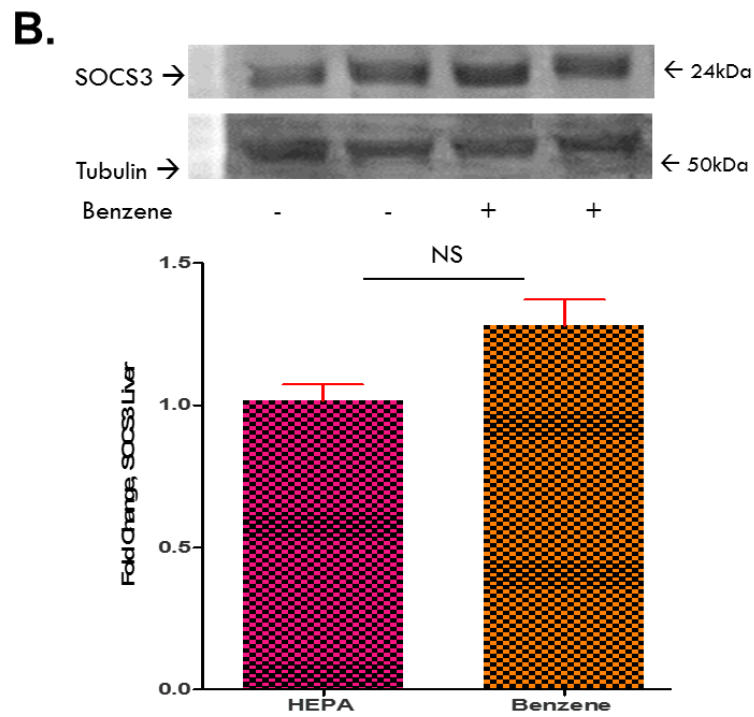
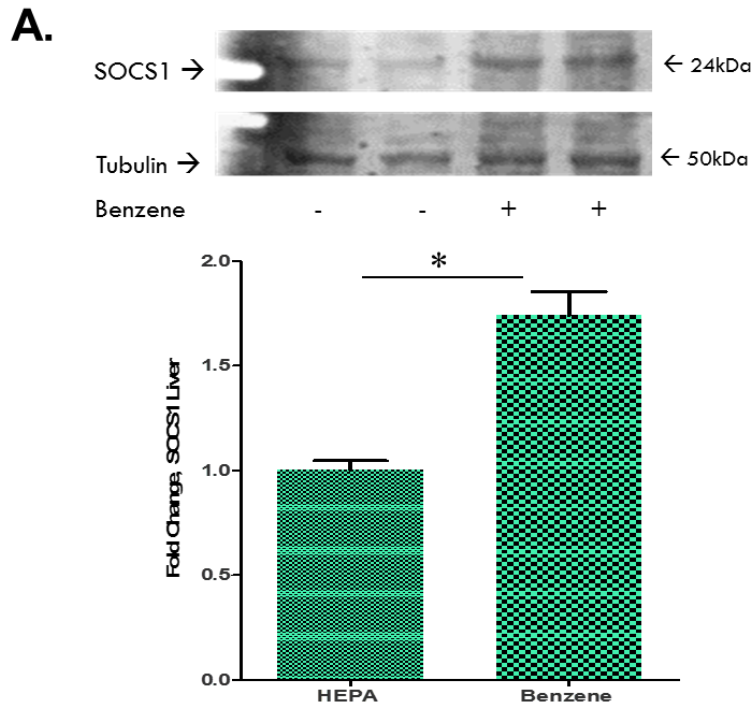


Figure 23. Benzene exposure and cytokine regulating proteins. Mice were exposed to HFA or 50ppm benzene for 2wks and then euthanized. Levels of the cytokine suppressor proteins SOCS1 (A) and SOCS3 (B) were determined in liver homogenates by Western blot analysis. Tubulin blots were used as loading controls. Illustrated are representative blots (upper panels) and normalized data (lower panels). n=4 mice/treatment; *p<0.05.

Figure 24.

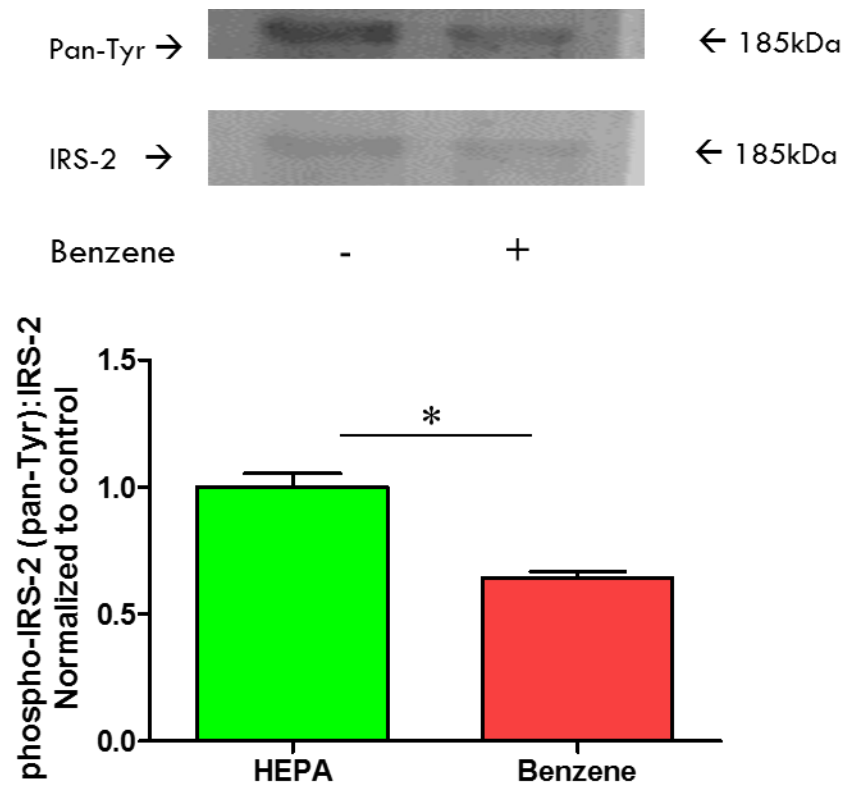


Figure 24. IRS-2 pan-tyrosine phosphorylation in liver. Mice were exposed to HFA or 50ppm benzene for 2wks and then euthanized. IRS-2 was immunoprecipitated from liver homogenates, collected proteins resolved by SDS-PAGE and transferred to nitrocellulose. The blots were probed with a pan-phospho-tyrosine antibody and an IRS-2 antibody. Illustrated are representative blots (upper panels) and quantitative data (lower panels). n=5 mice/treatment; *p<0.05.

To ascertain whether targets of NF κ B were upregulated a panel of cytokines were measured. Transcripts (mRNA) of inflammatory cytokines IL-1 β , IL-6, TNF α , and MIP-1 α were assayed in liver of benzene and HFA-exposed mice. IL-1 β , IL-6, TNF α demonstrated no significant increase in the liver after 2wks of exposure. However, MIP-1 α was upregulated 1.94-fold in liver tissue of benzene-exposed animals relative to HFA-exposed mice controls (p=0.007, n=10) (Figure 22). Benzene-exposed animals also displayed a 1.91-fold increase in MIP-1 α in skeletal muscle relative to controls (p=0.003, n=8). After finding cytokine levels elevated in both liver and skeletal muscle, we measured the abundance of both SOCS1 and SOCS3 (Figure 23). In these experiments we found SOCS1 elevated (1.74-fold, p=0.004, n=4) in the liver of 2wk benzene-exposed mice while the upward trend in SOCS3 expression did not reach significance (1.28-fold, p=0.058, n=4). Due to the inhibitory relationship of SOCS1 expression on IRS2 phosphorylation we immunoprecipitated IRS-2 to detect tyrosine phosphorylation of the substrate (Figure 24). Benzene-exposed animals displayed decreased IRS-2 total tyrosine phosphorylation relative to total IRS-2 as compared with phosphorylation of HFA-exposed controls.

Anti-oxidant 4-hydroxy TEMPO intervention and metabolic indices. Given the suggestive evidence that oxidative stress may be mediating the insulin resistant phenotype seen in benzene-exposed animals, the anti-oxidant (4-hydroxy TEMPO, or TEMPOL) was administered via drinking water *ad libitum* to a group of animals. Mice receiving TEMPOL intervention, but exposed to benzene showed significantly lower FPG (Figure 26) than their benzene-exposed

counterparts receiving no anti-oxidant intervention (i.e. normal drinking water). Additionally, there was no significant increase in FPG of TEMPOL administered, benzene-exposed mice compared with TEMPOL administered, HFA-exposed mice. Correspondingly, FPI of benzene-exposed animals receiving TEMPOL was decreased when compared with benzene-exposed animals without intervention. There was no significant difference in FPI between HFA exposed animals receiving TEMPOL and benzene-exposed animals with TEMPOL intervention ($p=0.40$). Composite HOMA-IR score of benzene-exposed mice without intervention was 34% higher ($p=0.018$) than benzene-exposed animals with TEMPOL intervention. Correspondingly, benzene-exposed animals receiving anti-oxidant intervention received demonstrated normoglycemic responses to glucose and insulin bolus in GTT and ITT assays (Figure 27), suggesting that altered insulin sensitivity was mediated by oxidative stress.

Intracellular insulin signaling appeared to be protected by TEMPOL intervention (Figure 28). Induction of insulin-stimulated phosphorylation of Akt in liver of benzene-exposed animals without intervention was significantly less than benzene-exposed animals receiving TEMPOL. Animals receiving TEMPOL intervention exposed to HEPA or benzene showed no significant difference in induction capacity for Akt phosphorylation upon insulin stimulation ($p=0.56$, $n=5$). Similar results were found in skeletal muscle of TEMPOL treated animals. Insulin-stimulated Akt phosphorylation in skeletal muscle of benzene-exposed animals receiving intervention was 77% greater than benzene-exposed animals without intervention ($p=0.05$, $n=5-12$).

TEMPOL intervention and measures of oxidative stress. TEMPOL treated animals exposed to volatile benzene displayed greater hepatic GSH concentrations (Figure 30) than did benzene-exposed animals without intervention. Skeletal muscle measurements of GSH displayed similar trends, with anti-oxidant treated, benzene-exposed mice displaying higher concentrations of GSH relative to their non-intervention benzene-exposed cohort. Another marker of ROS exposure, MDA, showed corresponding trends with anti-oxidant treated, benzene-exposed animals. That is, these animals displayed significantly lower concentrations of MDA than non-intervention, benzene-exposed animals (Figure 30).

TEMPOL intervention and measures of inflammation. Following measurements of reduced levels of oxidative stress in liver and skeletal muscle, we then ascertained whether inflammation is also decreased in benzene-exposed and TEMPOL treated animals relative to benzene without intervention cohort (Figure 31). Levels of phosphorylated NF κ B p65 relative to total NF κ B p65 were decreased in benzene-exposed, TEMPOL treated animals relative to benzene-exposed only animals in liver ($p=0.002$) and skeletal muscle ($p=0.041$).

After documenting decreased NF κ B p65 activation, we assayed for NF κ B p65 regulated MIP-1 α in liver and skeletal muscle (Figure 31). Transcript of MIP-1 α was found to be decreased in TEMPOL treated, benzene-exposed animals relative to benzene-exposed mice in liver ($p=0.044$) and skeletal muscle ($p=0.002$).

Accordingly, suppressors of cytokines (SOCS) proteins in benzene-exposed, TEMPOL treated mice were measured to assess if corresponding changes would occur contemporaneously with lower cytokine levels (Figure 32). SOCS1 demonstrated a decrease in benzene-exposed, TEMPOL treated mice relative to non-intervention mice in liver ($p=0.006$). No change was seen in SOCS3 expression with TEMPOL intervention receiving animals. Corresponding to the change in SOCS1 expression, benzene-exposed, TEMPOL-treated animals exhibited an increase in pan-tyrosine phosphorylation of IRS-2 (Figure 33) relative to non-intervention benzene-exposed animals.

Influence of high fat diet (60%) on benzene induced insulin resistance.

Mice on 6wks of HFD or NC were exposed to filtered air or benzene and metabolic indices were measured. Mice exposed to benzene on HFD demonstrated a significant 9.2% increase in FPG levels relative to air exposed (Figure 28), HFD mice ($p=0.03$) and an 8.7% increase in FPG relative to NC fed benzene-exposed mice ($p=0.01$). However, the relative increase of FPG compared with diet matched control for benzene-exposed animals on HFD was only a 9.2% increase relative to control while NC animals exposed to benzene exhibited a 13.0% increase compared with NC fed, air exposed animals, suggesting an additive effect to IR but not potentiating. Moreover, intracellular assessment of insulin signaling in HFD fed, benzene-exposed animals demonstrated no further diminishment of insulin-stimulated phosphorylation of Akt compared with NC fed benzene-exposed mice (Figure 34).

Figure 25.

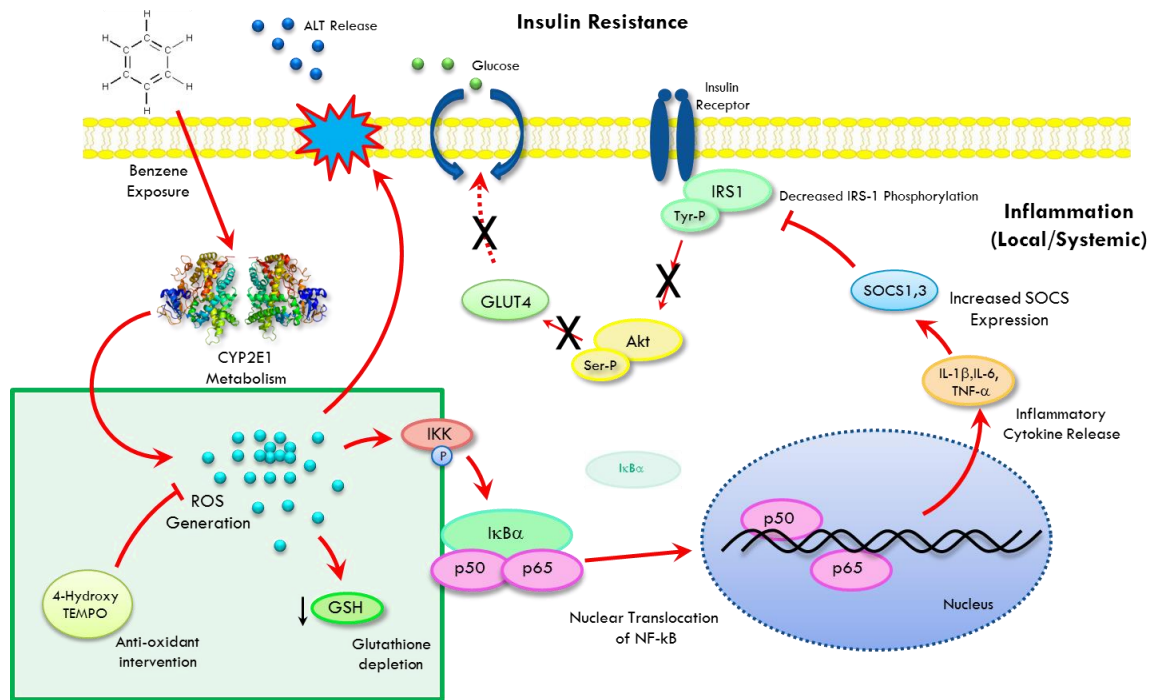


Figure 25. Schematic of benzene-induced liver injury and insulin resistance with anti-oxidant intervention. In this proposed model for benzene-induced pathology, benzene metabolism by CYP2E1 generates oxidative stress, induces inflammatory signaling pathways, upregulates cytokines, and upregulates SOCS proteins thereby inhibiting insulin signaling pathways. Here we highlight the point of intervention achieved with anti-oxidant 4-hydroxy TEMPO (TEMPOL) administration acting through a spin trap mechanism.

Figure 26.

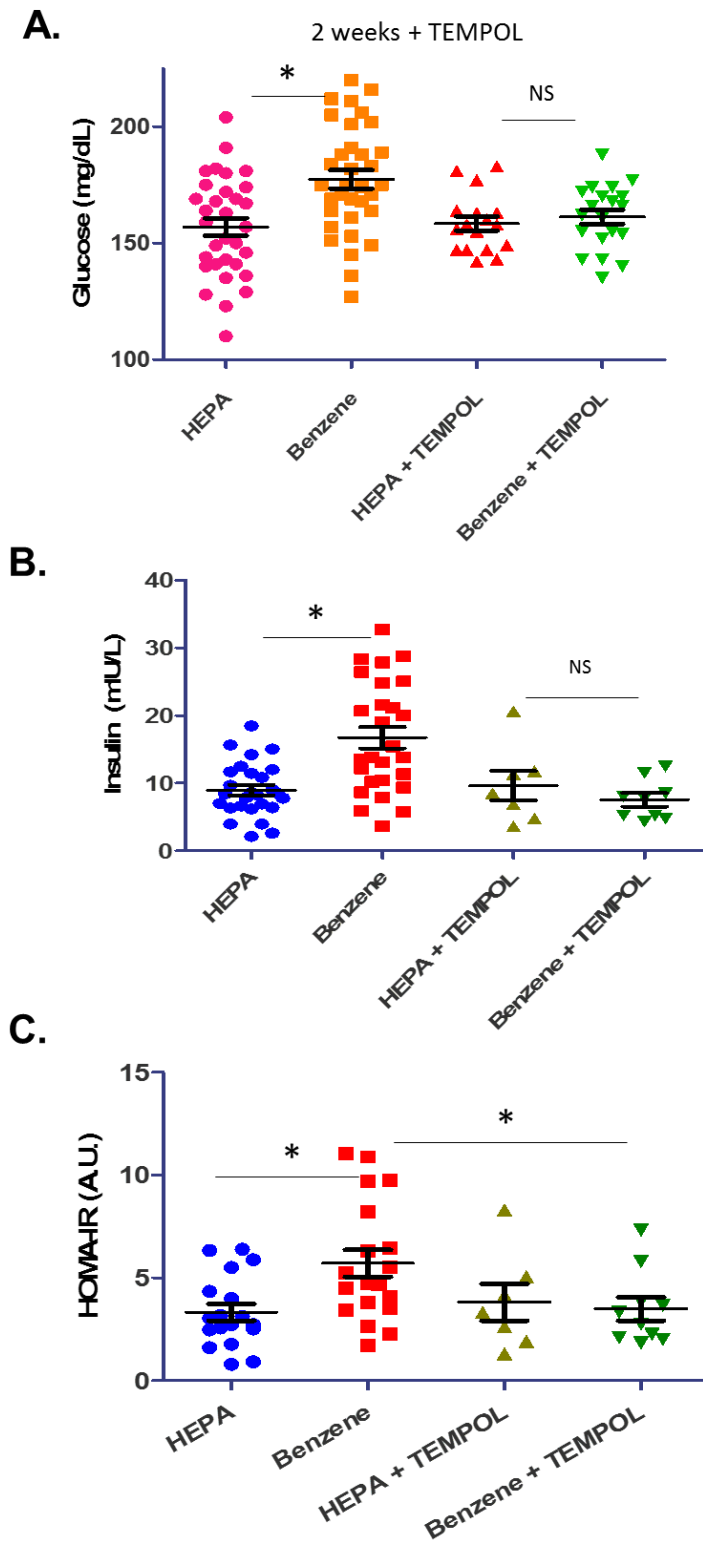


Figure 26. TEMPOL intervention and glycemic indices. Mice were exposed to HFA or 50ppm benzene in 3 separate exposures drinking normal water or that supplemented with 1mM TEMPOL. After 2wks of exposure, levels of FPG (A), FPI (B), were measured as previously described. We also calculated a HOMA-IR score (C). FPG: n=17-34 mice/treatment; FPI and HOMA-IR: n=10-20 mice/treatment; *p<0.05.

Figure 27.

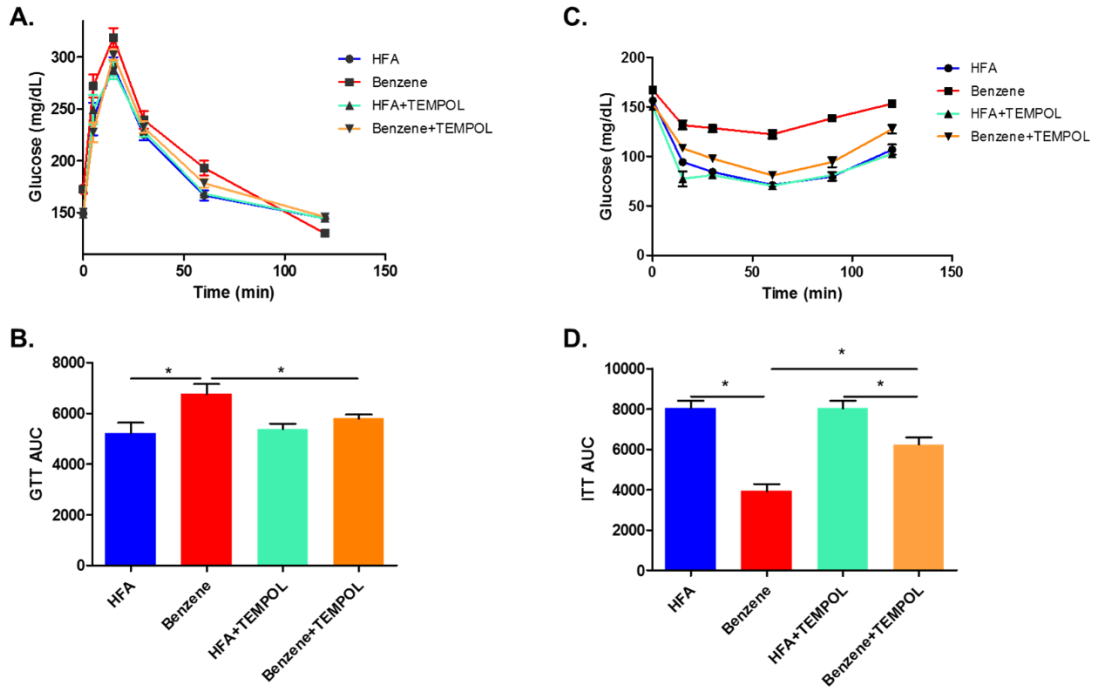
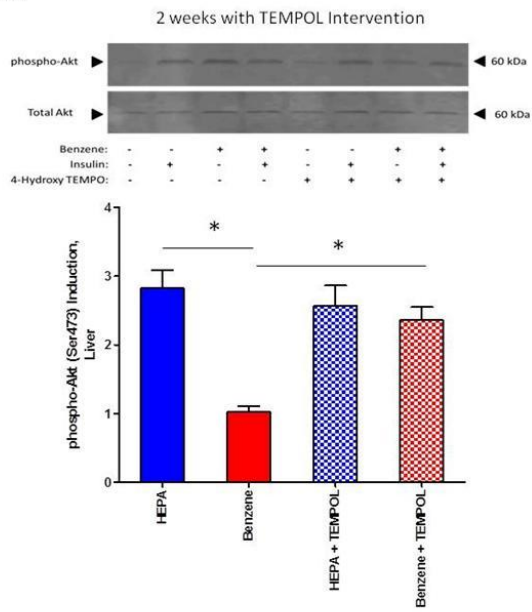


Figure 27. TEMPOL reverses glucose intolerance. Mice were exposed to HFA or 50ppm benzene drinking normal water or that supplemented with 1mM TEMPOL. After 2wks of exposure, GTTs (A) and ITTs (C) were performed. We also determined an AUC for the GTT (B) and the ITT (D). n=10 mice/treatment; *p<0.05.

Figure 28.

A.



B.

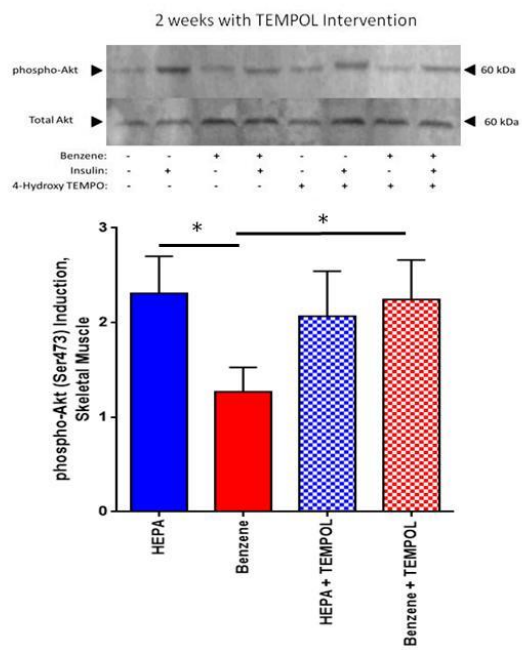


Figure 28. Anti-oxidant intervention and Akt phosphorylation. Mice were exposed to HFA or 50ppm benzene for 2wks drinking normal water or that supplemented with 1mM TEMPOL. The mice were then injected with insulin or saline for 15min prior to euthanasia. Levels of phospho-Akt and total Akt were determined in homogenates of liver (A), and skeletal muscle (B). Illustrated are representative blots (upper panels) and normalized data (lower panels). n=5-10 mice/treatment; *p<0.05.

Figure 29.

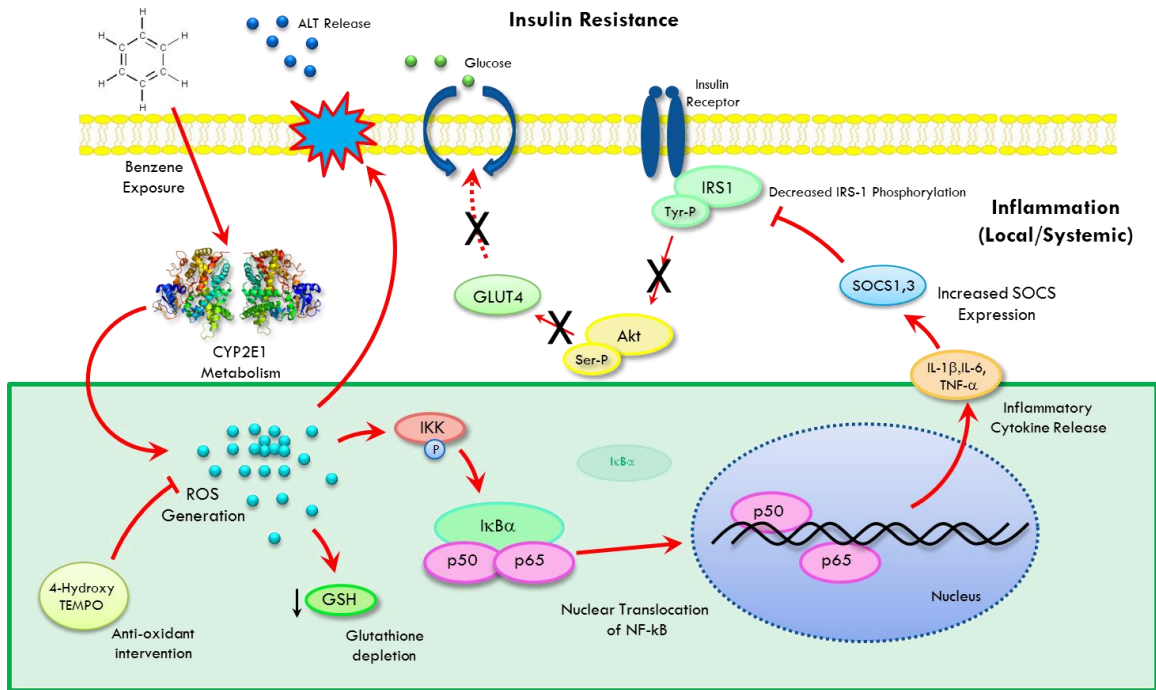


Figure 29. Schematic of benzene-induced liver injury and downstream changes influenced in mice by TEMPOL intervention. In this proposed model for benzene-induced pathology, benzene metabolism by CYP2E1 generates oxidative stress, induces inflammatory signaling pathways, upregulates cytokines, and upregulates SOCS proteins, thereby inhibiting insulin signaling pathways. Here is highlighted the downstream pathways influenced by TEMPOL intervention.

Figure 30.

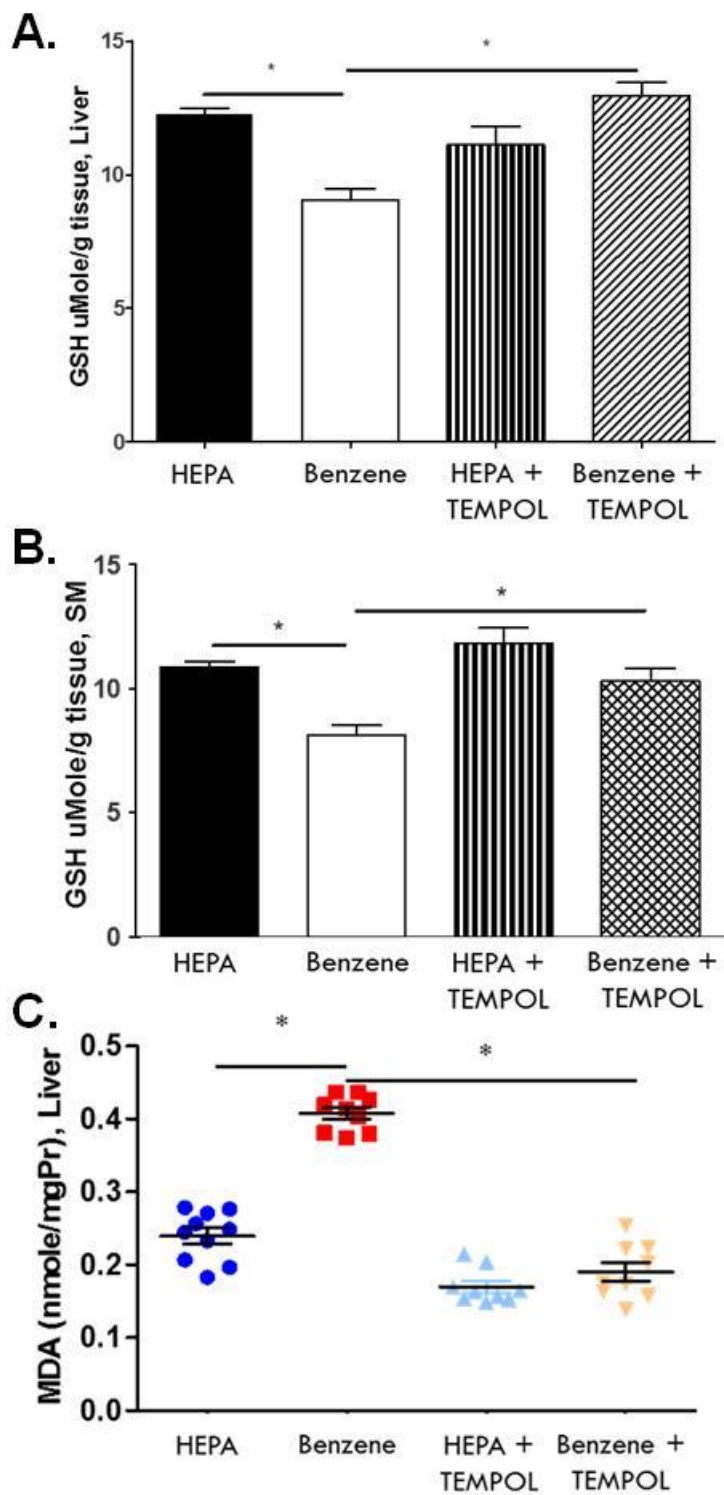


Figure 30. TEMPOL and oxidative stress. Mice were exposed to HFA or 50ppm drinking normal water or that supplemented with 1mM TEMPOL. After 2wks of exposure the mice were euthanized and levels of GSH determined in homogenates of liver (A) and skeletal muscle (B). MDA levels were also measured in liver (C). n=7-10 mice/treatment; *p<0.05.

Figure 31.

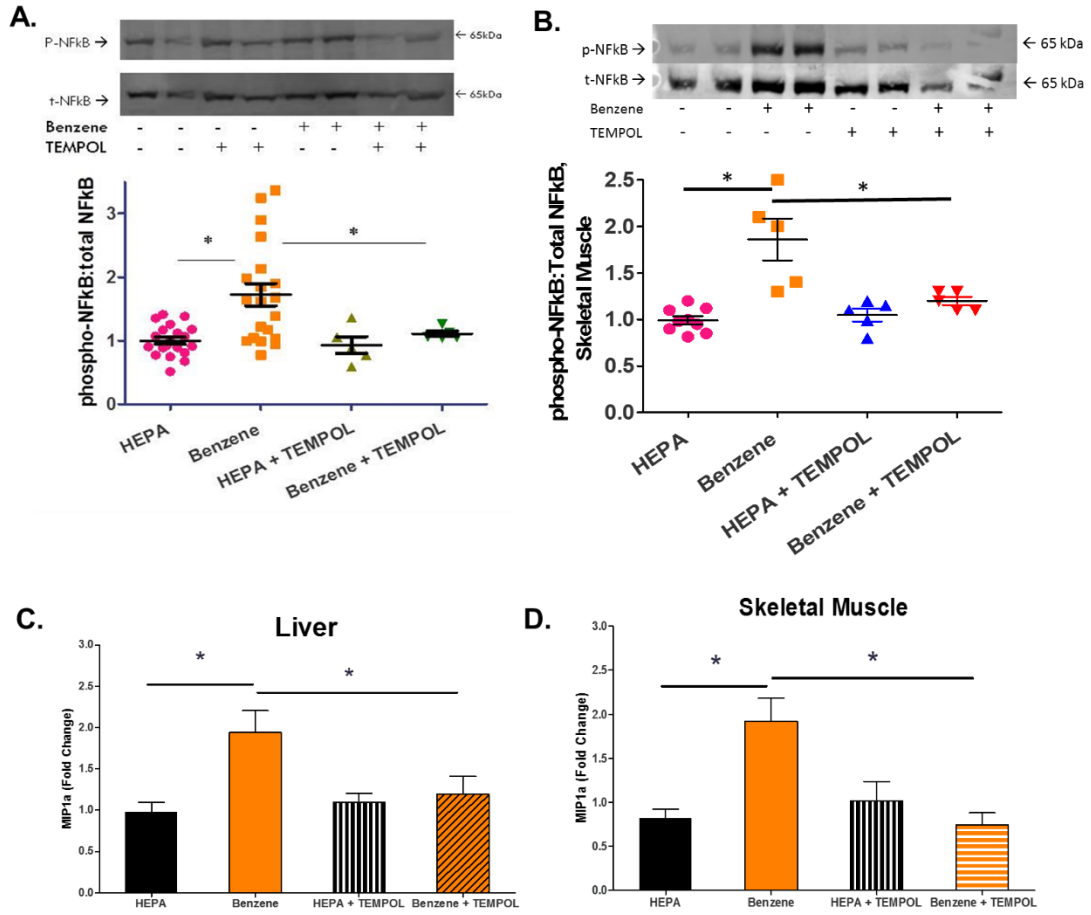
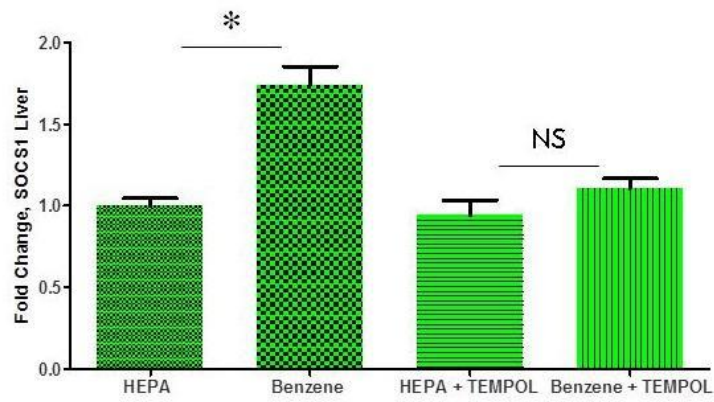
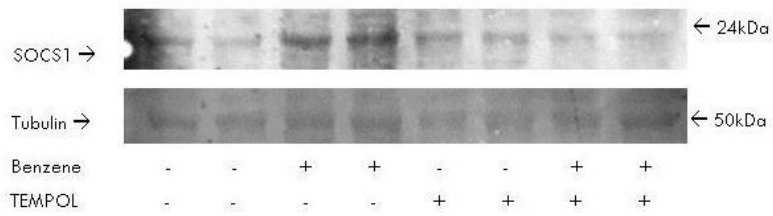


Figure 31. TEMPOL intervention and inflammatory signaling. Mice were exposed to HFA or 50ppm benzene for 2wks drinking normal water or 1mM TEMPOL and then euthanized. Levels of NF κ B p65 phosphorylation and total NF κ B p65 in liver (A) and skeletal muscle (B) homogenates were determined by Western blotting. Illustrated are representative blots (upper panels) and normalized data (lower panels). Quantitative PCR of selected cytokine transcripts was performed on RNA preparations of liver (C) and skeletal muscle (D). Illustrated are the fold changes using GAPDH as housekeeping control gene. n=5-21 mice/treatment; *p<0.05.

Figure 32.

A.



B.

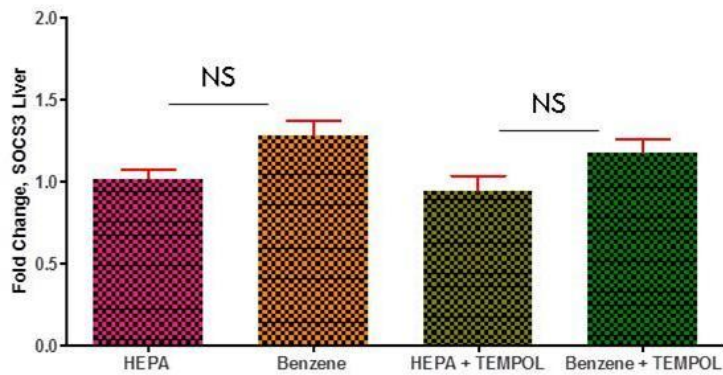
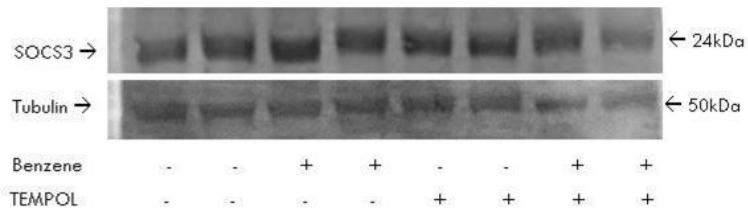


Figure 32. Anti-oxidant and SOCS proteins. Mice were exposed to HFA or 50ppm benzene for 2wks drinking normal water or 1mM TEMPOL supplemented water and then euthanized. Levels of the cytokine suppressor proteins SOCS1 (A) and SOCS3 (B) were determined in liver homogenates by Western blot analysis. Tubulin blots were used as loading controls. Illustrated are representative blots (upper panels) and normalized data (lower panels). n=4 mice/treatment; *p<0.05.

Figure 33.

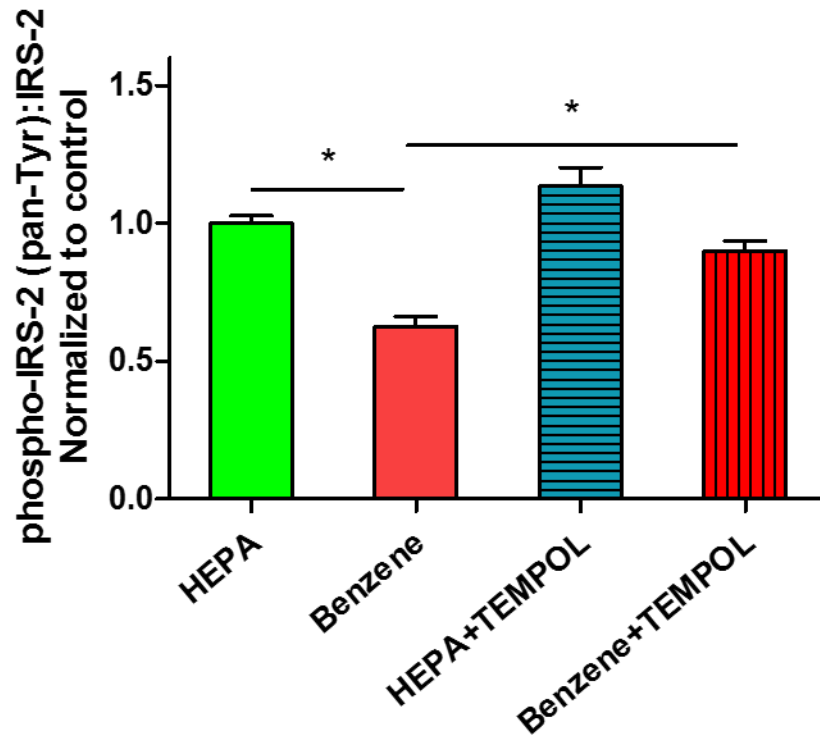
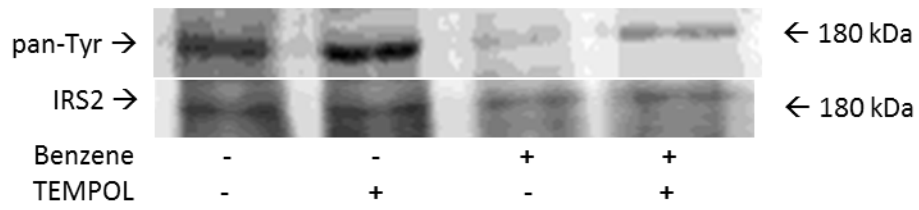


Figure 33. Anti-oxidant and IRS-2 phosphorylation. Mice were exposed to HFA or 50ppm benzene for 2wks drinking normal water or 1mM TEMPOL supplemented water and then euthanized. IRS-2 was immunoprecipitated from liver homogenates, collected proteins resolved by SDS-PAGE and transferred to nitrocellulose. The blots were probed with a pan-phospho-tyrosine antibody and an IRS-2 antibody. Illustrated are representative blots (upper panel) and quantitative data (lower panel). n=3-5 mice/treatment; *p<0.05.

Figure 34.

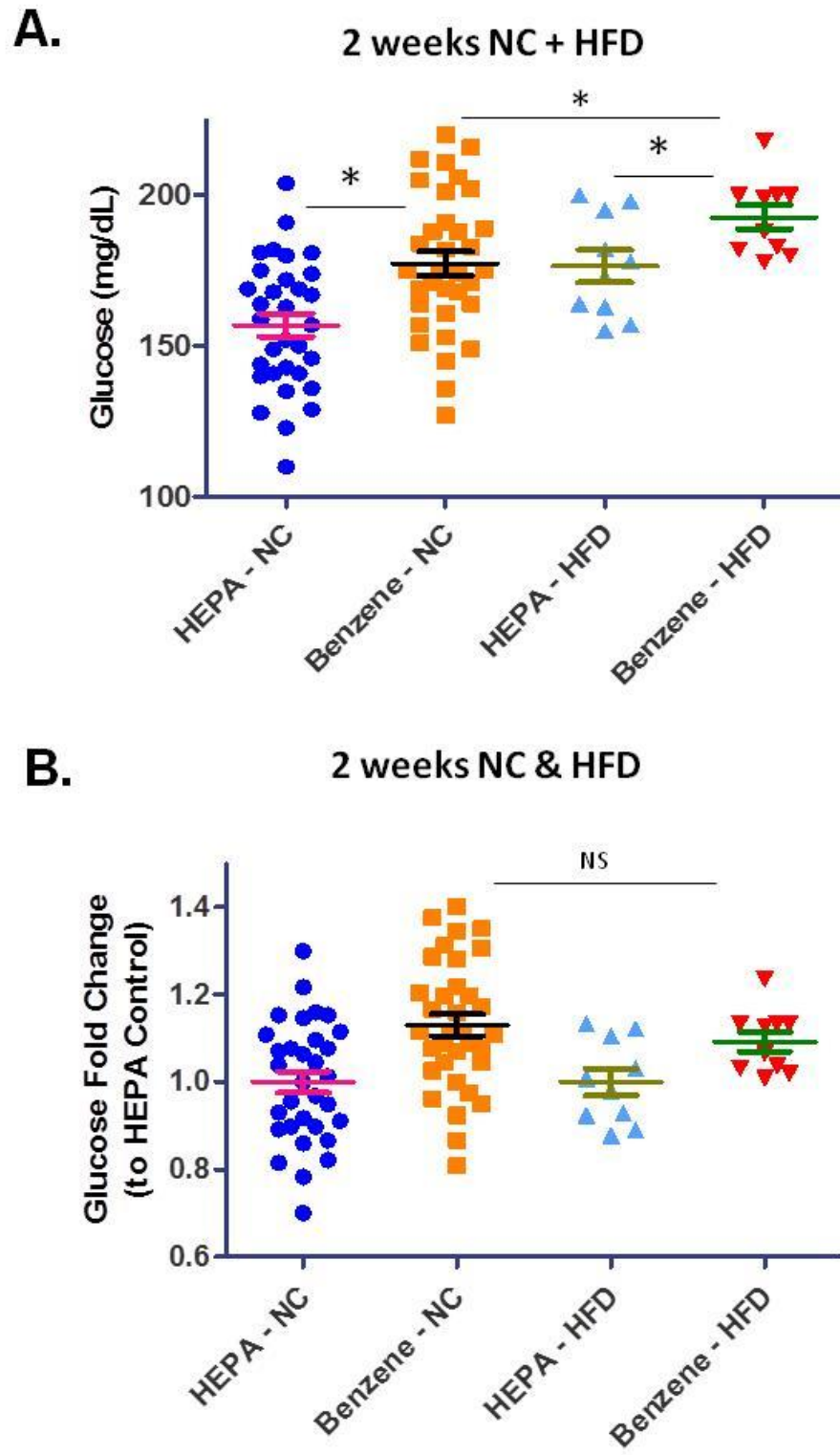


Figure 34. HFD-fed mice, benzene exposure and FPG. Mice were fed a normal chow diet or HFD for 6wk and then exposed to HFA or 50ppm benzene for 2wks. At this time fasting plasma glucose levels (A) were measured and a relative increase of FPG calculated (B). n=10-34 mice/treatment; *p<0.05.

Figure 35.

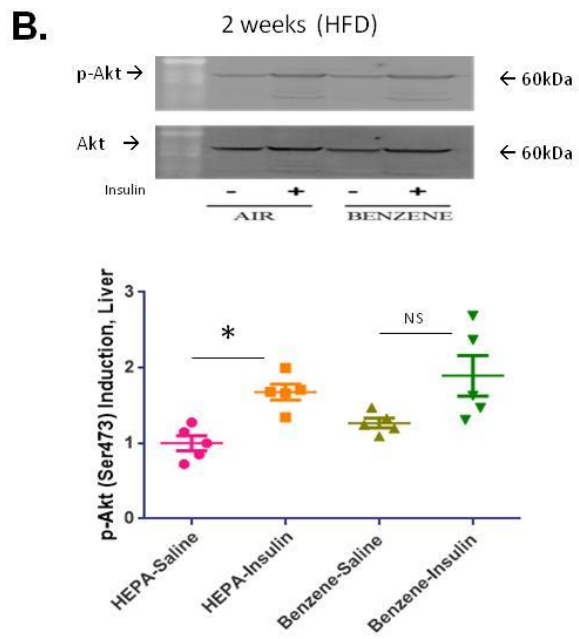
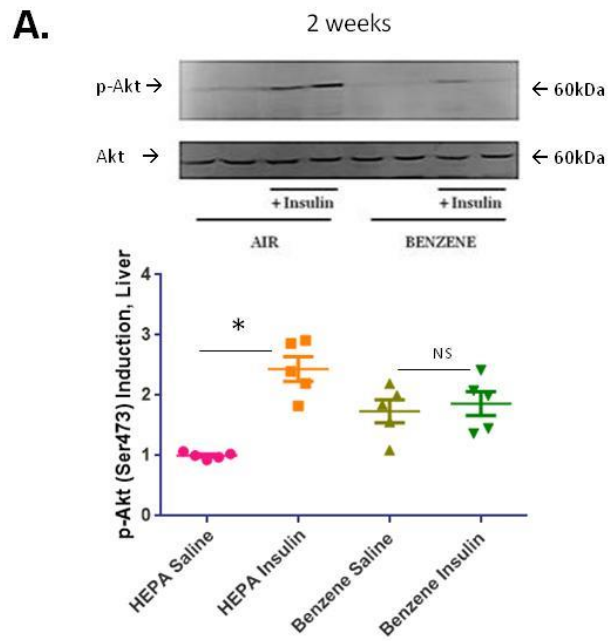
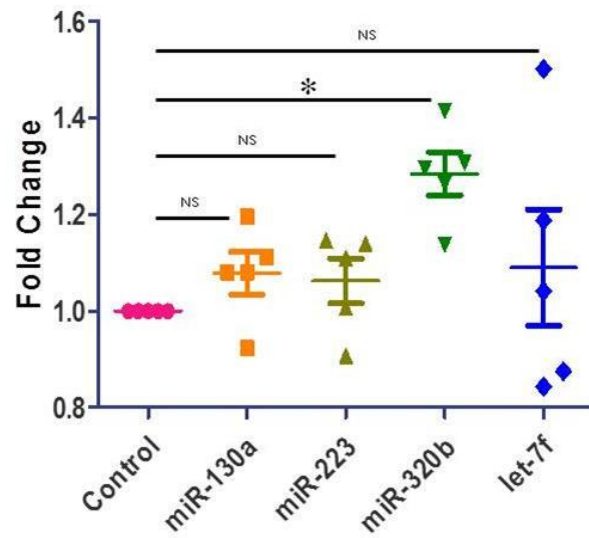


Figure 35. Insulin-stimulated Akt phosphorylation and HFD. Mice were exposed to HFA or 50ppm benzene for 2wks and given normal chow diet (A) or HFD (B) for 6wks and then injected with saline or insulin 15min before euthanasia. Levels of insulin-stimulated phospho-Akt were then measured in homogenates of collected livers. Illustrated are representative blots of phospho-Akt and pan-Akt (upper panels). Also illustrated are grouped data from 1 individual experiment and 5 animals. *p<0.05

Figure 36.

A.



B.

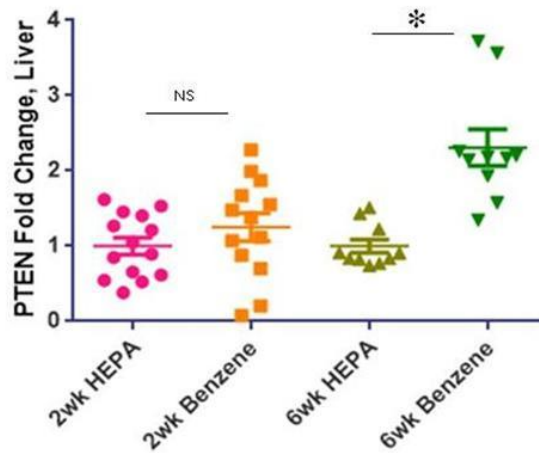
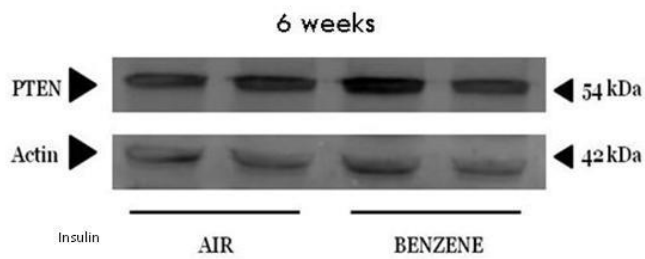


Figure 36. miRNAs, PTEN expression and benzene exposure. Mice were exposed to HFA or 50ppm benzene for 2 or 6wks and then euthanized. Quantitative PCR of selected transcripts was performed on miRNA preparations of liver (A) of 2wk exposed mice. Illustrated are the fold changes using sno202 as housekeeping control gene. Levels of PTEN and actin in liver (B) homogenates from 2wk and 6wk exposed animals were determined by Western blotting. Illustrated are representative blots (upper panel) and normalized data (lower panel). n=5-14 mice/treatment; *p<0.05.

Influence of miRNAs and PTEN regulation on benzene induced insulin resistance. Reported miRNAs (i.e. miR-130a, miR-223, miR-320b, miR-let-7) affecting PTEN expression were assayed in air and benzene-exposed mouse (no intervention) liver. The miR-320b was found to be elevated after 2wks ($p < 0.05$) but a significant increase in PTEN expression was not found until animals had been exposed to benzene for 6wks, suggesting PTEN is not involved in the acute insulin resistant response following benzene exposure (Figure 36).

Discussion

The major findings of this study are that acute exposure to volatile benzene induces insulin resistance and that administration of anti-oxidant TEMPOL, protects against this ROS generated change in metabolism. These results support a causal role for benzene and ROS in regulating insulin signaling. These data suggest that this benzene-induced insulin resistance is mediated by oxidative stress and inflammation that exert an inhibitory effect on insulin signaling. Given the ubiquitous nature of benzene exposure, these observations taken collectively support the notion that benzene exposure may play a role in the growing, global epidemic of diabetes. Previously it has been shown that the metabolism of benzene by CYP2E1 generates ROS and inflammation (239). Additionally, it has been shown that CYP2E1KO mice are protected against high-fat diet-induced obesity and insulin resistance (240) and that hepatocyte CYP2E1 overexpression leads to impaired hepatic insulin signaling (241). However, it has not been shown that exposure to environmentally relevant levels of volatile

benzene, acting through CYP2E1 metabolism and ROS generation may be sufficient to induce insulin resistance.

Several lines of evidence collected during this study support the notion that volatile benzene exposure induces insulin resistance via oxidative stress mediated pathways. Given our current findings we cannot completely rule out the minor extent to which reactive benzene-metabolite intermediaries may play a role in this process, previous studies demonstrating the extensive ROS generation of CYP2E1 and the abundant urinary metabolites suggest that few reactive metabolites form adducts and react independently before being conjugated by secondary enzymatic processes that facilitate excretion of these molecules. Additionally, our global application of anti-oxidant treatment does not provide specific answers regarding the most abundant tissue-source of oxidative stress. However, previous studies have demonstrated the overwhelming abundance of hepatic CYP2E1 relative to other tissues, which suggests most CYP2E1 generated ROS will be hepatic (242). Moreover, CYP2E1KO mice exposed to benzene generated no genotoxic effects typically without detection of any benzene metabolite (243, 244). This coupled with the finding of this study that repeatedly shows tissue specific injury (e.g. increased MDA, proportionally increased inhibition of Akt phosphorylation, etc) to liver more than other tissues suggest that this is likely the greatest extramedullary location of damage. Also, that benzene exposure results in a ROS mediated occurrence of insulin resistance is supported by the application of an antioxidant which may diminish the subtle insulin resistant phenotype.

How does benzene induce oxidative stress-mediated insulin resistance? Our data imply that ROS generated following benzene exposure signals inflammatory pathways play an important role in modulating insulin sensitivity. Previous studies have demonstrated a decrease in IRS-1 and IRS-2 tyrosine phosphorylation in CYP2E1 overexpressing rat hepatocytes (241). This same study demonstrated decreased Akt phosphorylation along with increased lipid peroxidation with CYP2E1 overexpression suggesting that insulin signaling and oxidative stress are both influenced by CYP2E1. These studies fully support our data that demonstrate an increase in oxidative stress (i.e. increased MDA and decreased GSH) and decreased insulin sensitivity (i.e. diminution of Akt serine phosphorylation and IRS-2 tyrosine phosphorylation) following benzene exposure and increased CYP2E1 activity. However, our studies are more detailed and robust. We demonstrate whole body physiological responses with changes in FPG, FPI, HOMA-IR, GTTs and ITTs. At the molecular level we can demonstrate the presence of oxidative stress in many compartments, but primarily in the liver. Here we see an increase in lipid peroxidation (i.e. MDA), a decrease in hepatic GSH, and a decrease in MCB not only in circulating cells but in bone marrow derived cells as well. Clearly, the benzene stimulus is sufficient to generate oxidative stress.

To determine whether benzene exposure might be associated with inflammation associated insulin resistance, markers of inflammation such as NF κ B, cytokines, and suppressors of cytokines (SOCS) were assayed. The transcription factor NF κ B is a powerful regulator of the inflammatory signaling

response and can be activated by ROS. ROS can phosphorylate IKK, which then dissociates I κ K α from NF κ B subunits p50 and p65. After NF κ B subunits dissociate from the complex they are capable of being phosphorylated. Following phosphorylation, NF κ B subunits then translocate to the nucleus to upregulate mRNAs involved in initiating the inflammatory signaling cascade. In 2 and 6wk benzene-exposed mice, phosphorylation of NF κ B p65 was elevated compared with HFA-exposed controls in liver and skeletal muscle. Relative NF κ B phosphorylation levels increased in liver and increased in statistical significance in skeletal muscle tissues with increasing exposure duration. With the elevated phosphorylation of p65 subunit of NF κ B, targets of NF κ B were measured in liver tissue. Transcript (mRNA) levels of IL-1 β , IL-6, TNF α demonstrated no significant change with benzene exposure while MIP-1 α was upregulated 1.94-fold (p=0.007). Transcript levels of MIP-1 α in skeletal muscle of benzene-exposed animals were upregulated 1.91-fold (p=0.003).

Other studies have also demonstrated reported increases in hepatic oxidative stress along with NF κ B subunit phosphorylation followed by partial NF κ B gene target transcription (245) and we surmise the selective gene targeting by p65 is likely multifactorial. There are five subunits or members to the mammalian NF κ B family (p65/RelA, RelB/p100, c-Rel, p50, and p52). These members form numerous dimeric complexes that can activate many target genes through attachment to the κ B enhancer. While the NF κ B family collectively targets over 150 genes, not all subunits target all 150 genes. For instance, p100

and p52 are closely associated with TNF α regulation while p65 tightly regulates MIP-1 α (a.k.a. CCL3), IFN β and IL-8 (246-250). This division of tasks required by each NF κ B subunit allows for specificity of response. Additionally, not all varieties of cells respond in the same way to a particular signal because they lack the necessary transduction molecules or receptors. The selectivity of response can be altered by what is known as the combinatorial response of promoter/enhancer regions, which requires more than one NF κ B subunit or other transcription factor to induce transcription of a particular gene. As mentioned above, selective activation or binding of NF κ B subunits also plays a role in transcription. Thus, there are many reasons why other gene targets of the five member NF κ B family may not be upregulated. Additionally, it is reasonable that if the liver contains 90% of the body's macrophages (as tissue-resident Kupffer cells), that the primary cytokine response would be the elevation of a cytokine dubbed the "macrophage inflammatory protein-1 α ." More convincingly though, is the tight regulation of MIP-1 α by the p65 subunit and the evidenced activation of this subunit.

The association of increased MIP-1 α levels with a specific increase in SOCS1 expression coupled with a decrease in IRS-2 tyrosine phosphorylation highly suggests that SOCS1 recruitment to suppress MIP-1 α levels is having an ancillary effect of inhibiting IRS-2 phosphorylation. Studies demonstrating the tight regulation of MIP-1 α by SOCS1 rather than by SOCS3 reaffirms the biological plausibility of these findings (251, 252). Moreover, the increase in

SOCS1 expression likely explains the concomitant decrease in IRS-2 tyrosine phosphorylation. SOCS1 has been shown to inhibit IRS-2 tyrosine phosphorylation as well as to facilitate IRS-2 ubiquitination (253, 254). Although this study did not detect decreased levels of IRS-2 (suggesting IRS-2 ubiquitination), data showed decreased IRS-2 tyrosine phosphorylation. Hence, the likelihood that benzene exposure is influencing insulin sensitivity via oxidative stress induced inflammation that drives increased SOCS1 levels to inhibit IRS-2 tyrosine phosphorylation is well supported by our observations.

The transience of this phenomena was tested by allowing mice exposed to benzene for 2wks to remain unexposed for 4wks before assaying for glucose and insulin levels. After 4wks of recovery, benzene-exposed animals surprisingly exhibited 20% increase ($p=0.036$, $n=7$) compared with the filtered air controls allowed to rest for the same length of time (Figure 20). FPI and HOMA-IR values of four-week recovery benzene-exposed animals also demonstrated a trending increase, though because so few animals were available for insulin testing this likely kept these values from reaching significance ($p=0.1$, $n=3$ for FPI and HOMA-IR). HOMA- β demonstrated no trending change in this small cohort.

Due to the suggestive evidence that oxidative stress may be mediating the insulin resistant phenotype seen in benzene-exposed animals, we then applied an anti-oxidant (4-hydroxy TEMPO, or TEMPOL) intervention to this study. With the administration of TEMPOL we found a return to baseline in in all indices of oxidative stress (i.e. GSH, MDA), inflammation (i.e. phospho-NF κ B p65, MIP-1 α levels, SOCS expression) and insulin signaling (Akt serine phosphorylation,

IRS-2 tyrosine phosphorylation). Additionally, this particular anti-oxidant has demonstrated the capacity to mitigate the effects of oxidative stress and therefore block the subsequent development of insulin resistance, inflammation and atherosclerosis (255-257).

Additionally, we investigated if lifestyle factors, such as HFD, might increase sensitivity to benzene exposure. Other studies have demonstrated an increase in the benzene metabolizing enzyme's (CYP2E1) expression and activity in obese organisms and that CYP2E1KO mice are protected from weight gain and insulin resistance when maintained on a high fat diet (240, 258). Also, investigations have demonstrated a potentiated CYP2E1-mediated (ethanol) injury is seen in obese organisms, suggesting increased sensitivity to the insult (259). Here we hypothesized that animals on a HFD exposed to benzene would demonstrate a more severe insulin resistance phenotype than animals exposed to benzene on a normal chow diet. Increased lipid levels coupled with possible increases in CYP2E1 activity would plausibly increase lipid peroxidation and efficiency of benzene metabolism causing greater concentrations of ROS to accumulate acutely. However, this exaggerated insulin resistance phenotype was not demonstrated in HFD fed animals exposed to benzene. This might be due to the subtle nature of the initial observation with normal chow animals along with a sufficient level of CYP2E1 endogenously present to metabolize benzene at the 50 ppm level of exposure. Increased CYP2E1 expression beyond that level would not necessarily drive a benzene-dependent increase in insulin resistance. Additionally, such a change might not be seen at times examined and thus either

a longer duration of HFD and/or benzene exposure administration may be needed to elicit such effects.

Finally, we wanted to investigate whether miRNAs may play a role in benzene-induced insulin resistance. It has been reported that specific miRNA profiles affecting PTEN expression are altered following benzene exposure (260-262). While many miRNAs regulate insulin signaling pathways, we only assayed the miRNAs reported to be affected by benzene exposure. These miRNAs largely target PTEN expression, a negative regulator of PI3K. However, only one of the four miRNAs (i.e. miR-320b) tested were elevated and subsequent interrogation of PTEN expression suggested that PTEN was unlikely to play a role in benzene-induced insulin resistance at after 2wks of exposure. Thus, given the current listing of altered miRNAs following benzene exposure that are likely to affect insulin signaling, it seems that miRNA and PTEN play a minimal role in the initiation of benzene-induced insulin resistance.

As the link between insulin resistance and inflammation becomes clearer, it is likely that we will begin to see surprising contributors to the global epidemics of insulin resistance and diabetes. Probable actors in this scenario will be constituents of air pollution. For instance, exposure to fine particulate matter (PM_{2.5}) has been shown to increase oxidative stress, inflammation, atherosclerosis and CV mortality (257, 263, 264). Moreover, it has been reported that if the USA reduced the mean levels PM_{2.5} by just 3.9 $\mu\text{g}/\text{m}^3$ would prevent 7,978 heart failure hospitalizations and save \$300 million dollars per year (265). Other factors like ozone appear to be playing a role not only in generating

oxidative stress but insulin resistance (266, 267). Furthermore, increased probability for exhibiting elevated HOMA-IR scores was observed for participants carrying risk genotypes in glutathione S-transferase genes (GSTM1, GSTT1, and GSTP1). Glutathione S-transferase enzymes mitigate oxidative stress and therefore these results suggest that the HOMA-IR increase is mediated by ROS (266). It is likely, that benzene will soon be added to the list of respirable, ubiquitous pollutants that generate cardiometabolic disruption. The hallmark profile of generating local and systemic oxidative stress and inflammation sets the stage for the promotion of insulin resistance and many other disorders. A study associating the benzene metabolite *t,t*-MA with HOMA-IR scores in 505 elderly adults (≥ 60 years) suggests that increased benzene exposure is associated with increased oxidative stress (i.e. urinary MDA) and HOMA-IR scores. While this is the first study to demonstrate such an association, it does not rigorously attempt to address a mechanism by which this association is likely, while our study conclusively shows a causative effect from benzene exposure on insulin signaling. Interestingly, both of these studies align in that the association between *t,t*-MA and HOMA-IR is driven by elevated fasting plasma insulin levels rather than by fasting plasma glucose. This aberrant increase in FPI rather than FPG is also indicative of the current model of T2D progression from insulin resistance.

As insulin resistance and T2D prevalence surges in areas where none existed before excessive pollution was generated by industrial complexes, it is likely that we will find that genetic susceptibility will only play a minor role in

differential prevalence of pathology, and that the environment's constituents will be the overwhelmingly greatest factor in progression of this particular pathology.

Conclusion

Volatile benzene exposure (50 ppm x 6h/d x 14d) appears to induce oxidative stress, inflammation and, overall, a subtle hyperglycemic but marked hyperinsulinemic phenotype in C57Bl/6 mice. This phenotype is prevented by the administration of anti-oxidant, TEMPOL. Additionally, under the conditions tested, a HFD does not appear to potentiate the insulin resistance in benzene-exposed mice. However, while the oxidative stress-mediated insulin resistance does not produce gross pathology (e.g. T2D after 6wks of exposure), this environmentally relevant exposure level used for these experiments suggests that benzene could be playing a role in the global epidemic of inflammation-driven insulin resistance and related diseases.

CHAPTER IV
BENZENE EXPOSURE AND HEMATOPOIETIC AND ENDOTHELIAL
PROGENITOR CELLS

Introduction

Benzene is known to have especially toxic effects to cells residing within the medullary cavity (i.e. inner bone marrow), especially hematopoietic stem cells (HSCs). However, many stem cell populations reside within the medullary cavity besides HSCs, such as endothelial progenitor cells (EPCs). One of the first signs to suggest the existence of HSCs was found in individuals exposed to lethal doses of radiation in 1945, but these cells were more articulately described by Till and McCulloch in the 1960s (268). Though EPCs also reside in the bone marrow and had been speculated about since the 1960s, the existence of these cells was not substantiated until the 1990s (269). As such, much less is known about the physiology of these cells.

What is known about EPCs is that they are necessary and sufficient for the growth of vascular tissue (angiogenesis and vasculogenesis) and that their relative abundance predicts cardiovascular events and mortality in humans. These cells are critically important in repairing the damaged endothelium and are vital to vascular health. As benzene has been used to study the behavior of bone marrow-resident HSCs, we used benzene to ascertain whether benzene

affects bone marrow-resident EPCs. Additionally, we also investigated the relative sensitivity of each of these cell types to the same toxic benzene exposure.

Another component of this study utilized mice placed on a high fat diet (HFD) which were then exposed to HEPA-filtered air (HFA) or volatile benzene. The HFD plus benzene exposure was of interest for two reasons. First, obesity has been reported to potentiate CYP2E1 mediated toxicities, and thus may sensitize animals to benzene exposure. Second, obesity clearly increases vulnerability to diseases and concurrently alters hematopoiesis and decreases viability of HSCs. It is unknown exactly how this disruption occurs, but it is speculated that anything from inflammation and ROS to adipocyte intrusion of the medullary cavity may alter the processes and viability of these cells (270). Additionally, obesity is a risk factor for cardiovascular disease development. Moreover, obesity is associated with decreased levels of EPCs (271, 272) despite evidence of damaged endothelium, a signal that would recruit EPCs under normal physiological conditions. This suggests that EPCs in the bone marrow may be depleted, may not be differentiating or that there is a bone marrow mobilization defect (as seen with type 2 diabetes [T2D]).

We used benzene not only as a tool to study EPC and HSC physiology, also to sustain important information concerning the potential effects of benzene on EPCs and therefore cardiovascular health (273). Cardiovascular tissues and EPCs have demonstrated a high sensitivity to inhaled pollutants and several

studies have shown that inhalation of toxic substances such as cigarette smoke and particulate matter (PM_{2.5}) cause significant cardiovascular injury (274-276). Understanding the effects of benzene on different stem cell populations residing within the same niche may provide novel information relating to future development of pathology as well as unique characteristics of these progenitor cells.

Methods

Volatile benzene exposure and HFD administration.

All procedures were approved by the University of Louisville Institutional Animal Care and Use Committee. Benzene exposures were performed as detailed in Chapter II. Briefly, mice were maintained on NC or HFD with normal drinking water or TEMPOL intervention and subsequently exposed to HFA or volatile benzene for 14d or 6wks. Necropsy was performed immediately after the final exposure.

Peripheral blood EPC detection and bone marrow-derived EPC and hematopoietic lineage assay and flow cytometry

Whole blood (300-400 μ L) was lysed (4 ml; BD PharmLyse, BD BioSciences, San Jose, CA, USA; 10 min, RT) and after centrifugation (5min, 400 x g, RT), the supernatant was aspirated and the lysing/centrifugation/aspiration steps were repeated. The cell pellet was resuspended in 1 % FBS/PBS and divided into two

equal fractions. One fraction was fluorescently-labeled with anti-Sca-1 and anti-Flk-1 antibodies tagged with FITC and APC, respectively. Following centrifugation (5min, 400 x g, RT), mononuclear cells were re-suspended in 1 % FBS/PBS. The FITC-Sca-1 (BD BioSciences) and APC-Flk-1 (BD BioSciences) antibodies were added to cells and incubated for 30min on ice. Cells were then washed with 1 % FBS/PBS and centrifuged (5min, 400 x g, RT). Cells re-suspended in 1 % FBS/PBS (400 μ L) were analyzed using a LSRII flow cytometer (BD BioSciences). Based on forward and side scatter, small non-debris events in a sub-lymphocyte population (sized using fluorescent beads, BD Biosciences) were gated electronically and displayed in a two-color dot plot. Data were subsequently analyzed using FACSDiva v6.0 software (BD Biosciences), and double positive events were normalized per 50,000 events or per IJL of assay volume. For bone marrow-derived EPC detection the same staining procedure was performed for aspirates as with peripheral blood EPCs. The same preparatory steps were taken for the hematopoietic lineage assay from bone marrow aspirates but lineage markers were used in lieu of more general markers for endothelial and stem cell capacity. Briefly, bone marrow aspirates are washed with with 1 mL of PBS/1% BSA and then centrifuged for 500 x g for 5min. The supernatant is decanted and the pellet vortexed before being resuspended in an antibody master mix solution for 30min on ice. The master mix contains the following markers, Sca-1-FITC, CD16/32 Fc γ R-PE, lin-e450, CD45-APC, CD34-Alexa 700, CD117 (C-kit)-APCe780. After the incubation the cells are washed with PBS/BSA, and centrifuged at 500 x g for 5min. The supernatant is decanted,

the pellet vortexed and resuspended in 250 μ L PBS/BSA and data is acquired on the LSRII flow cytometer.

Cell culture procedures

Endothelial colony forming cells (ECFCs) were cultured with endothelial basal media (Clonetics/Lonza) supplemented with 20% FBS (Invitrogen, Carlsbad, CA, USA), human endothelial growth factor (hEGF), hydrocortisone, gentamycin/amphotericin B (GA) and bovine brain extract (BBE) (SingleQuot®, Clonetics/Lonza) under standard cell culture conditions (37°C, 5% CO₂). Bone marrow outgrowth cells were aspirated from the femur and tibia of both legs of exposed mice with 1 mL phosphate buffered saline (PBS) (Gibco/Life Technologies). Half of the aspirate was aliquoted for hematopoietic lineage assay analysis, 50 μ L was used for the HSC CFU differentiation and the remainder was then washed twice in PBS before plating onto fibronectin coated 6-well plates (Corning) in endothelial basal media (Clonetics/Lonza) supplemented with 20% FBS (Invitrogen, Carlsbad, CA, USA), human endothelial growth factor (hEGF), hydrocortisone, gentamycin/amphotericin B (GA) and bovine brain extract (BBE) (SingleQuot®, Clonetics/Lonza) under standard cell culture conditions (37°C, 5% CO₂). Cells were allowed to adhere and medium was changed every 48h. After 7-10d of culture, the cells were used for functional assays (i.e. proliferation and adhesion assays). For treatment of cells with benzene metabolites, cultures were treated with 1,4-benzoquinone (Sigma) or hydroquinone (Sigma) overnight before commencing the with the assay.

Differentiation assay with bone marrow aspirates.

Differentiation assay (a.k.a. HSC CFU assay) was performed using bone marrow aspirates, which were plated on to 35mm x 10mm tissue culture dishes (Falcon/Becton Dickinson) in a differentiation medium (Methocult/StemCell). Standard HSC CFU assay protocols were followed via manufacturer's suggestion. Briefly, MethoCult medium was thawed overnight at 2 - 8°C. Animals were euthanized and femurs and tibias were removed from each mouse. Bone marrow was aspirated from femur and tibia of both legs with 1 mL sterile phosphate buffered saline (PBS) (Gibco/Life Technologies), and 50µL was aliquoted for differentiation assay purposes. Bone marrow aspirates were kept on ice until needed. Cells were counted and 2.5×10^4 cells were added to thawed aliquots of MethoCult media, vortexed and allowed to rest before using a luer lock syringe attached to a 16 gauge blunt-end needle to dispense the suspended cells onto 35mm x 10mm tissue culture plates (Falcon/Becton Dickinson). Cells were cultured under normal conditions for 3d before counting by light microscopy.

Proliferation assay of BMO cells and ECFCs.

To measure proliferation, the CyQuant proliferation assay (Thermo Fisher) was used. Assay was performed according to product specifications and assay was performed in a 96 well plate. Briefly, we added an equal volume of provided 2x detection reagent to BMO or ECFCs in culture. Cells were then incubated with

the detection reagent for 60min at 37°C. Subsequently, fluorescence of the plated cells was determined using appropriate wavelengths (i.e., excitation 480 nm, emission 535 nm).

Adhesion assay of BMO cells and ECFCs.

To measure adhesion, harvested bone marrow outgrowth cells (BMOs) or ECFCs were incubated with 5 μ M calcein AM (Life Technologies) at 37°C for 30min. The BMOs or ECFCs were washed, centrifuged at 400 x g for 5min and resuspended in media and allowed to incubate at 37°C for an additional 30min. Cells were then added to confluent S17 bone marrow stromal cells (gift from Dr. Kenneth Dorschkind, University of California, Los Angeles) in a 24 well plate at 10⁵ cells/well. At time points of interest, the wells were aspirated, washed, and fluorescence detected in a BioTek plate reader. The percent adhesion was determined based upon the maximum fluorescence of 10⁵ cell aliquots. Background fluorescence was determined using wells coated with BSA.

Results

Effect of benzene exposure on bone marrow-resident hematopoietic stem cells. 2wks of volatile benzene exposure resulted in a significant decrease of megakaryocyte-erythroid progenitor (MEP), granulocyte-monocyte progenitor (GMP) and multipotent progenitor (MPP) cell types (Figure 37A). Common myeloid progenitor (CMP) and hematopoietic progenitor (HPC) cell types were

unchanged. No corresponding change was evident in the CBC of these mice (Chapter II). 6wks of volatile benzene exposure displayed a different hematopoietic lineage variance than did 2wks of benzene exposure (Figure 37B). After 6wks of benzene exposure GMPs were elevated ($p < 0.05$) were as HPCs whereas decreased.

Effect of benzene exposure on bone marrow derived hematopoietic stem cell differentiation. Bone marrow aspirates were plated for 3d in a differentiation medium directly after collection. Three days after 2wks of benzene exposure a 45% decrease in hematopoietic stem cell colony-forming units (HSC CFU) of the granulocyte-monocyte phenotype (GM) were found to be decreased relative to HFA exposed animals (Figure 38A). 6wks of exposure demonstrated a trending 23% reduction ($p = 0.088$) in HSC CFU-GMs relative to HFA. An insignificant trending decrease was displayed in HSC CFUs with a non-granulocyte-monocyte phenotype (“other”) after 6wks of benzene exposure (Figure 38B).

Effect of benzene exposure on bone marrow derived and circulating EPCs. Opposing changes in circulating EPC abundance was displayed after 2 and 6wks of benzene exposure (Figure 39A). 2wks of benzene exposure corresponded to a 40% increase in circulating EPCs while 6wks of exposure showed a 48% significant decrease in circulating EPCs. No significant change in EPC abundance following benzene exposure was seen until 6wks of inhalation wherein a 58% decrease was observed (Figure 39B). In addition, monochlorobimane (MCB) mean fluorescence intensity (MFI) was reduced by 66%

and 76% in peripheral blood and bone marrow derived EPCs, respectively. This suggests that while cell abundance is not altered, they were under oxidative stress.

Effect of benzene exposure plus HFD on bone marrow-resident hematopoietic stem. HFA versus HFA exposed, HFD fed animals demonstrated a significant change in many hematopoietic lineage cell types, including relative increases in MEPs and HPCs and decreases in GMPs and MPPs (Figure 40). Reductions in benzene-exposed, HFD fed animals compared with HFA exposed, HFD fed mice demonstrated decreases in MEPs and HPCs, while reduction in benzene-exposed, HFD fed mice compared with benzene exposure alone was seen in GMPs and HPCs.

Effect of benzene exposure plus HFD on bone marrow derived hematopoietic stem cell differentiation. Mice administered HFD demonstrated an additive depletion of HSC CFU-GMs compared with NC animals (Figure 41A). Benzene-exposed, HFD fed mice displayed a similar relative reduction in HSC CFU-GMs that was seen when comparing HFA to benzene. However, the lower decrease of HSC CFU-GMs in HFA exposed HFD fed mice compared with HFA exposed suggests that HFD conferred additional differentiation defect susceptibility independent of benzene exposure. Mice belonging to the HFA exposed, HFD fed cohort demonstrated an increase in relative HSC CFU-other relative to HFA (Figure 41B). While benzene-exposed, HFD fed mice displayed a diminution in development relative to HFA exposed, HFD fed mice, it is clear that benzene-exposed, HFD fed animals did not display a significant HSC

Figure 37.

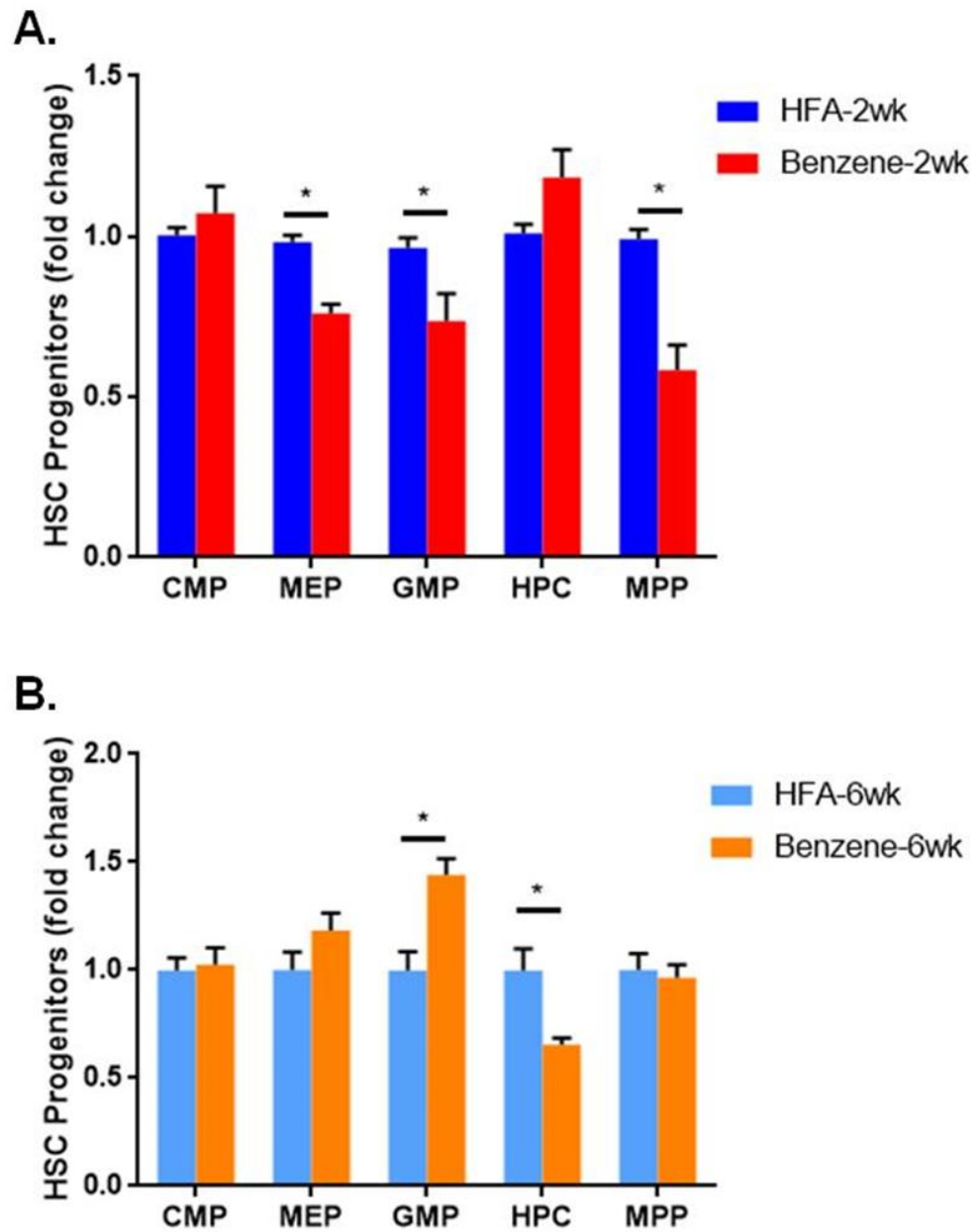


Figure 37. Benzene exposure and bone marrow-resident hematopoietic stem cell populations. Mice were exposed to HFA or 50ppm benzene for 2wks or 6wks and euthanized and bone marrow flushed in sterile PBS. Samples from 4 separate exposures were analyzed to assess relative abundance of cells within the hematopoietic lineage by cytometry. The results document CMP, MEP, GMP, HPC, and MPP from 2wk (A) and 6wk (B) exposures are displayed in the above figure. n=10-30 mice/treatment; *p<0.05.

Figure 38.

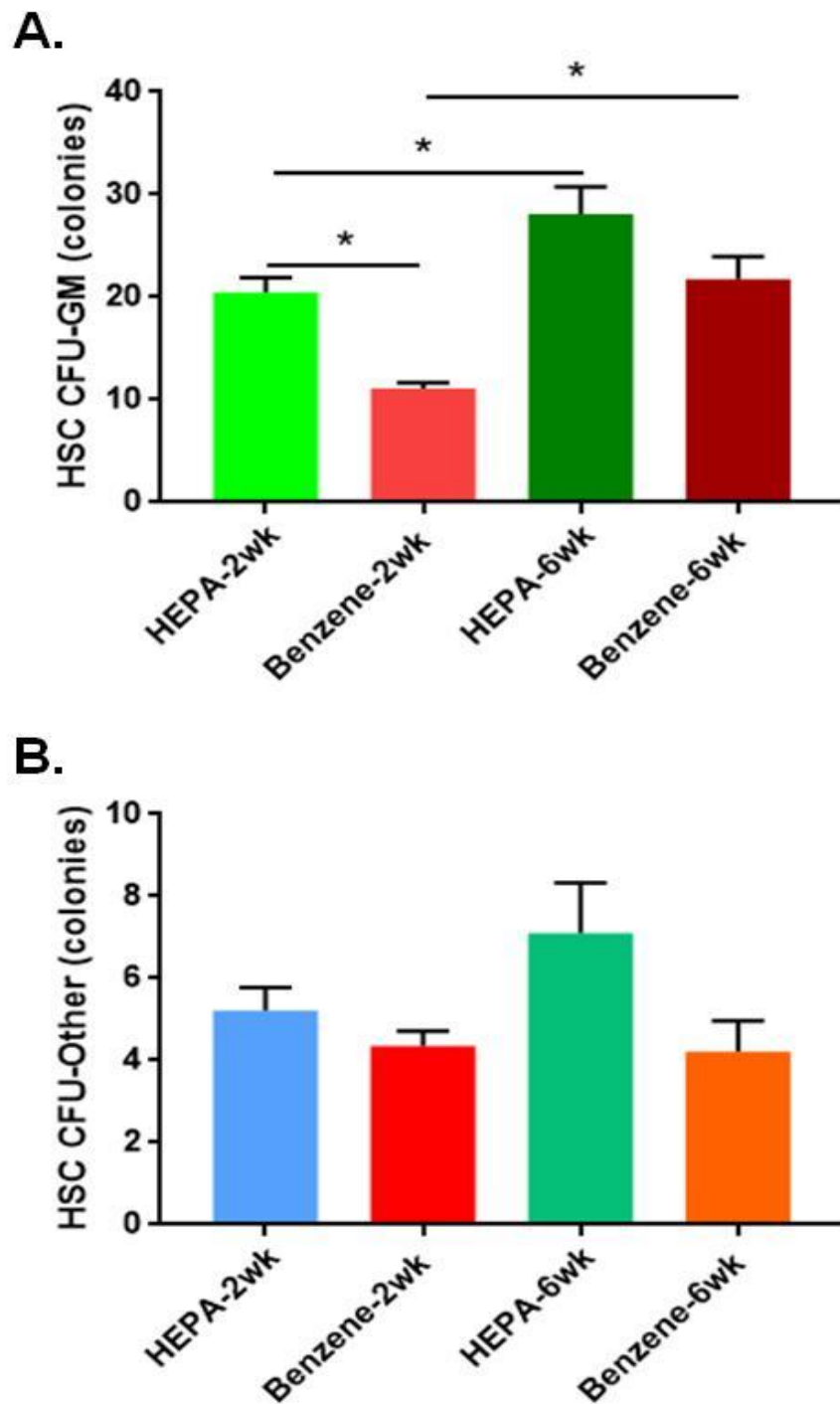


Figure 38. Benzene exposure and HSC CFU outgrowth. Mice were exposed to HFA or 50ppm benzene for 2wks or 6wks and euthanized and bone marrow flushed in sterile PBS. Samples from 4 separate exposures were analyzed to assess relative abundance of cluster forming units of granulocyte-monocyte (HSC CFU-GM) (A) or other units (HSC CFU-Other) (B). 2wk: n=20-27 mice/treatment; 6wk: n=9-10 mice/treatment; *p<0.05.

Figure 39.

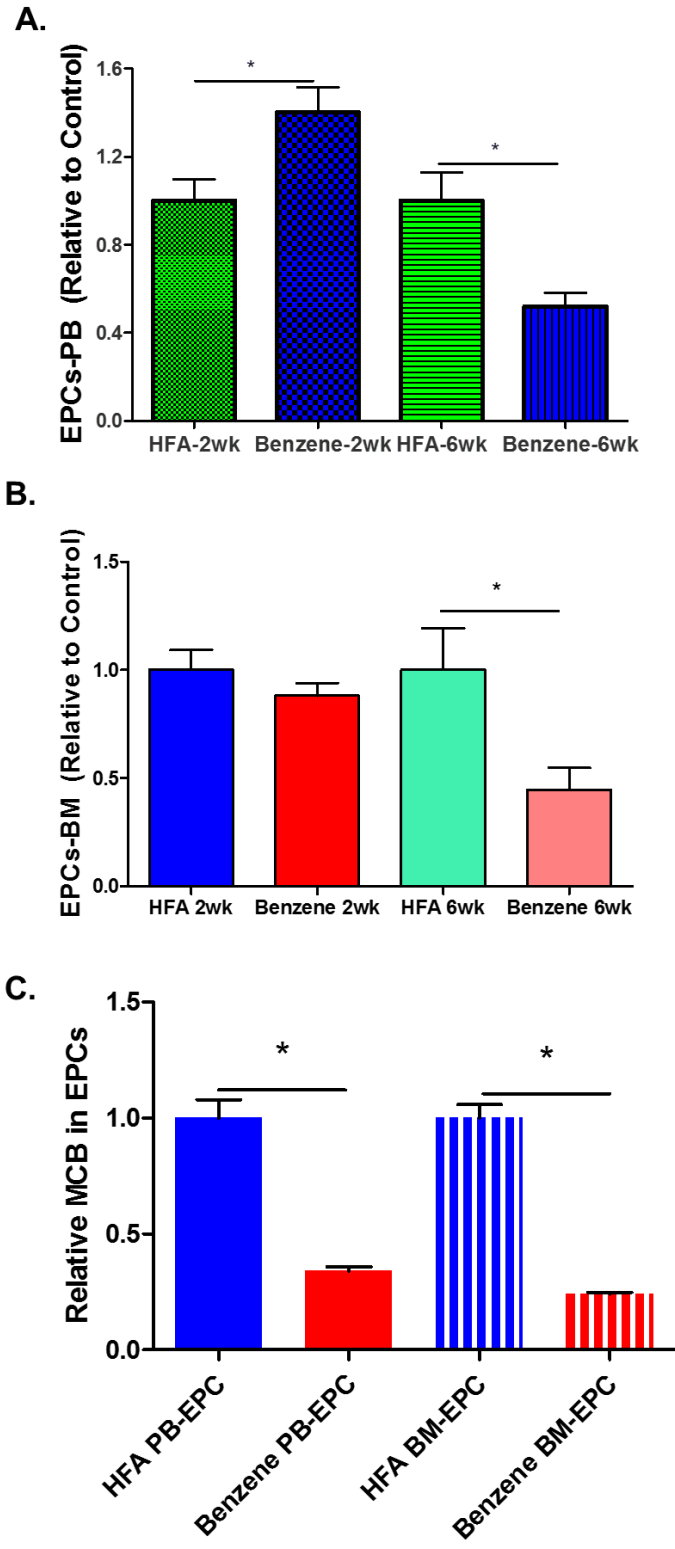


Figure 39. Circulating and bone marrow-derived EPCs and benzene exposure. Mice were exposed to HFA or 50ppm benzene for 2wks or 6wks and euthanized, peripheral blood was collected and bone marrow flushed in sterile PBS. Samples from 4 separate exposures were analyzed to assess relative abundance of and oxidative stress in circulating and bone marrow-derived EPCs. The results document relative abundance of circulating EPCs (A) BM-derived EPCs (B) and circulating and BM-derived EPC relative MCB fluorescence. 2wk PB and BM EPCs: n=25-28 mice/treatment; 6wk PB and BM EPCs: MCB in EPCs: n=8-10 mice/treatment; *p<0.05.

CFU-other increase or decrease. Many of the HSC CFU-other populations are thought to be largely composed of erythrocyte progenitors, which in agreement with the increase in MEP levels with HFA exposed, HFD fed mice compared with HFA exposed animals.

Effect of benzene exposure plus HFD on bone marrow-derived and circulating EPCs. While HFA exposed, HFD-fed animals demonstrated no change in baseline circulating EPCs compared with HFA, it is apparent that benzene-exposed, HFD fed animals demonstrated a 56% decrease in these cells relative to HFA exposed animals on HFD (Figure 42A). Additionally, HFD plus benzene-exposed mice displayed a significant diminution of circulating EPCs relative to benzene-exposed animals. The bone marrow EPCs from mice on HFD displayed significant reductions with or without benzene exposure (Figure 42B) relative to their NC, exposure-matched counterparts. Additionally, benzene-exposed, HFD fed animals displayed a slight increase in BM EPCs relative to HFA exposed animals on HFD.

EPCs show functional defects with exposure to benzene or benzene metabolites. Bone marrow derived EPCs from benzene-exposed animals showed increased rates of adhesion to bone marrow stromal S17 cells relative to HFA *ex vivo* (Figure 43A), while a similar increase in adhesion of ECFCs is seen to stromal S17 cells *in vitro* with benzene metabolite treatment relative to vehicle controls (Figure 43B). Additionally, ECFCs treated *in vitro* with benzene metabolites show a decreased rate of proliferation relative to controls (Figure 43C).

Figure 40.

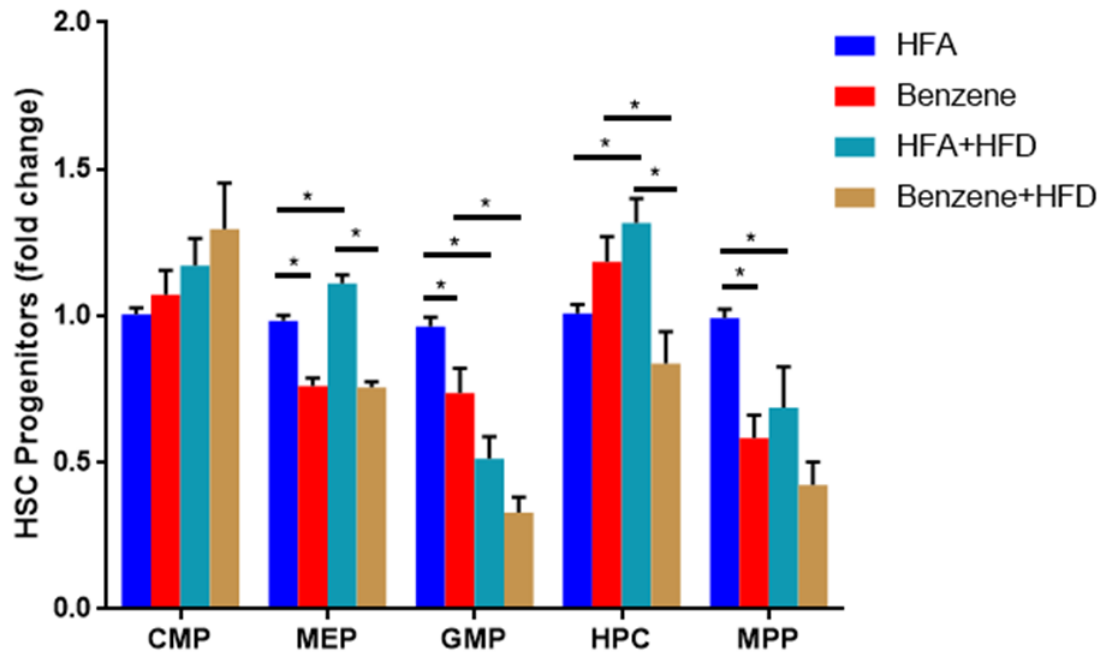


Figure 40. HFD, benzene exposure and bone marrow-resident hematopoietic stem cells. Mice were exposed to HFA or 50ppm benzene for 2wks and fed a normal chow diet or HFD for 8wks. Animals were euthanized and bone marrow flushed in sterile PBS. Samples from 4 separate exposures were analyzed to assess relative abundance of cells within the hematopoietic lineage by cytometry. Illustrated are results for CMP, MEP, GMP, HPC, and MPP. n=20-30 mice/treatment; *p<0.05.

Figure 41.

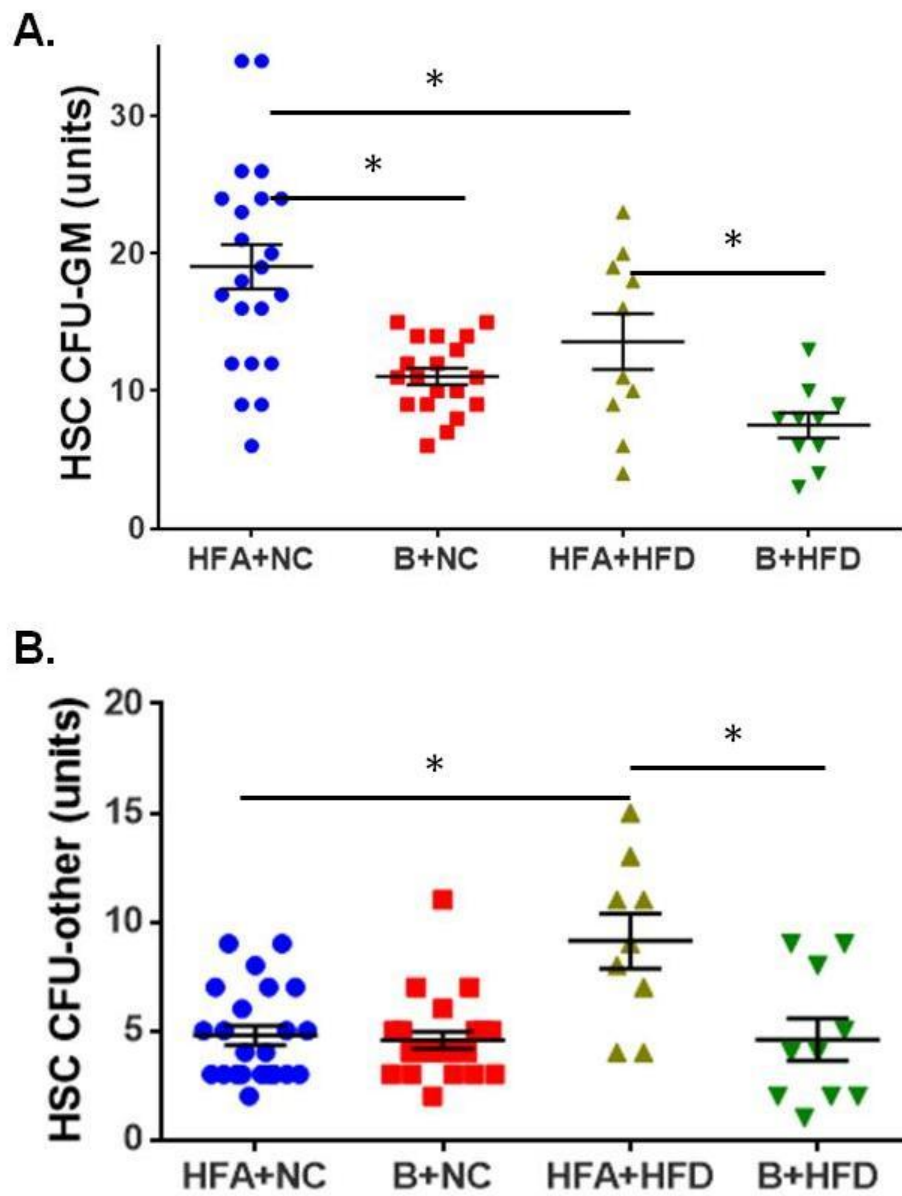


Figure 41. Benzene, HFD and HSC CFUs. Mice were exposed to HFA or 50ppm benzene for 2wks and fed normal chow diet or HFD. Animals were euthanized and bone marrow flushed in sterile PBS. Samples from 4 separate exposures were analyzed to assess relative abundance of cluster forming units of granulocyte-monocyte (HSC CFU-GM) (A) or other units (HSC CFU-Other) (B). n=10-20 mice/treatment; *p<0.05.

Figure 42.

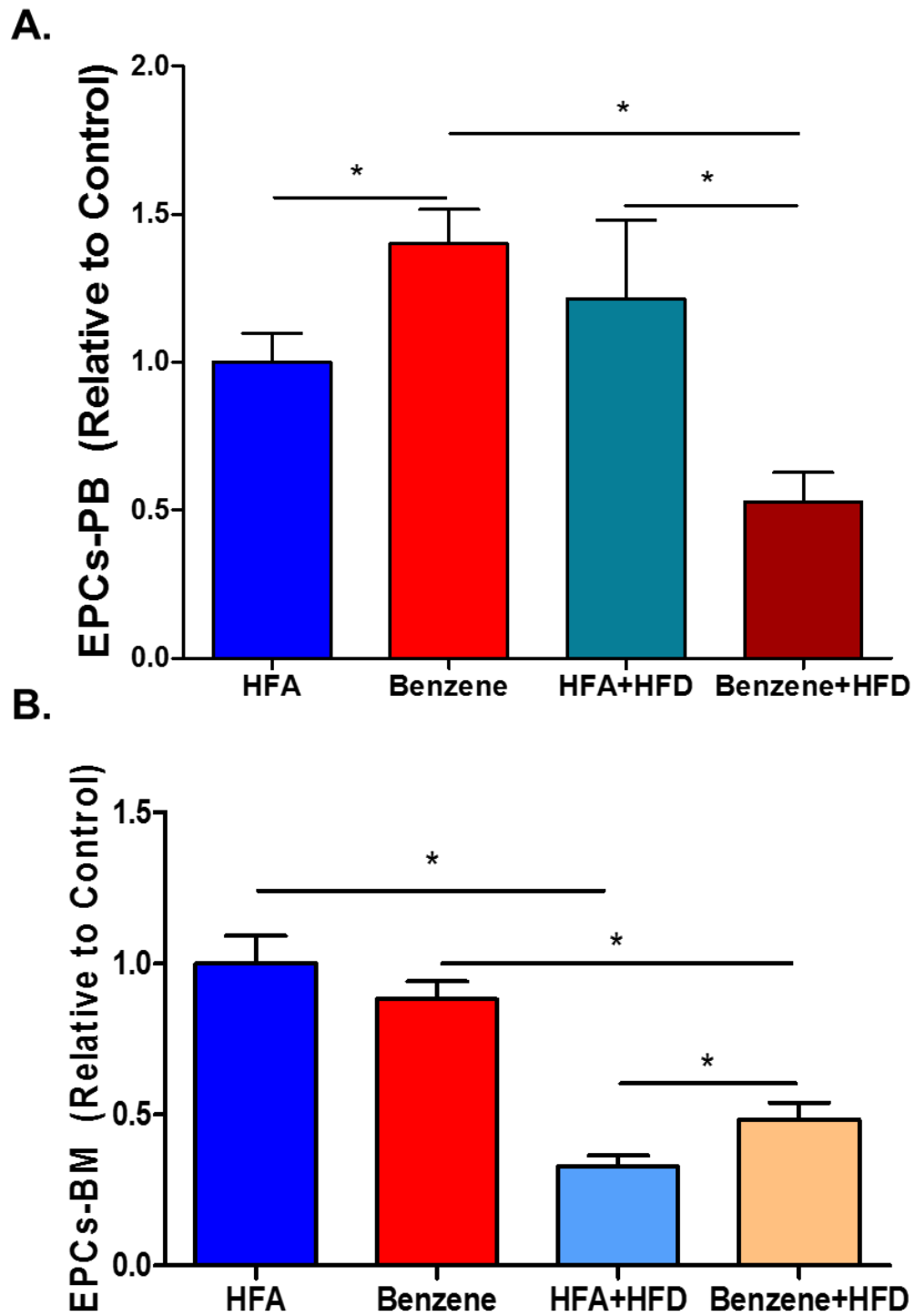
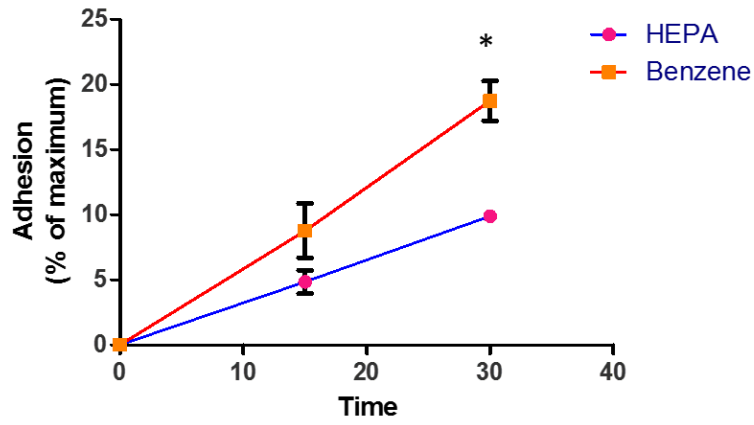


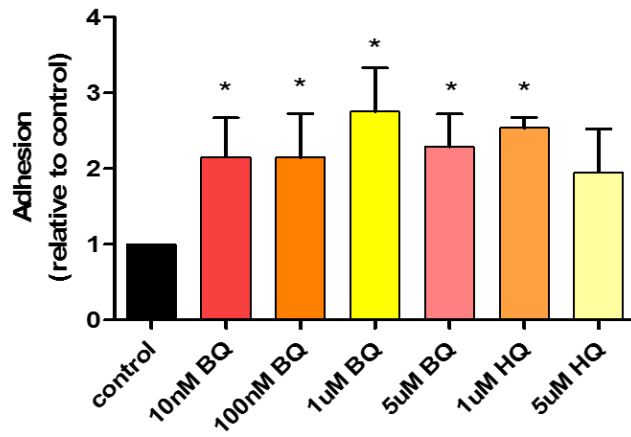
Figure 42. Benzene, HFD and circulating and BM EPCs. Mice were exposed to HFA or 50ppm benzene for 2wks and fed normal chow diet or HFD. Animals were euthanized, peripheral blood was collected and bone marrow flushed in sterile PBS. Samples from 4 separate exposures were analyzed to assess relative abundance of circulating (A) and bone marrow-derived (B) EPCs. n=10-28 mice/treatment; *p<0.05

Figure 43.

A.



B.



C.

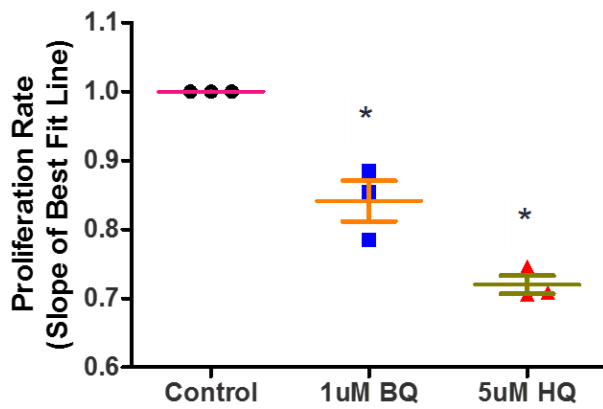


Figure 43. EPC adhesion, proliferation and benzene exposure. Mice were exposed to HFA or 50ppm benzene for 2wks. Animals were euthanized, and bone marrow flushed in sterile PBS. BM outgrowth cells were cultured as described. Samples from 2 separate exposures were analyzed to assess *ex vivo* adhesion of bone marrow-derived outgrowth endothelial progenitor cells (A) to S17 bone marrow stromal cells. Human endothelial progenitor cells (endothelial colony forming cells [ECFCs]) were incubated with benzene metabolites as described in methods and *in vivo* adhesion (B) to S17 bone marrow stromal cells and proliferation rates (C) were analyzed. Panel A: n=4 mice/treatment; Panel B: n=3-6 experiments; Panel C: n=3 experiments; *p<0.05.

Discussion

This study is the first of its kind to document the differential susceptibility of bone marrow derived hematopoietic and endothelial stem cells to benzene exposure *in vivo*, *ex vivo* and *in vitro*. Additionally, this study provides new biomarkers that precede and predict peripheral cytopenia alterations most commonly measured as indicators of benzene exposure. Results from this study clearly show a dynamic equilibrium in the bone marrow niche specific to duration of benzene exposure and diet. Interestingly, while stem cell abundance was the primary measurement for sensitivity, other endpoints (e.g. MCB, adhesion rates, proliferation rates) proved a remarkable predictor of stem cell abundance. Thus future studies would be greatly edified by researching further the functional and adaptive changes of these various populations.

The outcomes of these experiments generated a glimpse into the health and response of the stem cell niche in response to benzene exposure while suggesting interesting biomarkers for assessment of benzene exposure. While CBCs are the standard, easily measured variable, frequently used to assess current susceptibility to benzene exposure, we have found in these NC mice to have altered hematopoietic differentiation that precedes and predicts altered CBCs. Depletion of HSC CFU-GMs was also found to arise as an indicator of future CBC changes. While we used bone marrow for HSC CFU assays, this experiment can be completed with cells from the peripheral blood and may be a more reliable indicator of acute exposure. However, HSC CFU-GMs and hematopoietic lineage did not show the same depletions after 6wks of benzene

exposure relative to their HFA controls, suggesting that these effects may be transient or briefly compensated in a manner after initial depletion. Interestingly, peripheral blood and bone marrow EPCs demonstrated a progressive diminution in both compartments after 6wks of benzene exposure, possibly implying that effects on these cells is more cumulative and lasting than in HSCs.

With benzene-exposed, HFD-fed animals, the effect on these stem cell populations was markedly pronounced. Large depletions were seen in hematopoietic lineage subtypes GMP and HPC relative to benzene and HFA while MPP and MEP remained suppressed in benzene-exposed, HFD-fed animals relative to HFA exposed controls. The change is striking when coupled with the depletion of the HSC CFU-GMs of the differentiation assay along with significant reduction of neutrophils and lymphocytes of benzene-exposed, HFD-fed mice relative to HFA-exposed, HFD-fed controls. EPCs showed a response in animals of the benzene-exposed, HFD-fed cohort that demonstrate both a general EPC depletion in the bone marrow relative to HFA, but an increase in cells relative to HFA-exposed, HFD-fed animals. These benzene-exposed, HFD-fed animals also show a decrease in PB EPCs relative to HFA-exposed, HFD-fed and HFA-exposed controls. Though a HFD may be the primary driver of depleted BM EPCs at this time point, it appears that benzene exposure is inhibiting EPC egress from the bone marrow to the peripheral blood. This might explain the relative increase in BM EPCs but the significant decrease in PB EPCs of benzene-exposed, HFD-fed mice relative to HFA-exposed, HFD-fed controls. Interestingly, bone marrow outgrowth EPCs from benzene-exposed

mice demonstrate an increased rate of adhesion to bone marrow stromal S17 cells relative to HFA controls. This increased adhesion rate is replicated with benzene metabolite treatment of human EPCs (ECFCs) relative to vehicle treated control. Additionally, ECFCs treated with benzene metabolites show decreased proliferation rates. These proliferation assays suggest that benzene may also be playing a role in the diminution of EPC abundance in the benzene-exposed, HFD-fed mice.

Damage to the bone marrow tissue will be phenotypically reflected in the tissues into which these bone marrow-derived, differentiated cells will come to function. Most crudely this is exemplified in bone marrow irradiation and inherent subsequent depletion of hematopoietic stem cells driving pancytopenia. A subtler and more specific example may be reflected in type 2 diabetics (T2D) having diminished abundance of circulating endothelial progenitor cells (EPCs) while still maintaining a population within the bone marrow having a mobilization defect. This lack of circulating EPCs inhibits the repair of accumulating vascular injury, leading to a dysfunctional endothelium and greater cardiovascular risk. Here, we use benzene, an agent especially toxic to the bone marrow, as an effective tool in assessing relative sensitivity of bone marrow derived stem cells to toxicity. Our focus in these investigations assesses responses in the stem cell niche to benzene exposure coupled with interventions and attributing relative rapidity and intensity of response by hematopoietic progenitor cells, cardiac progenitor cells and endothelial progenitor cells.

There may be many reasons why stem cell subpopulations have variance in vulnerability to particular stimuli. Decreased proximity to the source of the insult (i.e. oxidative stress) may inherently expose a cell to higher concentrations of a particular agent. This is quite plausible, as the bone marrow niche is composed of many discrete areas defined by their proximate location to anatomical landmarks. The endosteal niche (or the endosteum) is a slender piece of vascular, connective tissue coating the interior surface of the medullary cavity. This area is home to quiescent HSCs and 80% of less differentiated hematopoietic stem cells (HSCs). As HSCs differentiate they move towards the perivascular niche where they may egress from the BM by way of vasculature. Thus, more differentiated cells are likely to be affected by vascular stressors. In our hematopoietic lineage assays we see a greater effect on more differentiated cells (MEPs and GMPs) with less effect on CMPs, MPPs and HPCs. Given the relative distance of exposure that these cells have to any vascular driven disruption, these changes would be in agreement with this possibility. Additionally, if the source of stress happens because the cell expresses a particular enzyme that catalyzes a reaction with noxious byproducts (e.g. the conversion of hydroquinone to benzoquinone via myeloperoxidase, prevalent in granulocyte precursors) then those cells are more likely to be negatively influenced. Again, the repeated depletion of GMPs and HSC CFU-GMs suggest that this may be a reason why HSC CFU-GMs are more affected than HSC CFU-others and why GMPs deplete more readily than MEP populations. Conversely, cells may have decreased expression or activity of enzymes capable of

mediating benzene metabolite-induced oxidative stress (e.g. glutathione, superoxide dismutase, etc). This could happen with age or if additional stress is added to the system (e.g. HFD).

This differential toxicity may result in abnormal proliferation of progenitor cells or blocked differentiation pathways leading to deficits in fully differentiated cells. Additionally, a decrease in fully differentiated cells may result from decreased mobilization of cells from the perivascular niche to the peripheral vasculature thus resulting in fewer cells reaching the tissue in which they play a functional role. In these investigations we see strong potential for decreased proliferation rates and decreased EPC egress to play a role in cardiovascular pathological development with intermediate to chronic benzene exposure.

Given that the health of progenitor populations is a sensitive predictor of physiological outcomes in the respective differentiated cell and tissue populations it is imperative to understand which progenitor population is influenced by a particular pollutant. While the specific mechanism conferring susceptibility to each stem cell type is beyond the scope of this study, we seek to draw attention to the relative susceptibility of certain stem cell populations exposed benzene in order to ascertain relative risk of disease (i.e. hematological versus cardiovascular) following benzene exposure.

These studies show that hematopoiesis is acutely sensitive to benzene exposure, while intermediate and long term exposures have varied responses with regard to relative abundance of precursor cells. EPCs demonstrate a diminution with 6wks of benzene exposure with altered function after 2wks of

exposure. Cells treated with benzene metabolites BQ and HQ demonstrate similar results in function along with additional decreased proliferation rates. While it is not abundantly clear from these studies whether hematopoiesis or cardiovascular health will be more greatly affected by benzene exposure, it is abundantly clear that cardiovascular health will likely be affected by benzene exposure due to depleted EPC abundance and function. This possibility for cardiovascular injury is novel and has remained largely unstudied. Furthermore, it is clear that HFD plays a clear role in disrupting the bone marrow niche and that benzene exposure and HFD feeding potentiates injury to stem cells implying that lifestyle factors will strongly alter susceptibility to hematopoietic and cardiovascular health.

CHAPTER V

CONCLUDING DISCUSSION

These studies were carried out to expand the understanding of the effects of volatile benzene exposure on the cardiovascular and hematopoietic systems. More specifically, our hypothesis addressed whether the effects of benzene-induced, hepatic CYP2E1-generated ROS would play a role in inflammation, tissue injury, insulin resistance, and vascular repair. To this end, we characterized the general response of mice to benzene exposure measuring indices of tissue injury, vascular health while monitoring complete blood counts (Table 7). We also assessed markers of oxidative stress, inflammation, glycemic indices and insulin signaling pathways (Table 8). Lastly, we looked how benzene exposure influences hematopoietic progenitor cells and endothelial progenitor cells (*in vivo* and *ex vivo*) (Table 9). These results tell us that volatile benzene exposure induces oxidative stress, inflammation, insulin resistance, tissue damage and possibly deficiencies in vascular repair. Notably, these data also show that changes in these outcomes occur at levels similar to the lowest observed adverse effect levels in hematotoxicity studies. Therefore, these signs of inflammation, oxidative stress and vascular disruption are just as likely to be having acute effects following benzene exposure as is hematotoxicity.

While we cannot rule out changes due to oxidative stress generated by extra-hepatic CYP2E1-mediated ROS or by damage caused by reactive metabolite adduct formation, previous studies suggest that these are unlikely scenarios. To further address the former statement, it would be beneficial to utilize a transgenic animal model overexpressing an antioxidant (e.g. superoxide dismutase) to validate that the oxidative stress-induced changes are liver specific. However, previously mentioned studies have provided detailed tissue expression data for CYP2E1 and have demonstrated that the enzyme is primarily hepatic. Furthermore, studies involving CYP2E1KO animals exposed to benzene exhibit complete protection from hematopoietic and genotoxic effects, while generating no significant level of benzene metabolite. Additional investigations with overexpressing CYP2E1 hepatocytes demonstrated increased oxidative stress. These studies show that CYP2E1 is primarily hepatic, necessary for benzene metabolism and toxicity and generate increased levels of oxidative stress that reduce cell viability. Other studies have shown protection from HFD-induced weight gain and insulin resistance in CYP2E1KO mice compared with wild type animals. Increased activity of CYP2E1 is strongly associated with weight gain and loss in humans, a condition highly associated with oxidative stress and inflammation. Lastly while reactive benzene metabolites are briefly formed, most metabolites are conjugated and excreted before forming adducts with other molecules. These studies provide biological plausibility for the data shown here.

Notably, these changes are occurring at levels nearing the LOAEL in animal models acutely exposed to benzene. Given that the benzene-induced IR

phenotype presents before hallmark benzene-associated cytopenias suggests that changes in insulin sensitivity may be a better indicator of benzene exposure than altered circulating blood populations. One study looking at elderly men's level of urinary benzene metabolite (i.e. *t,t*-MA), HOMA-IR score and oxidative stress levels confirm our results. This study found positive correlations between *t,t*-MA and HOMA-IR as well as with *t,t*-MA and oxidative stress.

Our results also suggest that vascular damage occurs at 2 and 6wks of exposure as seen with elevated PB EPCs and increased circulating endothelial-derived microparticle levels at 2 and 6wks of exposure, respectively. A likely disruption in vascular repair capacity may be inferred due to diminished PB and BM-derived EPC levels at 6wks of exposure. This suggests that acute and chronic exposure may play a role in development of accumulating vascular damage which could lead to development of CV complications.

Together, these data give plausibility for simultaneous disruption of cardiovascular, metabolic, and hematopoietic processes following benzene exposure. Given the increased environmental release of benzene through industrial activities and worldwide exposure to benzene through cigarette smoking that is commensurate with the rapid increase in pre-diabetes and CVD prevalence it is possible that chronic, ubiquitous benzene exposure is playing a role in the development of these pathologies.

Table 7. Characteristics of response to benzene exposure.

General Characteristics		
Endpoint	2wk Benzene	6wk Benzene
CBC	-	↓↓
ALT	↑	-
AST	↑	-
ALT:AST	-	-
Albumin	↓	↑
Body Weight	-	-
Liver:Body Weight	↑	-
HDL	↑	↑
LDL	-	↑↑
LDL:HDL	-	↑
Total Cholesterol	-	-
TRG	-	-
EMP	-	↑↑
Act. EMP	-	↑↑
LMP	-	↑↑
PMP	-	-
PLAgg	↑↑	↑↑
Immune Cells	-	-

Illustrated are the changes in general characteristics seen in mice after indicated exposures.

↑ = moderate increase (0.1 – 1.4-fold, $p < 0.05$) for indicated exposure; ↑↑ = greater increase (≥ 1.5 -fold, $p < 0.05$), - = no change ($p \geq 0.05$), NM = not measured; ↓ = moderate decrease (0.1-1.4-fold, $p < 0.05$), ↓↓ = greater decrease (≥ 1.5 -fold, $p < 0.05$)

Table 8. Indices of oxidative stress, inflammation and IR.

Oxidative stress, Inflammation and IR			
Endpoint	2wk Benzene	2wk Benzene + TEMPOL	6wk Benzene
FPG	↑	-	-
FPI	↑	-	↑↑
HOMA-IR	↑↑	-	↑↑
HOMA-b	↑↑	-	↑
GTT	↑	-	NM
ITT	↓↓	↓	NM
phospho-Akt _{liver}	↓↓	-	↓↓
phospho-Akt _{SM}	↓↓	-	↓↓
GSH _{liver}	↓	-	↓↓
GSH _{SM}	↓	-	↓↓
MCB _{lymphocytes}	↓↓	-	NM
MDA _{liver}	↑↑	-	NM
phospho-NFkB _{liver}	↑↑	-	↑↑
phospho-NFkB _{SM}	↑↑	-	↑↑
MIP1a _{liver}	↑↑	-	NM
MIP1a _{SM}	↑↑	-	NM
SOCS1 _{liver}	↑↑	-	NM
SOCS3 _{liver}	-	-	NM
phospho-IRS-2	↓	-	NM
miR130a	-	NM	NM
miR223	-	NM	NM
miR320b	↑	NM	NM
miR let7f	-	NM	NM
PTEN	-	NM	↑↑

Illustrated are the changes in oxidative stress, inflammation and IR seen in mice after indicated exposures.

↑ = moderate increase (0.1 – 1.4-fold, p<0.05) for indicated exposure; ↑↑ = greater increase (≥1.5-fold, p<0.05), - = no change (p≥0.05), NM = not measured; ↓ = moderate decrease (0.1-1.4-fold, p<0.05), ↓↓ = greater decrease (≥1.5-fold, p<0.05)

Table 9. Hematopoietic and endothelial progenitor cells.

Hematopoietic and Endothelial Progenitor Cells			
Endpoint	2wk Benzene	2wk Benzene + HFD	6wk Benzene
CMP	-	-	-
MEP	↓	↓	-
GMP	↓	-	↑
HPC	-	↓	↓
MPP	↓	-	-
HSC CFU-GM	↓↓	↓	↓
HSC CFU-Other	-	↓↓	-
PB EPC	↑	↓↓	↓↓
BM EPC	-	↑	↓↓
PB EPC MCB	↓↓	NM	NM
BM EPC MCB	↓↓	NM	NM
EPC Adhesion <i>ex vivo</i>	↑↑	NM	NM

Illustrated are the changes in hematopoietic and endothelial progenitor cells seen in mice after indicated exposures.

↑ = moderate increase (0.1 – 1.4-fold, p<0.05) for indicated exposure; ↑↑ = greater increase (≥1.5-fold, p<0.05), - = no change (p≥0.05), NM = not measured; ↓ = moderate decrease (0.1-1.4-fold, p<0.05), ↓↓ = greater decrease (≥1.5-fold, p<0.05)

REFERENCES

1. Kojima N, Mitomo A, Itaya Y, Mori S, Yoshida S. Adsorption removal of pollutants by active coques produced from sludge in the energy recycle process of wastes. *Waste management (New York, NY)*. 2002;22(4):399-404.
2. Cockburn A, Barraco RA, Reyman TA, Peck WH. Autopsy of an Egyptian mummy. *Science*. 1975;187(4182):1155-60.
3. Shaw AB. Knappers' rot. Silicosis in East Anglian flint-knappers. *Medical history*. 1981;25(2):151-68.
4. Brimblecombe P. The antiquity of 'smokeless zones'. *Atmospheric Environment (1967)*. 1987;21(11):2485-.
5. Gari L. Notes on air pollution in Islamic heritage. *Hamdard Medicus*. 1987;30:40-8.
6. Bowler CB, P. Control of Air Pollution in Manchester prior to the Public Health Act, 1875. *Environment and History*. 2000;6(1):71-98.
7. Allen WE. *Transatlantic crossing : American visitors to Britain and British visitors to America in the nineteenth century*. New York: Morrow; 1971.
8. Brimblecombe P. *The big smoke : A history of air pollution in London since medieval times*. London: Methuen; 1987.
9. *Public Health Act of 1848.*, (1848).
10. Melosi MV. *Pollution and Reform in American Cities 1870-1930*. Austin: University of Texas Press; 1980.
11. Brimblecombe PB, C. *The Silent Countdown*. Berlin: Springer-Verlag; 1990.
12. Bernstein HT. The mysterious disappearance of Edwardian London fog. *The London Journal*. 1975;1:189-206.
13. Russell WT. The influence of London fog on mortality from respiratory diseases. *The Lancet*. 1924:335-9.
14. Bates DV. *Environmental Health Risks and Public Policy: Decision-making in Free Societies*. Seattle: Washington University Press; 1994.
15. Ng M, Freeman MK, Fleming TD, et al. Smoking prevalence and cigarette consumption in 187 countries, 1980-2012. *JAMA*. 2014;311(2):183-92.
16. Organization WH. *WHO Report on the Global Tobacco Epidemic, 2011*. Geneva: World Health Organization, 2011.
17. Registry AftSaD. *Toxicological Profile for Benzene*. U.S. Department of Health and Human Services, 2007.
18. Davis DL, Bell ML, Fletcher T. A look back at the London smog of 1952 and the half century since. *Environ Health Perspect*. 2002;110(12):A734-5.
19. Hunt A, Abraham JL, Judson B, Berry CL. Toxicologic and epidemiologic clues from the characterization of the 1952 London smog fine particulate matter in archival autopsy lung tissues. *Environ Health Perspect*. 2003;111(9):1209-14.
20. NDRC. *Environmental Laws and Treaties*. NDRC, 2016.

21. Quenel P, Zmirou D, Dab W, Le Tertre A, Medina S. Premature deaths and long-term mortality effects of air pollution. *International journal of epidemiology*. 1999;28(2):362.
22. Rehfuess E, Corvalan C, Neira M. Indoor air pollution: 4000 deaths a day must no longer be ignored. *Bull World Health Organ*. 2006;84(7):508.
23. Pope CA, 3rd, Ezzati M, Dockery DW. Fine-particulate air pollution and life expectancy in the United States. *N Engl J Med*. 2009;360(4):376-86.
24. Division OoAQPaSHaEI. Quantitative Health Risk Assessment for Particulate Matter Research Triangle Park: U.S. Environmental Protection Agency, 2010.
25. Dockery DW, Pope CA, 3rd, Xu X, Spengler JD, Ware JH, Fay ME, et al. An association between air pollution and mortality in six U.S. cities. *N Engl J Med*. 1993;329(24):1753-9.
26. Pope CA, 3rd, Burnett RT, Thurston GD, Thun MJ, Calle EE, Krewski D, et al. Cardiovascular mortality and long-term exposure to particulate air pollution: epidemiological evidence of general pathophysiological pathways of disease. *Circulation*. 2004;109(1):71-7.
27. Krewski D, Burnett RT, Goldberg M, Hoover K, Siemiatycki J, Abrahamowicz M, et al. Reanalysis of the Harvard Six Cities Study, part II: sensitivity analysis. *Inhalation toxicology*. 2005;17(7-8):343-53.
28. Krewski D, Burnett RT, Goldberg MS, Hoover K, Siemiatycki J, Abrahamowicz M, et al. Validation of the Harvard Six Cities Study of particulate air pollution and mortality. *N Engl J Med*. 2004;350(2):198-9.
29. Standards OoAQPa. Our Nation's Air: Status and Trends Through 2008. Research Triangle Park: U.S. Environmental Protection Agency, 2010.
30. Ibrahim AL, Zee YC, Osebold JW. The effects of ozone on the respiratory epithelium and alveolar macrophages of mice. I. Interferon production. *Proceedings of the Society for Experimental Biology and Medicine Society for Experimental Biology and Medicine (New York, NY)*. 1976;152(4):483-8.
31. Saltzman BE, Svirbely JL. Ozone toxicity and substances associated with its production. *AMA archives of industrial health*. 1957;15(2):111-8.
32. Bell ML, McDermott A, Zeger SL, Samet JM, Dominici F. Ozone and short-term mortality in 95 US urban communities, 1987-2000. *Jama*. 2004;292(19):2372-8.
33. Pershagen G, Rylander E, Norberg S, Eriksson M, Nordvall SL. Air pollution involving nitrogen dioxide exposure and wheezing bronchitis in children. *International journal of epidemiology*. 1995;24(6):1147-53.
34. Gairola CG, Wu H, Gupta RC, Diana JN. Mainstream and sidestream cigarette smoke-induced DNA adducts in C7Bl and DBA mice. *Environ Health Perspect*. 1993;99:253-5.
35. Brunnemann KD, Kagan MR, Cox JE, Hoffmann D. Analysis of 1,3-butadiene and other selected gas-phase components in cigarette mainstream and sidestream smoke by gas chromatography-mass selective detection. *Carcinogenesis*. 1990;11(10):1863-8.
36. FDA. Progress and Effectiveness of tile Implementation of the Family Smoking Prevention and Tobacco Control Act U.S. Department of Health and Human Services: Food and Drug Administration, 2013.
37. AIHA. Odor thresholds for chemicals with established occupational health standards. Fairfax, VA: American Industrial Hygiene Association, 1989.
38. Morris ET. *Frangrance: the story of perfume from Cleopatra to Chanel*. New York, NY: Charles Scribner's Sons; 1984.
39. Faraday M. On new compounds of carbon and hydrogen, and on certain other products obtained during the decomposition of oil by heat. *Philosophical Transactions of the Royal Society*. 1825;115:440-66.

40. Mitscherlich E. Über das Benzol und die Säuren der Oel- und Talgarten [On benzol and oily and fatty types of acids]. *Annalen der Pharmacie*. 1834;9(1):39-48.
41. Hofmann AW. Über eine sichere Reaction auf Benzol [On a reliable test for benzene]. *Annalen der Chemie und Pharmacie*. 1845;55:200-5.
42. Read J. *From alchemy to chemistry*. New York: Dover Publications; 1995.
43. Lonsdale K. The Structure of the Benzene Ring in Hexamethylbenzene. *Proceedings of the Royal Society*. 1929;123:494.
44. Eveleth WT. *Basic and intermediate chemicals*. 5th Edition ed. Fairfield, NJ: Kline & Company, Inc; 1990.
45. Fruscella W. Benzene: Kirk-Othmer Encyclopedia of Chemical Technology (1999-2014). . Hoboken, NJ: John Wiley and Sons; 2014.
46. C&EN. Top 50 chemicals production rose modestly last year. *Chem Eng News*. 1994;72(15):12-3.
47. Wallace LAN, W.C.; Ziegenfus, R.; et al. . The Los Angeles team study: Personal exposures, indoor-outdoor air concentrations, and breath concentrations of 25 volatile organic compounds. *J Exp Anal Environ Epidemiol* 1991;1(2):157-92.
48. Yu R, Weisel CP. Measurement of benzene in human breath associated with an environmental exposure. *Journal of exposure analysis and environmental epidemiology*. 1996;6(3):261-77.
49. Inventory TR. *Toxics Release Inventory (TRI) Data: Environmental Defense Fund; 2016 [Benzene Release]*.
50. Pate CTA, R.; Pitts, J.N. The gas phase reaction of O₃ with a series of aromatic hydrocarbons. . *J Environ Sci Health*. 1976;All:1-10.
51. Wallace LA. Major sources of benzene exposure. . *Environ Health Perspect* 1989;82:165-9.
52. Fraser MPC, G.R.; Simoneit, B.R.T. . Gas-phase and particle-phase organic compounds emitted from motor vehicle traffic in a Los Angeles roadway tunnel. . *Environ Sci Technol*. 1998. ;32:2051-60.
53. Administration OSH. *Chemical Hazards and Toxic Substances* Washington, D.C.: U.S. Department of Labor: Occupational Safety & Health Administration; [<https://www.osha.gov/SLTC/hazardoustoxicsubstances/> legally enforceable standards]. Available from: <https://www.osha.gov/SLTC/hazardoustoxicsubstances/>.
54. CDC. The National Institute for Occupational Safety and Health (NIOSH) cdc.gov: CDC; 2016 [updated 03/07/2016. Description of legal differences between OSHA and NIOSH]. Available from: <https://www.cdc.gov/niosh/npg/pgintrod.html>.
55. Organization WH. *Exposure to benzene: a major public health concern*. Geneva, Switzerland: World Health Organization, 2010.
56. Srbova JT, J.; Skramovsky, S. . Absorption and elimination of inhaled benzene in man. . *Arch Ind Hyg Occup Med*. 1950;2:1-8.
57. Nomiyama KN, H. . Respiratory retention, uptake and excretion of organic solvents in man: Benzene, toluene, n-hexane, trichloroethylene, acetone, ethyl acetate and ethyl alcohol. . *Int Arch Arbeitsmed*. 1974;32:75-83.
58. Pekari KV, S.; Heikkila, P.; et al. . Biological monitoring of occupational exposure to low levels of benzene. . *Scand J Work Environ Health* 1992. ;18(5):317-22.
59. Tauber J. Instant benzol death. *J Occup Med*. 1970;12:91-2.
60. Winek CLC, W.D. Benzene and toluene fatalities. *J Occup Med*. 1971;13:259-61.
61. Dowty BJL, J.L.; Storer, J. . The transplacental migration and accumulation in blood of volatile organic constituents. *Pediatr Res*. 1976;10:696-701.

62. Travis CCB, J.C. Protein binding of benzene under ambient exposure conditions. . *Toxicol Ind Health*. 1989;5(6):1017-24.
63. Rickert DEB, T.S.; Bus, J.S.; et al. . Benzene disposition in the rat after exposure by inhalation. . *Toxicology and applied pharmacology*. 1979;49:417-23.
64. Schrenk HHY, W.P.; Pearce, S.J.; et al. . Absorption, distribution and elimination of benzene by body tissues and fluids of dogs exposed to benzene vapor. . *J Ind Hyg Toxicol* 1941;23:20-34.
65. Porteous JW, Williams RT. Studies in detoxication. 20. The metabolism of benzene. II. The isolation of phenol, catechol, quinol and hydroxyquinol from the ethereal sulphate fraction of the urine of rabbits receiving benzene orally. *The Biochemical journal*. 1949;44(1):56-61.
66. Parke DV, Williams RT. Studies in detoxication. XLIX. The metabolism of benzene containing (14C1) benzene. *The Biochemical journal*. 1953;54(2):231-8.
67. Williams RT. *Detoxication Mechanisms*. London, England: Chapman and Hall; 1959. 188-94 p.
68. Jaffe M. Uber die Aufspaltung des Benzolrings im Organismus. *Z Physiol Chem*. 1909;62:58-67.
69. Drummond JC, Finar IL. Muconic acid as a metabolic product of benzene. *The Biochemical journal*. 1938;32(1):79-84.
70. Sabourin PJ, Bechtold WE, Birnbaum LS, Lucier G, Henderson RF. Differences in the metabolism and disposition of inhaled [3H]benzene by F344/N rats and B6C3F1 mice. *Toxicology and applied pharmacology*. 1988;94(1):128-40.
71. Snyder R, Kocsis JJ. Current concepts of chronic benzene toxicity. *CRC critical reviews in toxicology*. 1975;3(3):265-88.
72. Rusch GM, Leong BK, Laskin S. Benzene metabolism. *Journal of toxicology and environmental health Supplement*. 1977;2:23-36.
73. Snyder CA. *Benzene*. 2nd Edition ed. Amsterdam, Netherlands: Elsevier; 1987.
74. Henderson RF, Sabourin PJ, Bechtold WE, Griffith WC, Medinsky MA, Birnbaum LS, et al. The effect of dose, dose rate, route of administration, and species on tissue and blood levels of benzene metabolites. *Environ Health Perspect*. 1989;82:9-17.
75. Ghittori S, Fiorentino ML, Maestri L, Cordioli G, Imbriani M. Urinary excretion of unmetabolized benzene as an indicator of benzene exposure. *Journal of toxicology and environmental health*. 1993;38(3):233-43.
76. Inoue O, Seiji K, Kasahara M, Nakatsuka H, Watanabe T, Yin SG, et al. Quantitative relation of urinary phenol levels to breathzone benzene concentrations: a factory survey. *British journal of industrial medicine*. 1986;43(10):692-7.
77. Cole CE, Tran HT, Schlosser PM. Physiologically based pharmacokinetic modeling of benzene metabolism in mice through extrapolation from in vitro to in vivo. *Journal of toxicology and environmental health Part A*. 2001;62(6):439-65.
78. Lindstrom AB, Yeowell-O'Connell K, Waidyanatha S, Golding BT, Tornero-Velez R, Rappaport SM. Measurement of benzene oxide in the blood of rats following administration of benzene. *Carcinogenesis*. 1997;18(8):1637-41.
79. Vogel EG, H. Benzene oxide-oxepin valence tautomerism. . *Angew Chem Int Ed Engl*. 1967;6(5):385-476.
80. Jerina DD, J.; Witkop, B.; et al. . Role of arene oxide-oxepin system in the metabolism of aromatic substances. I. In vitro conversion of benzene oxide to a premercapturic acid and a dihydrodiol. . *Arch Biochem Biophys*. 1968;128:176-83.

81. Nebert DWR, A.L.; Vandale, S.E.; et al. . NAD(P)H:quinone oxidoreductase (NQO1) polymorphism, exposure to benzene, and predisposition to disease: A huGE review. . Genet Med. 2002;4(2):6270.
82. Schrenk D, Bock KW. Metabolism of benzene in rat hepatocytes. Influence of inducers on phenol glucuronidation. Drug Metab Dispos. 1990;18(5):720-5.
83. Bleasdale C, Kennedy G, MacGregor JO, Nieschalk J, Pearce K, Watson WP, et al. Chemistry of muconaldehydes of possible relevance to the toxicology of benzene. Environ Health Perspect. 1996;104 Suppl 6:1201-9.
84. Guengerich FP. Oxidative cleavage of carboxylic esters by cytochrome P-450. J Biol Chem. 1987;262(18):8459-62.
85. Nebert DW, Nelson DR, Coon MJ, Estabrook RW, Feyereisen R, Fujii-Kuriyama Y, et al. The P450 superfamily: update on new sequences, gene mapping, and recommended nomenclature. DNA and cell biology. 1991;10(1):1-14.
86. Nelson DR, Koymans L, Kamataki T, Stegeman JJ, Feyereisen R, Waxman DJ, et al. P450 superfamily: update on new sequences, gene mapping, accession numbers and nomenclature. Pharmacogenetics. 1996;6(1):1-42.
87. Porter TD, Coon MJ. Cytochrome P-450. Multiplicity of isoforms, substrates, and catalytic and regulatory mechanisms. J Biol Chem. 1991;266(21):13469-72.
88. Rendic S, Di Carlo FJ. Human cytochrome P450 enzymes: a status report summarizing their reactions, substrates, inducers, and inhibitors. Drug metabolism reviews. 1997;29(1-2):413-580.
89. Guengerich FP. Uncommon P450-catalyzed reactions. Current drug metabolism. 2001;2(2):93-115.
90. Loida PJ, Sligar SG. Molecular recognition in cytochrome P-450: mechanism for the control of uncoupling reactions. Biochemistry. 1993;32(43):11530-8.
91. Kuthan H, Ullrich V. Oxidase and oxygenase function of the microsomal cytochrome P450 monooxygenase system. European journal of biochemistry / FEBS. 1982;126(3):583-8.
92. White RE. The involvement of free radicals in the mechanisms of monooxygenases. Pharmacology & therapeutics. 1991;49(1-2):21-42.
93. Knight JA. Free radicals: their history and current status in aging and disease. Annals of clinical and laboratory science. 1998;28(6):331-46.
94. Kehrer JP. Free radicals as mediators of tissue injury and disease. Critical reviews in toxicology. 1993;23(1):21-48.
95. Bondy SC. Reactive oxygen species: relation to aging and neurotoxic damage. Neurotoxicology. 1992;13(1):87-100.
96. Nordmann R, Ribiere C, Rouach H. Implication of free radical mechanisms in ethanol-induced cellular injury. Free radical biology & medicine. 1992;12(3):219-40.
97. Cederbaum AI. Microsomal generation of reactive oxygen species and their possible role in alcohol hepatotoxicity. Alcohol and alcoholism (Oxford, Oxfordshire) Supplement. 1991;1:291-6.
98. Blanck J, Ristau O, Zhukov AA, Archakov AI, Rein H, Ruckpaul K. Cytochrome P-450 spin state and leakiness of the monooxygenase pathway. Xenobiotica; the fate of foreign compounds in biological systems. 1991;21(1):121-35.
99. Nakazawa H, Genka C, Fujishima M. Pathological aspects of active oxygens/free radicals. The Japanese journal of physiology. 1996;46(1):15-32.
100. McCord JM. Iron, free radicals, and oxidative injury. Seminars in hematology. 1998;35(1):5-12.

101. Halliwell B. Antioxidant defence mechanisms: from the beginning to the end (of the beginning). *Free radical research*. 1999;31(4):261-72.
102. Yu BP. Cellular defenses against damage from reactive oxygen species. *Physiological reviews*. 1994;74(1):139-62.
103. Rosen GM, Pou S, Ramos CL, Cohen MS, Britigan BE. Free radicals and phagocytic cells. *FASEB journal : official publication of the Federation of American Societies for Experimental Biology*. 1995;9(2):200-9.
104. Wu D, Cederbaum AI. Ethanol-induced apoptosis to stable HepG2 cell lines expressing human cytochrome P-450E1. *Alcoholism, clinical and experimental research*. 1999;23(1):67-76.
105. Lee SS, Buters JT, Pineau T, Fernandez-Salguero P, Gonzalez FJ. Role of CYP2E1 in the hepatotoxicity of acetaminophen. *J Biol Chem*. 1996;271(20):12063-7.
106. Gorsky LD, Koop DR, Coon MJ. On the stoichiometry of the oxidase and monooxygenase reactions catalyzed by liver microsomal cytochrome P-450. *Products of oxygen reduction*. *J Biol Chem*. 1984;259(11):6812-7.
107. Ekstrom G, Ingelman-Sundberg M. Rat liver microsomal NADPH-supported oxidase activity and lipid peroxidation dependent on ethanol-inducible cytochrome P-450 (P-450IIE1). *Biochem Pharmacol*. 1989;38(8):1313-9.
108. Lieber CS. Microsomal ethanol-oxidizing system (MEOS): the first 30 years (1968-1998)--a review. *Alcoholism, clinical and experimental research*. 1999;23(6):991-1007.
109. Lieber CS. Cytochrome P-450E1: its physiological and pathological role. *Physiological reviews*. 1997;77(2):517-44.
110. Raucy JL, Lasker JM, Kraner JC, Salazar DE, Lieber CS, Corcoran GB. Induction of cytochrome P450IIE1 in the obese overfed rat. *Molecular pharmacology*. 1991;39(3):275-80.
111. Hong JY, Pan JM, Gonzalez FJ, Gelboin HV, Yang CS. The induction of a specific form of cytochrome P-450 (P-450j) by fasting. *Biochem Biophys Res Commun*. 1987;142(3):1077-83.
112. Johansson I, Lindros KO, Eriksson H, Ingelman-Sundberg M. Transcriptional control of CYP2E1 in the perivenous liver region and during starvation. *Biochem Biophys Res Commun*. 1990;173(1):331-8.
113. Woodcroft KJ, Hafner MS, Novak RF. Insulin signaling in the transcriptional and posttranscriptional regulation of CYP2E1 expression. *Hepatology*. 2002;35(2):263-73.
114. Lin HL, Parsels LA, Maybaum J, Hollenberg PF. N-Nitrosodimethylamine-mediated cytotoxicity in a cell line expressing P450 2E1: evidence for apoptotic cell death. *Toxicology and applied pharmacology*. 1999;157(2):117-24.
115. Lin HL, Roberts ES, Hollenberg PF. Heterologous expression of rat P450 2E1 in a mammalian cell line: in situ metabolism and cytotoxicity of N-nitrosodimethylamine. *Carcinogenesis*. 1998;19(2):321-9.
116. Andrews LSL, E.W.; Witmer, C.M.; et al. Effects of toluene on metabolism, disposition, and hematopoietic toxicity of [3H] benzene. *Biochem Pharmacol*. 1977;26:293-300.
117. Gill DP, Jenkins VK, Kempen RR, Ellis S. The importance of pluripotential stem cells in benzene toxicity. *Toxicology*. 1980;16(2):163-71.
118. Tuo J, Loft S, Thomsen MS, Poulsen HE. Benzene-induced genotoxicity in mice in vivo detected by the alkaline comet assay: reduction by CYP2E1 inhibition. *Mutation research*. 1996;368(3-4):213-9.
119. Gad-El Karim MM, Sadagopa Ramanujam VM, Legator MS. Correlation between the induction of micronuclei in bone marrow by benzene exposure and the excretion of

- metabolites in urine of CD-1 mice. *Toxicology and applied pharmacology*. 1986;85(3):464-77.
120. Cheung C, Yu AM, Ward JM, Krausz KW, Akiyama TE, Feigenbaum L, et al. The cyp2e1-humanized transgenic mouse: role of cyp2e1 in acetaminophen hepatotoxicity. *Drug Metab Dispos*. 2005;33(3):449-57.
 121. Rothman N, Smith MT, Hayes RB, Traver RD, Hoener B, Campleman S, et al. Benzene poisoning, a risk factor for hematological malignancy, is associated with the NQO1 609C->T mutation and rapid fractional excretion of chlorzoxazone. *Cancer research*. 1997;57(14):2839-42.
 122. Gut I, Nedelcheva V, Soucek P, Stopka P, Vodicka P, Gelboin HV, et al. The role of CYP2E1 and 2B1 in metabolic activation of benzene derivatives. *Archives of toxicology*. 1996;71(1-2):45-56.
 123. Powley MW, Carlson GP. Species comparison of hepatic and pulmonary metabolism of benzene. *Toxicology*. 1999;139(3):207-17.
 124. Powley MW, Carlson GP. Cytochromes P450 involved with benzene metabolism in hepatic and pulmonary microsomes. *Journal of biochemical and molecular toxicology*. 2000;14(6):303-9.
 125. Sheets P, Carlson G. Kinetic factors involved in the metabolism of benzene in mouse lung and liver. *Journal of toxicology and environmental health Part A*. 2004;67(5):421-30.
 126. Snyder R, Chepiga T, Yang CS, Thomas H, Platt K, Oesch F. Benzene metabolism by reconstituted cytochromes P450 2B1 and 2E1 and its modulation by cytochrome b5, microsomal epoxide hydrolase, and glutathione transferases: evidence for an important role of microsomal epoxide hydrolase in the formation of hydroquinone. *Toxicology and applied pharmacology*. 1993;122(2):172-81.
 127. Snyder R, Witz G, Goldstein BD. The toxicology of benzene. *Environ Health Perspect*. 1993;100:293-306.
 128. Chepiga TA, Yang CS, Snyder R. Benzene metabolism by two purified, reconstituted rat hepatic mixed function oxidase systems. *Advances in experimental medicine and biology*. 1991;283:261-5.
 129. Parke DV. Introduction: Session on metabolism. *Environ Health Perspect*. 1989;82:7-8.
 130. Henschler R, Glatt HR. Induction of Cytochrome P4501A1 in Haemopoietic Stem Cells by Hydroxylated Metabolites of Benzene. *Toxicology in vitro : an international journal published in association with BIBRA*. 1995;9(4):453-7.
 131. Irons RD. Molecular models of benzene leukemogenesis. *Journal of toxicology and environmental health Part A*. 2000;61(5-6):391-7.
 132. Ross D. Metabolic basis of benzene toxicity. *European journal of haematology Supplementum*. 1996;60:111-8.
 133. Ross D. The role of metabolism and specific metabolites in benzene-induced toxicity: evidence and issues. *Journal of toxicology and environmental health Part A*. 2000;61(5-6):357-72.
 134. Smith MT. Overview of benzene-induced aplastic anaemia. *European journal of haematology Supplementum*. 1996;60:107-10.
 135. Smith MT. The mechanism of benzene-induced leukemia: a hypothesis and speculations on the causes of leukemia. *Environ Health Perspect*. 1996;104 Suppl 6:1219-25.
 136. Snyder R. Recent developments in the understanding of benzene toxicity and leukemogenesis. *Drug and chemical toxicology*. 2000;23(1):13-25.
 137. Snyder R. Overview of the toxicology of benzene. *Journal of toxicology and environmental health Part A*. 2000;61(5-6):339-46.

138. Snyder R, Hedli CC. An overview of benzene metabolism. *Environ Health Perspect.* 1996;104 Suppl 6:1165-71.
139. Snyder R, Kalf GF. A perspective on benzene leukemogenesis. *Critical reviews in toxicology.* 1994;24(3):177-209.
140. Caro AA, Cederbaum AI. Oxidative stress, toxicology, and pharmacology of CYP2E1. *Annual review of pharmacology and toxicology.* 2004;44:27-42.
141. Kessova I, Cederbaum AI. CYP2E1: biochemistry, toxicology, regulation and function in ethanol-induced liver injury. *Current molecular medicine.* 2003;3(6):509-18.
142. Jimenez-Lopez JM, Cederbaum AI. CYP2E1-dependent oxidative stress and toxicity: role in ethanol-induced liver injury. *Expert opinion on drug metabolism & toxicology.* 2005;1(4):671-85.
143. Wu D, Cederbaum AI. Removal of glutathione produces apoptosis and necrosis in HepG2 cells overexpressing CYP2E1. *Alcoholism, clinical and experimental research.* 2001;25(4):619-28.
144. Gong P, Cederbaum AI. Nrf2 is increased by CYP2E1 in rodent liver and HepG2 cells and protects against oxidative stress caused by CYP2E1. *Hepatology.* 2006;43(1):144-53.
145. Cederbaum AI. Cytochrome P450 2E1-dependent oxidant stress and upregulation of anti-oxidant defense in liver cells. *Journal of gastroenterology and hepatology.* 2006;21 Suppl 3:S22-5.
146. Nieto N, Friedman SL, Cederbaum AI. Stimulation and proliferation of primary rat hepatic stellate cells by cytochrome P450 2E1-derived reactive oxygen species. *Hepatology.* 2002;35(1):62-73.
147. Nieto N, Friedman SL, Cederbaum AI. Cytochrome P450 2E1-derived reactive oxygen species mediate paracrine stimulation of collagen I protein synthesis by hepatic stellate cells. *J Biol Chem.* 2002;277(12):9853-64.
148. Liu H, Jones BE, Bradham C, Czaja MJ. Increased cytochrome P-450 2E1 expression sensitizes hepatocytes to c-Jun-mediated cell death from TNF-alpha. *American journal of physiology Gastrointestinal and liver physiology.* 2002;282(2):G257-66.
149. Leclercq IA, Da Silva Morais A, Schroyen B, Van Hul N, Geerts A. Insulin resistance in hepatocytes and sinusoidal liver cells: mechanisms and consequences. *Journal of hepatology.* 2007;47(1):142-56.
150. Muniyappa R, Montagnani M, Koh KK, Quon MJ. Cardiovascular actions of insulin. *Endocrine reviews.* 2007;28(5):463-91.
151. Petersen KF, Shulman GI. Etiology of insulin resistance. *The American journal of medicine.* 2006;119(5 Suppl 1):S10-6.
152. Alberti KG, Zimmet P, Shaw J. Metabolic syndrome--a new world-wide definition. A Consensus Statement from the International Diabetes Federation. *Diabetic medicine : a journal of the British Diabetic Association.* 2006;23(5):469-80.
153. Alberti KG, Zimmet PZ. Definition, diagnosis and classification of diabetes mellitus and its complications. Part 1: diagnosis and classification of diabetes mellitus provisional report of a WHO consultation. *Diabetic medicine : a journal of the British Diabetic Association.* 1998;15(7):539-53.
154. Executive Summary of The Third Report of The National Cholesterol Education Program (NCEP) Expert Panel on Detection, Evaluation, And Treatment of High Blood Cholesterol In Adults (Adult Treatment Panel III). *Jama.* 2001;285(19):2486-97.
155. Simmons D, Thompson CF. Prevalence of the metabolic syndrome among adult New Zealanders of Polynesian and European descent. *Diabetes Care.* 2004;27(12):3002-4.

156. Ko GT, Cockram CS, Chow CC, Yeung V, Chan WB, So WY, et al. High prevalence of metabolic syndrome in Hong Kong Chinese--comparison of three diagnostic criteria. *Diabetes research and clinical practice*. 2005;69(2):160-8.
157. Qiao Q, Gao W, Zhang L, Nyamdorj R, Tuomilehto J. Metabolic syndrome and cardiovascular disease. *Annals of clinical biochemistry*. 2007;44(Pt 3):232-63.
158. Bogardus C, Lillioja S, Mott DM, Hollenbeck C, Reaven G. Relationship between degree of obesity and in vivo insulin action in man. *The American journal of physiology*. 1985;248(3 Pt 1):E286-91.
159. Saltiel AR, Kahn CR. Insulin signalling and the regulation of glucose and lipid metabolism. *Nature*. 2001;414(6865):799-806.
160. Pirola L, Johnston AM, Van Obberghen E. Modulation of insulin action. *Diabetologia*. 2004;47(2):170-84.
161. Kubota N, Tobe K, Terauchi Y, Eto K, Yamauchi T, Suzuki R, et al. Disruption of insulin receptor substrate 2 causes type 2 diabetes because of liver insulin resistance and lack of compensatory beta-cell hyperplasia. *Diabetes*. 2000;49(11):1880-9.
162. Liu SC, Wang Q, Lienhard GE, Keller SR. Insulin receptor substrate 3 is not essential for growth or glucose homeostasis. *J Biol Chem*. 1999;274(25):18093-9.
163. Burgering BM, Coffey PJ. Protein kinase B (c-Akt) in phosphatidylinositol-3-OH kinase signal transduction. *Nature*. 1995;376(6541):599-602.
164. Meshkani R, Taghikhani M, Larijani B, Khatami S, Khoshbin E, Adeli K. The relationship between homeostasis model assessment and cardiovascular risk factors in Iranian subjects with normal fasting glucose and normal glucose tolerance. *Clinica chimica acta; international journal of clinical chemistry*. 2006;371(1-2):169-75.
165. Goodyear LJ, Giorgino F, Sherman LA, Carey J, Smith RJ, Dohm GL. Insulin receptor phosphorylation, insulin receptor substrate-1 phosphorylation, and phosphatidylinositol 3-kinase activity are decreased in intact skeletal muscle strips from obese subjects. *The Journal of clinical investigation*. 1995;95(5):2195-204.
166. Bjornholm M, Kawano Y, Lehtihet M, Zierath JR. Insulin receptor substrate-1 phosphorylation and phosphatidylinositol 3-kinase activity in skeletal muscle from NIDDM subjects after in vivo insulin stimulation. *Diabetes*. 1997;46(3):524-7.
167. Shulman GI. Cellular mechanisms of insulin resistance. *The Journal of clinical investigation*. 2000;106(2):171-6.
168. Tamemoto H, Kadowaki T, Tobe K, Yagi T, Sakura H, Hayakawa T, et al. Insulin resistance and growth retardation in mice lacking insulin receptor substrate-1. *Nature*. 1994;372(6502):182-6.
169. Withers DJ, Gutierrez JS, Towery H, Burks DJ, Ren JM, Previs S, et al. Disruption of IRS-2 causes type 2 diabetes in mice. *Nature*. 1998;391(6670):900-4.
170. Weickert MO, Pfeiffer AF. Signalling mechanisms linking hepatic glucose and lipid metabolism. *Diabetologia*. 2006;49(8):1732-41.
171. Kile BT, Schulman BA, Alexander WS, Nicola NA, Martin HM, Hilton DJ. The SOCS box: a tale of destruction and degradation. *Trends in biochemical sciences*. 2002;27(5):235-41.
172. Kaszubska W, Falls HD, Schaefer VG, Haasch D, Frost L, Hessler P, et al. Protein tyrosine phosphatase 1B negatively regulates leptin signaling in a hypothalamic cell line. *Molecular and cellular endocrinology*. 2002;195(1-2):109-18.
173. Butler M, McKay RA, Popoff IJ, Gaarde WA, Wittchell D, Murray SF, et al. Specific inhibition of PTEN expression reverses hyperglycemia in diabetic mice. *Diabetes*. 2002;51(4):1028-34.

174. Elchebly M, Payette P, Michaliszyn E, Cromlish W, Collins S, Loy AL, et al. Increased insulin sensitivity and obesity resistance in mice lacking the protein tyrosine phosphatase-1B gene. *Science*. 1999;283(5407):1544-8.
175. Ahmad F, Azevedo JL, Cortright R, Dohm GL, Goldstein BJ. Alterations in skeletal muscle protein-tyrosine phosphatase activity and expression in insulin-resistant human obesity and diabetes. *The Journal of clinical investigation*. 1997;100(2):449-58.
176. Haj FG, Zabolotny JM, Kim YB, Kahn BB, Neel BG. Liver-specific protein-tyrosine phosphatase 1B (PTP1B) re-expression alters glucose homeostasis of PTP1B^{-/-} mice. *J Biol Chem*. 2005;280(15):15038-46.
177. Clement S, Krause U, Desmedt F, Tanti JF, Behrends J, Pesesse X, et al. The lipid phosphatase SHIP2 controls insulin sensitivity. *Nature*. 2001;409(6816):92-7.
178. Liao J, Barthel A, Nakatani K, Roth RA. Activation of protein kinase B/Akt is sufficient to repress the glucocorticoid and cAMP induction of phosphoenolpyruvate carboxykinase gene. *J Biol Chem*. 1998;273(42):27320-4.
179. Michael MD, Kulkarni RN, Postic C, Previs SF, Shulman GI, Magnuson MA, et al. Loss of insulin signaling in hepatocytes leads to severe insulin resistance and progressive hepatic dysfunction. *Molecular cell*. 2000;6(1):87-97.
180. Bruning JC, Michael MD, Winnay JN, Hayashi T, Horsch D, Accili D, et al. A muscle-specific insulin receptor knockout exhibits features of the metabolic syndrome of NIDDM without altering glucose tolerance. *Molecular cell*. 1998;2(5):559-69.
181. Kim JK, Michael MD, Previs SF, Peroni OD, Mauvais-Jarvis F, Neschen S, et al. Redistribution of substrates to adipose tissue promotes obesity in mice with selective insulin resistance in muscle. *The Journal of clinical investigation*. 2000;105(12):1791-7.
182. Nakae J, Biggs WH, 3rd, Kitamura T, Cavenee WK, Wright CV, Arden KC, et al. Regulation of insulin action and pancreatic beta-cell function by mutated alleles of the gene encoding forkhead transcription factor Foxo1. *Nature genetics*. 2002;32(2):245-53.
183. Ginsberg HN, Zhang YL, Hernandez-Ono A. Regulation of plasma triglycerides in insulin resistance and diabetes. *Archives of medical research*. 2005;36(3):232-40.
184. Grundy SM. Hypertriglyceridemia, atherogenic dyslipidemia, and the metabolic syndrome. *Am J Cardiol*. 1998;81(4a):18b-25b.
185. Adiels M, Olofsson SO, Taskinen MR, Boren J. Overproduction of very low-density lipoproteins is the hallmark of the dyslipidemia in the metabolic syndrome. *Arteriosclerosis, thrombosis, and vascular biology*. 2008;28(7):1225-36.
186. Olofsson SO, Boren J. Apolipoprotein B: a clinically important apolipoprotein which assembles atherogenic lipoproteins and promotes the development of atherosclerosis. *Journal of internal medicine*. 2005;258(5):395-410.
187. Stillemark-Billton P, Beck C, Boren J, Olofsson SO. Relation of the size and intracellular sorting of apoB to the formation of VLDL 1 and VLDL 2. *Journal of lipid research*. 2005;46(1):104-14.
188. Avramoglu RK, Qiu W, Adeli K. Mechanisms of metabolic dyslipidemia in insulin resistant states: deregulation of hepatic and intestinal lipoprotein secretion. *Frontiers in bioscience : a journal and virtual library*. 2003;8:d464-76.
189. Lin MC, Gordon D, Wetterau JR. Microsomal triglyceride transfer protein (MTP) regulation in HepG2 cells: insulin negatively regulates MTP gene expression. *Journal of lipid research*. 1995;36(5):1073-81.
190. Theriault A, Cheung R, Adeli K. Expression of apolipoprotein B in vitro in cell-free lysates of HepG2 cells: evidence that insulin modulates ApoB synthesis at the translational level. *Clinical biochemistry*. 1992;25(5):321-3.

191. Phung TL, Roncone A, Jensen KL, Sparks CE, Sparks JD. Phosphoinositide 3-kinase activity is necessary for insulin-dependent inhibition of apolipoprotein B secretion by rat hepatocytes and localizes to the endoplasmic reticulum. *J Biol Chem.* 1997;272(49):30693-702.
192. Sparks JD, Phung TL, Bolognino M, Sparks CE. Insulin-mediated inhibition of apolipoprotein B secretion requires an intracellular trafficking event and phosphatidylinositol 3-kinase activation: studies with brefeldin A and wortmannin in primary cultures of rat hepatocytes. *The Biochemical journal.* 1996;313 (Pt 2):567-74.
193. Au CS, Wagner A, Chong T, Qiu W, Sparks JD, Adeli K. Insulin regulates hepatic apolipoprotein B production independent of the mass or activity of Akt1/PKBalpha. *Metabolism: clinical and experimental.* 2004;53(2):228-35.
194. Horton JD, Shah NA, Warrington JA, Anderson NN, Park SW, Brown MS, et al. Combined analysis of oligonucleotide microarray data from transgenic and knockout mice identifies direct SREBP target genes. *Proceedings of the National Academy of Sciences of the United States of America.* 2003;100(21):12027-32.
195. Sansbury BE, Hill BG. Regulation of obesity and insulin resistance by nitric oxide. *Free radical biology & medicine.* 2014;73:383-99.
196. Riddell DR, Owen JS. Nitric oxide and platelet aggregation. *Vitamins and hormones.* 1999;57:25-48.
197. Gries A, Bode C, Peter K, Herr A, Bohrer H, Motsch J, et al. Inhaled nitric oxide inhibits human platelet aggregation, P-selectin expression, and fibrinogen binding in vitro and in vivo. *Circulation.* 1998;97(15):1481-7.
198. Sansbury BE, Cummins TD, Tang Y, Hellmann J, Holden CR, Harbeson MA, et al. Overexpression of endothelial nitric oxide synthase prevents diet-induced obesity and regulates adipocyte phenotype. *Circ Res.* 2012;111(9):1176-89.
199. Alessi MC, Juhan-Vague I. PAI-1 and the metabolic syndrome: links, causes, and consequences. *Arteriosclerosis, thrombosis, and vascular biology.* 2006;26(10):2200-7.
200. Hamsten A, de Faire U, Walldius G, Dahlen G, Szamosi A, Landou C, et al. Plasminogen activator inhibitor in plasma: risk factor for recurrent myocardial infarction. *Lancet (London, England).* 1987;2(8549):3-9.
201. Collet JP, Montalescot G, Vicaud E, Ankri A, Walylo F, Lesty C, et al. Acute release of plasminogen activator inhibitor-1 in ST-segment elevation myocardial infarction predicts mortality. *Circulation.* 2003;108(4):391-4.
202. Smith A, Patterson C, Yarnell J, Rumley A, Ben-Shlomo Y, Lowe G. Which hemostatic markers add to the predictive value of conventional risk factors for coronary heart disease and ischemic stroke? The Caerphilly Study. *Circulation.* 2005;112(20):3080-7.
203. Hotamisligil GS. Inflammation and metabolic disorders. *Nature.* 2006;444(7121):860-7.
204. Yuan M, Konstantopoulos N, Lee J, Hansen L, Li ZW, Karin M, et al. Reversal of obesity- and diet-induced insulin resistance with salicylates or targeted disruption of Ikkbeta. *Science.* 2001;293(5535):1673-7.
205. Cai D, Yuan M, Frantz DF, Melendez PA, Hansen L, Lee J, et al. Local and systemic insulin resistance resulting from hepatic activation of IKK-beta and NF-kappaB. *Nature medicine.* 2005;11(2):183-90.
206. Weisberg SP, McCann D, Desai M, Rosenbaum M, Leibel RL, Ferrante AW, Jr. Obesity is associated with macrophage accumulation in adipose tissue. *The Journal of clinical investigation.* 2003;112(12):1796-808.

207. Xu H, Barnes GT, Yang Q, Tan G, Yang D, Chou CJ, et al. Chronic inflammation in fat plays a crucial role in the development of obesity-related insulin resistance. *The Journal of clinical investigation*. 2003;112(12):1821-30.
208. Gregory SH, Wing EJ. Neutrophil-Kupffer cell interaction: a critical component of host defenses to systemic bacterial infections. *Journal of leukocyte biology*. 2002;72(2):239-48.
209. Jacob P, 3rd, Abu Raddaha AH, Dempsey D, Havel C, Peng M, Yu L, et al. Comparison of nicotine and carcinogen exposure with water pipe and cigarette smoking. *Cancer epidemiology, biomarkers & prevention : a publication of the American Association for Cancer Research, cosponsored by the American Society of Preventive Oncology*. 2013;22(5):765-72.
210. Appel BR, Guirguis G, Kim IS, Garbin O, Fracchia M, Flessel CP, et al. Benzene, benzo(a)pyrene, and lead in smoke from tobacco products other than cigarettes. *American journal of public health*. 1990;80(5):560-4.
211. Hattemer-Frey HA, Travis CC, Land ML. Benzene: environmental partitioning and human exposure. *Environ Res*. 1990;53(2):221-32.
212. Aksoy M, Erdem S, DinCol G. Leukemia in shoe-workers exposed chronically to benzene. *Blood*. 1974;44(6):837-41.
213. Collins JJ, Anteau SE, Swaen GM, Bodner KM, Bodnar CM. Lymphatic and hematopoietic cancers among benzene-exposed workers. *Journal of occupational and environmental medicine / American College of Occupational and Environmental Medicine*. 2015;57(2):159-63.
214. Li GL, Yin SN, Watanabe T, Nakatsuka H, Kasahara M, Abe H, et al. Benzene-specific increase in leukocyte alkaline phosphatase activity in rats exposed to vapors of various organic solvents. *Journal of toxicology and environmental health*. 1986;19(4):581-9.
215. Aoyama K. Effects of benzene inhalation on lymphocyte subpopulations and immune response in mice. *Toxicology and applied pharmacology*. 1986;85(1):92-101.
216. Tatrai E, Ungvary G, Hudak A, Rodics K, Lorincz M, Barcza G. Concentration dependence of the embryotoxic effects of benzene inhalation in CFY rats. *Journal of hygiene, epidemiology, microbiology, and immunology*. 1980;24(3):363-71.
217. Santesson CG. Über chronische vegiftungen mit steinkohlenteerbenzin: Vier todesfälle. . *Arch Hyg Berl* 1897;31:336-76.
218. Lan Q, Zhang L, Li G, Vermeulen R, Weinberg RS, Dosemeci M, et al. Hematotoxicity in workers exposed to low levels of benzene. *Science*. 2004;306(5702):1774-6.
219. Verma Y, Rana SV. Modulation of CYP450E1 and oxidative stress by testosterone in liver and kidney of benzene treated rats. *Indian journal of experimental biology*. 2008;46(8):568-72.
220. Li GX, Hirabayashi Y, Yoon BI, Kawasaki Y, Tsuboi I, Kodama Y, et al. Thioredoxin overexpression in mice, model of attenuation of oxidative stress, prevents benzene-induced hemato-lymphoid toxicity and thymic lymphoma. *Experimental hematology*. 2006;34(12):1687-97.
221. Boulanger CM, Scoazec A, Ebrahimian T, Henry P, Mathieu E, Tedgui A, et al. Circulating microparticles from patients with myocardial infarction cause endothelial dysfunction. *Circulation*. 2001;104(22):2649-52.
222. Rozen MG, Snyder CA, Albert RE. Depressions in B- and T-lymphocyte mitogen-induced blastogenesis in mice exposed to low concentrations of benzene. *Toxicology letters*. 1984;20(3):343-9.

223. Wan JX, Zhang ZB, Guan JR, Cao DZ, Ye R, Jin XP, et al. Genetic polymorphism of toxicant-metabolizing enzymes and prognosis of Chinese workers with chronic benzene poisoning. *Annals of the New York Academy of Sciences*. 2006;1076:129-36.
224. Tunsaringkarn T, Soogarun S, Palasuwan A. Occupational exposure to benzene and changes in hematological parameters and urinary trans, trans-muconic acid. *The international journal of occupational and environmental medicine*. 2013;4(1):45-9.
225. Gonzalez-Jasso E, Lopez T, Lucas D, Berthou F, Manno M, Ortega A, et al. CYP2E1 regulation by benzene and other small organic chemicals in rat liver and peripheral lymphocytes. *Toxicology letters*. 2003;144(1):55-67.
226. Shen M, Zhang L, Lee KM, Vermeulen R, Hosgood HD, Li G, et al. Polymorphisms in genes involved in innate immunity and susceptibility to benzene-induced hematotoxicity. *Experimental & molecular medicine*. 2011;43(6):374-8.
227. Yang J, Zhang L, Yu C, Yang XF, Wang H. Monocyte and macrophage differentiation: circulation inflammatory monocyte as biomarker for inflammatory diseases. *Biomarker research*. 2014;2(1):1.
228. Imhof BA, Aurrand-Lions M. Adhesion mechanisms regulating the migration of monocytes. *Nature reviews Immunology*. 2004;4(6):432-44.
229. Panteghini M. Aspartate aminotransferase isoenzymes. *Clinical biochemistry*. 1990;23(4):311-9.
230. Rothschild MA, Oratz M, Schreiber SS. Regulation of albumin metabolism. *Annual review of medicine*. 1975;26:91-104.
231. Bae JC, Seo SH, Hur KY, Kim JH, Lee MS, Lee MK, et al. Association between Serum Albumin, Insulin Resistance, and Incident Diabetes in Nondiabetic Subjects. *Endocrinology and metabolism (Seoul, Korea)*. 2013;28(1):26-32.
232. Dignat-George F, Boulanger CM. The many faces of endothelial microparticles. *Arteriosclerosis, thrombosis, and vascular biology*. 2011;31(1):27-33.
233. Agouni A, Andriantsitohaina R, Martinez MC. Microparticles as biomarkers of vascular dysfunction in metabolic syndrome and its individual components. *Current vascular pharmacology*. 2014;12(3):483-92.
234. Li S, Li X, Li J, Deng X, Li Y. Inhibition of oxidative-stress-induced platelet aggregation by androgen at physiological levels via its receptor is associated with the reduction of thromboxane A2 release from platelets. *Steroids*. 2007;72(13):875-80.
235. Gawaz M, Langer H, May AE. Platelets in inflammation and atherogenesis. *The Journal of clinical investigation*. 2005;115(12):3378-84.
236. Stokes KY, Granger DN. Platelets: a critical link between inflammation and microvascular dysfunction. *The Journal of physiology*. 2012;590(5):1023-34.
237. Wolfrum C, Stoffel M. Coactivation of Foxa2 through Pgc-1beta promotes liver fatty acid oxidation and triglyceride/VLDL secretion. *Cell metabolism*. 2006;3(2):99-110.
238. McGuinness OP, Ayala JE, Laughlin MR, Wasserman DH. NIH experiment in centralized mouse phenotyping: the Vanderbilt experience and recommendations for evaluating glucose homeostasis in the mouse. *American journal of physiology Endocrinology and metabolism*. 2009;297(4):E849-55.
239. Valencia-Olvera AC, Moran J, Camacho-Carranza R, Prospero-Garcia O, Espinosa-Aguirre JJ. CYP2E1 induction leads to oxidative stress and cytotoxicity in glutathione-depleted cerebellar granule neurons. *Toxicology in vitro : an international journal published in association with BIBRA*. 2014;28(7):1206-14.

240. Zong H, Armoni M, Harel C, Karnieli E, Pessin JE. Cytochrome P-450 CYP2E1 knockout mice are protected against high-fat diet-induced obesity and insulin resistance. *American journal of physiology Endocrinology and metabolism*. 2012;302(5):E532-9.
241. Schattenberg JM, Wang Y, Singh R, Rigoli RM, Czaja MJ. Hepatocyte CYP2E1 overexpression and steatohepatitis lead to impaired hepatic insulin signaling. *J Biol Chem*. 2005;280(11):9887-94.
242. Bieche I, Narjoz C, Asselah T, Vacher S, Marcellin P, Lidereau R, et al. Reverse transcriptase-PCR quantification of mRNA levels from cytochrome (CYP)1, CYP2 and CYP3 families in 22 different human tissues. *Pharmacogenetics and genomics*. 2007;17(9):731-42.
243. Valentine JL, Lee SS, Seaton MJ, Asgharian B, Farris G, Corton JC, et al. Reduction of benzene metabolism and toxicity in mice that lack CYP2E1 expression. *Toxicology and applied pharmacology*. 1996;141(1):205-13.
244. Carlson G. Influence of selected inhibitors on the metabolism of the styrene metabolite 4-vinylphenol in wild-type and CYP2E1 knockout mice. *Journal of toxicology and environmental health Part A*. 2004;67(12):905-9.
245. Lu H, Lei X, Zhang Q. Moderate activation of IKK2-NF-kB in unstressed adult mouse liver induces cytoprotective genes and lipogenesis without apparent signs of inflammation or fibrosis. *BMC gastroenterology*. 2015;15:94.
246. Pahl HL. Activators and target genes of Rel/NF-kappaB transcription factors. *Oncogene*. 1999;18(49):6853-66.
247. Giardino Torchia ML, Conze DB, Jankovic D, Ashwell JD. Balance between NF-kappaB p100 and p52 regulates T cell costimulation dependence. *Journal of immunology (Baltimore, Md : 1950)*. 2013;190(2):549-55.
248. Sun SC. Non-canonical NF-kappaB signaling pathway. *Cell research*. 2011;21(1):71-85.
249. Grove M, Plumb M. C/EBP, NF-kappa B, and c-Ets family members and transcriptional regulation of the cell-specific and inducible macrophage inflammatory protein 1 alpha immediate-early gene. *Molecular and cellular biology*. 1993;13(9):5276-89.
250. Yun JJ, Tsao MS, Der SD. Differential utilization of NF-kappaB RELA and RELB in response to extracellular versus intracellular polyIC stimulation in HT1080 cells. *BMC immunology*. 2011;12:15.
251. Qin H, Niyongere SA, Lee SJ, Baker BJ, Benveniste EN. Expression and functional significance of SOCS-1 and SOCS-3 in astrocytes. *Journal of immunology (Baltimore, Md : 1950)*. 2008;181(5):3167-76.
252. Ramirez-Martinez G, Cruz-Lagunas A, Jimenez-Alvarez L, Espinosa E, Ortiz-Quintero B, Santos-Mendoza T, et al. Seasonal and pandemic influenza H1N1 viruses induce differential expression of SOCS-1 and RIG-I genes and cytokine/chemokine production in macrophages. *Cytokine*. 2013;62(1):151-9.
253. Ueki K, Kondo T, Kahn CR. Suppressor of cytokine signaling 1 (SOCS-1) and SOCS-3 cause insulin resistance through inhibition of tyrosine phosphorylation of insulin receptor substrate proteins by discrete mechanisms. *Molecular and cellular biology*. 2004;24(12):5434-46.
254. Rui L, Yuan M, Frantz D, Shoelson S, White MF. SOCS-1 and SOCS-3 block insulin signaling by ubiquitin-mediated degradation of IRS1 and IRS2. *J Biol Chem*. 2002;277(44):42394-8.
255. Cannizzo B, Quesada I, Militello R, Amaya C, Miatello R, Cruzado M, et al. Tempol attenuates atherosclerosis associated with metabolic syndrome via decreased vascular

- inflammation and NADPH-2 oxidase expression. *Free radical research*. 2014;48(5):526-33.
256. Bourgoin F, Bachelard H, Badeau M, Lariviere R, Nadeau A, Pitre M. Effects of tempol on endothelial and vascular dysfunctions and insulin resistance induced by a high-fat high-sucrose diet in the rat. *Canadian journal of physiology and pharmacology*. 2013;91(7):547-61.
257. Habertzettl P, O'Toole TE, Bhatnagar A, Conklin DJ. Exposure to Fine Particulate Air Pollution Causes Vascular Insulin Resistance by Inducing Pulmonary Oxidative Stress. *Environ Health Perspect*. 2016.
258. Tomankova V, Liskova B, Skalova L, Bartikova H, Bousova I, Jourova L, et al. Altered cytochrome P450 activities and expression levels in the liver and intestines of the monosodium glutamate-induced mouse model of human obesity. *Life sciences*. 2015;133:15-20.
259. Cederbaum AI. CYP2E1 potentiates toxicity in obesity and after chronic ethanol treatment. *Drug metabolism and drug interactions*. 2012;27(3):125-44.
260. Bai W, Chen Y, Yang J, Niu P, Tian L, Gao A. Aberrant miRNA profiles associated with chronic benzene poisoning. *Experimental and molecular pathology*. 2014;96(3):426-30.
261. Wei H, Zhang J, Tan K, Sun R, Yin L, Pu Y. Benzene-Induced Aberrant miRNA Expression Profile in Hematopoietic Progenitor Cells in C57BL/6 Mice. *International journal of molecular sciences*. 2015;16(11):27058-71.
262. Liu Y, Chen X, Bian Q, Shi Y, Liu Q, Ding L, et al. Analysis of plasma microRNA expression profiles in a Chinese population occupationally exposed to benzene and in a population with chronic benzene poisoning. *Journal of thoracic disease*. 2016;8(3):403-14.
263. Rao X, Zhong J, Maiseyeu A, Gopalakrishnan B, Villamena FA, Chen LC, et al. CD36-dependent 7-ketocholesterol accumulation in macrophages mediates progression of atherosclerosis in response to chronic air pollution exposure. *Circ Res*. 2014;115(9):770-80.
264. Thurston GD, Burnett RT, Turner MC, Shi Y, Krewski D, Lall R, et al. Ischemic Heart Disease Mortality and Long-Term Exposure to Source-Related Components of U.S. Fine Particle Air Pollution. *Environ Health Perspect*. 2016;124(6):785-94.
265. Shah AS, Langrish JP, Nair H, McAllister DA, Hunter AL, Donaldson K, et al. Global association of air pollution and heart failure: a systematic review and meta-analysis. *Lancet (London, England)*. 2013;382(9897):1039-48.
266. Kim JH, Hong YC. GSTM1, GSTT1, and GSTP1 polymorphisms and associations between air pollutants and markers of insulin resistance in elderly Koreans. *Environ Health Perspect*. 2012;120(10):1378-84.
267. Valavanidis A, Vlachogianni T, Fiotakis K, Loridas S. Pulmonary oxidative stress, inflammation and cancer: respirable particulate matter, fibrous dusts and ozone as major causes of lung carcinogenesis through reactive oxygen species mechanisms. *Int J Environ Res Public Health*. 2013;10(9):3886-907.
268. Till JE, Mc CE. A direct measurement of the radiation sensitivity of normal mouse bone marrow cells. *Radiation research*. 1961;14:213-22.
269. Asahara T, Murohara T, Sullivan A, Silver M, van der Zee R, Li T, et al. Isolation of putative progenitor endothelial cells for angiogenesis. *Science*. 1997;275(5302):964-7.
270. Chen S, Sun L, Gao H, Ren L, Liu N, Song G. Visfatin and oxidative stress influence endothelial progenitor cells in obese populations. *Endocrine research*. 2015;40(2):83-7.

271. Bruyndonckx L, Hoymans VY, Frederix G, De Guchtenaere A, Franckx H, Vissers DK, et al. Endothelial progenitor cells and endothelial microparticles are independent predictors of endothelial function. *The Journal of pediatrics*. 2014;165(2):300-5.
272. Tsai TH, Chai HT, Sun CK, Yen CH, Leu S, Chen YL, et al. Obesity suppresses circulating level and function of endothelial progenitor cells and heart function. *Journal of translational medicine*. 2012;10:137.
273. Werner N, Kosiol S, Schiegl T, Ahlers P, Walenta K, Link A, et al. Circulating endothelial progenitor cells and cardiovascular outcomes. *N Engl J Med*. 2005;353(10):999-1007.
274. O'Toole TE, Hellmann J, Wheat L, Haberzettl P, Lee J, Conklin DJ, et al. Episodic exposure to fine particulate air pollution decreases circulating levels of endothelial progenitor cells. *Circ Res*. 2010;107(2):200-3.
275. Brook RD, Bard RL, Kaplan MJ, Yalavarthi S, Morishita M, Dvonch JT, et al. The effect of acute exposure to coarse particulate matter air pollution in a rural location on circulating endothelial progenitor cells: results from a randomized controlled study. *Inhalation toxicology*. 2013;25(10):587-92.
276. Kondo T, Hayashi M, Takeshita K, Numaguchi Y, Kobayashi K, Iino S, et al. Smoking cessation rapidly increases circulating progenitor cells in peripheral blood in chronic smokers. *Arteriosclerosis, thrombosis, and vascular biology*. 2004;24(8):1442-7.

CURRICULUM VITAE

NAME: Wesley T. Abplanalp

August 2016

PRESENT PRIMARY POSITION AND ADDRESS:

Doctoral Graduate Student
Department of Physiology
School of Medicine
Diabetes and Obesity Center
University of Louisville
580 South Preston St.
Delia Baxter Building, Rm 207
Louisville, KY 40202
Phone: (502) 852-4215
Email: wtabpl01@louisville.edu

BIOGRAPHICAL

DATE & PLACE OF BIRTH: July 21, 1981 – Cincinnati, OH USA

HOME ADDRESS: 233 Haldeman Ave., Louisville, KY 40206

EDUCATION

<u>Institution</u>	<u>Date</u>	<u>Degree</u>	<u>Subject</u>
Indiana University	2007	BS	Biology
University of Louisville	2014	MS	Physiology
University of Louisville	2016	PhD	Physiology

PAST PROFESSIONAL EXPERIENCE

2015	Guest Lecturer	Clinical Pathophysiology Sullivan University
------	----------------	---

2009–2011	Research Technologist II	Center for Diabetes and Obesity Research University of Louisville
2008-2009	Field Biologist	Fort Knox, Armored Vehicle Division Virginia Commonwealth University
2007-2008	Field Biologist	Malheur National Wildlife Refuge Department of Interior

SERVICE

2012-2013	Graduate Student Volunteer	AHA Walk/Run Fundraiser
2013-2015	Graduate Student Volunteer	IPIBS New Student Orientation University of Louisville
2015	Volunteer	Louisville Housing Authority Playground Build Construction Project for Parkway Neighborhood Residents
2016	Volunteer	Stoddard Johnston Scholar House Playground Build Construction Project for Residents

MEMBERSHIP IN SCIENTIFIC SOCIETIES

2015-Present	Student/Trainee Member, American Heart Association (Council on Basic Cardiovascular Sciences)
2015-Present	Student/Trainee Member, Arteriosclerosis, Vascular Biology and Thrombosis (ATVB)
2012-Present	Student/Trainee Member, Society of Toxicology (SOT)

2012-Present Student/Trainee Member, Ohio Valley Society of Toxicology Chapter (OVSOT)

AWARDS, HONORS and INVITED PRESENTATIONS

2012 IPIBS Fellowship, University of Louisville
2013 IPIBS Fellowship, University of Louisville
2014 National Society of Toxicology Travel Award
2016 OVSOT Finalist and Invited Platform Speaker for Outstanding Abstract

RESEARCH ACTIVITIES

Active areas of interest:

- Vascular Consequences of Exposure to Air Pollution
- Regulation of Insulin Signaling
- Role of Extracellular Vesicles in Physiological and Pathophysiological States
- Progenitor Cell Physiology

PUBLICATIONS

1. **Abplanalp W**, Conklin DJ, Cantor JM, Ginsberg MH, Wysoczynski M, Bhatnagar A, O'Toole TE. Enhanced integrin $\alpha 4\beta 1$ -mediated adhesion contributes to a mobilization defect of endothelial progenitor cells in diabetes. *Diabetes*. (Accepted, In Press)
2. Pope CA, Bhatnagar A, McCracken JM, **Abplanalp W**, Conklin DJ, O'Toole TE. Fine Particulate Matter Air Pollution Is Associated with Biomarkers of Endothelial Injury and Systemic Inflammation. *Journal of the American College of Cardiology*. (Accepted, In Press)
3. O'Toole TE, **Abplanalp W**, Li X, Cooper N, Conklin DJ, Haberzettl P, Bhatnagar A. Acrolein decreases endothelial cell migration and insulin sensitivity through induction of let-7a. *Tox Sci* 2014 Aug 1;140(2):271-82.

4. DeJarnett N, Yeager R, Conklin DJ, Lee J, O'Toole TE, McCracken J, **Abplanalp W**, Srivastava S, Riggs DW, Hamzeh I, Wagner S, Chugh A, DeFilippis A, Ciszewski T, Wyatt B, Becher C, Higdon D, Ramos KS, Tollerud DJ, Myers JA, Rai SN, Shah J, Zafar N, Krishnasamy SS, Prabhu SD, Bhatnagar A. Residential Proximity to Major Roadways Is Associated with Increased Levels of AC133+ Circulating Angiogenic Cells. *Arterioscler Thromb Vasc Biol.* 2015 Nov;35(11):2468-77.
5. DeJarnett N, Conklin DJ, Riggs DW, Myers JA, O'Toole TE, Hamzeh I, Wagner S, Chugh A, Ramos KS, Srivastava S, Higdon D, Tollerud DJ, DeFilippis A, Becher C, Wyatt B, McCracken J, **Abplanalp W**, Rai SN, Ciszewski T, Xie Z, Yeager R, Prabhu SD, Bhatnagar A. Acrolein Exposure Is Associated with Increased Cardiovascular Disease Risk. *J Am Heart Assoc.* 2014 Aug 6;3(4).
6. **Abplanalp W**, DeJarnett N, Conklin DJ, Riggs DW, Hamzeh I, Srivastava S, Higdon D, McCracken J, Rai SN, Xie Z, Bhatnagar A, O'Toole TE. Benzene Exposure Is Associated with Decreased Circulating Angiogenic Cells and Increased Cardiovascular Disease Risk. *Environmental Health Perspectives.* (Submitted, Under Review)
7. **Abplanalp W**, Conklin DJ, Bhatnagar A, O'Toole TE. Exposure to Inhaled Fine Particulate Matter (PM_{2.5}) Induces Functional Defects in Bone Marrow-Derived Endothelial Progenitor Cells. (Submitted)

PRESENTATIONS

1. Tobacco Centers of Regulatory Science (TCORS) Symposium – Bethesda, MD – May 2016
2. Arteriosclerosis, Thrombosis and Vascular Biology Annual Meeting – Nashville, TN – May 2016
3. National SOT Conference – New Orleans, LA – March 2016
4. Ohio Valley Society of Toxicology (SOT) Symposium – Covington, KY – November 2015
5. Research Louisville – Louisville, KY – September 2015
6. Ohio Valley Society of Toxicology Student Symposium – Cincinnati, OH – June 2015

7. Vascular Research Seminar – Louisville, KY – April 2015
8. National SOT Conference – San Diego, CA – March 2015
9. Ohio Valley Society of Toxicology (SOT) Symposium – Louisville, KY – October 2014
10. Research Louisville – Louisville, KY – September 2014
11. Vascular Research Seminar – Louisville, KY – April 2014
12. National SOT Conference – Phoenix, AZ – March 2014
13. Ohio Valley Society of Toxicology (SOT) Symposium – Louisville, KY – October 2013
14. Research Louisville – Louisville, KY – September 2013